Anthropogenic microfibres in background natural environments in Ireland

A Thesis Submitted to the Committee on Graduate Studies in Partial Fulfilment of the Requirements for the Degree of Master of Science in the Faculty of Arts and Science

Trent University
Peterborough, Ontario, Canada
© Copyright by Brett Roblin 2019
Environmental and Life Sciences M.Sc. Graduate Program
September 2019

Abstract

Anthropogenic microfibres in background natural environments in Ireland

Brett Roblin

Microfibres, which are threadlike particles < 5 mm, are the most common type of microplastic reported in the environment. However, few studies have focused on their abundance in background natural environments. This study assessed the abundance of microfibres in rainfall samples (from four precipitation monitoring stations) and across three headwater lake catchments that were in remote, undeveloped areas, away from anthropogenic disturbance and anthropogenic emission sources (i.e., sites were background natural environments). Anthropogenic microfibres were observed in all samples using visual identification methods, with Raman spectroscopy confirming the presence of polyester film and synthetic pigments, e.g., indigo and hostasol green. The estimated annual average atmospheric deposition of microfibres was ~28,800 mf m⁻². Meteorological variables, e.g., rain, wind direction, and relative humidity were correlated with the abundance of microfibres. The average abundance of microfibres in headwater lake catchments was 24 mf g⁻¹ in moss, 0.70 mf m⁻³ in surface trawl, 9,690 mf m⁻³ in subsurface, 910 mf kg⁻¹ in lake sediment and 576 mf kg⁻¹ in lakeshore sediment. Keywords: Microfibres, Microplastics, Background Environments, Rainfall, Headwater Lake Catchments, Atmospheric Deposition

Acknowledgements

This thesis could not be possible without continued advice and support from many people. First, I would like to thank my supervisor Dr. Julian Aherne for his guidance, support and patience throughout this process. I would also like to thank my thesis committee Dr. Andrew Vreugdenhil and Dr. Chris Metcalfe for their feedback and support throughout the process of this project.

I would like to thank my friends and colleagues from the Environmental GeoSciences
Research Group and Sc. 105 & 106; Dane Blanchard, Spencer Gilbert-Parkes, Patrick
Levasseur, Stephen McGovarin, Kimber Munford, Becki Brown, and numerous other
people, for moral support, suggestions, and for sharing the everyday grind of being a
graduate student. I would also like to thank my family and Michelle Arentsen for all their
support and encouragement throughout this process.

This research would not be possible without the funding from the Irish Environmental Protection Agency, and the logistical support from: The National Parks and Wildlife Service, Inland Fisheries Ireland, and University College Dublin (specifically Dr. Thomas Cummins and Ms. Anne Killion). I would also like to thank Hazel Cathcart for helping me with field work. Special thanks go to Dr. Andrew Vreugdenhil and the Vreugdenhil Lab for guidance and access to their Raman Spectrometer as well as Debbie Lietz and the Biology Department for access to their stereomicroscope.

Table of Contents

Abstract	i
Acknowledgements	ii
List of Figures	v
List of Tables	<i>v</i> /
List of Appendices	vi
Chapter one: General introduction	1
1.1. Plastics in the environment	1
1.2. Microfibres	2
1.3. The sizes, shapes and colours of microfibres	3
1.4. Microfibres as pollutants	4
1.5. Microfibres in the environment	6
1.6. Transboundary air pollution	7
1.7. Thesis objectives	9
1.8. References	11
Chapter 2: Ambient atmospheric deposition of anthropogenic microfibres	19
2.1. Abstract	
2.2. Introduction	19
2.3. Materials and methods	22
2.3.1. Study sites	
2.3.2 Microfibre extractions	
2.3.3. Microscopy and microfibre identification	
2.3.5. Quality control	
2.3.6. Data analysis	
2.4. Results	
2.5. Discussion	32
2.6. Conclusion	37
2.7. References	38
2.8. Appendix	41
Chapter 3: Presence of microfibres in headwater lake catchments in Ireland	56
3.1. Abstract	
3.1. Abstract	56
3.2. Introduction	

3.3.1. Study sites	59
3.3.2. Field sampling	62
3.3.3. Microfibre extraction	
3.3.4. Microscopy and microfibre identification	65
3.3.5. Raman spectroscopy	
3.3.6. Quality control and data analysis	67
3.4. Results	69
3.4.1. Microfibre abundance in headwater lake catchments	69
3.3.2. Size and colour of microfibres	
3.4.3 Trajectory source receptor plot analysis	74
3.4.4. Raman analysis	74
3.5. Discussion	75
3.5.1. Abundance of microfibres in headwater lake catchments	75
3.5.2. Size and colour of microfibres	77
3.5.3. Raman analysis	78
3.6. Conclusion	80
3.7. References	81
3.8. Appendix	84
Chapter 4: Conclusion	99
4.1 General conclusions	99
4.2 Contributions to research	101
4.3 Recommendations	101
4.4. References	103

List of Figures

Figure 2.1. Location of the four precipitation chemistry monitoring stations in the current study. All stations are part of the European Monitoring and Evaluation Programme under the United Nations Economic Commission for Europe
Figure 2.2A-2.2D. A) The monthly microfibre counts, B) microfibres per litre (mf L ⁻¹), C) average microfibre length (mm) and D) estimated microfibre deposition (mf m ⁻²) observed in rainfall collected from the four precipitation chemistry stations, Oak Park (OP), Johnstown Castle (JC), Valentia (VA), and Malin Head (MH) during June 2017–May 2018. The black line indicates the median, the box represents the first and third quartiles, the whiskers represent minimum and maximum values and outliers are indicated by dots
Figure 2.3. The percentage of microfibres that each month contributed to the total number of microfibres at each of the four precipitation chemistry stations from June 2017–May 2018
Figure 3.1. Location of the three headwater lake catchments: Glendalough, Lough Maumwee and Lough Veagh. All lake catchments are part of International Cooperative Programme on Assessment and Monitoring of Effects of Air Pollution on Rivers and Lakes under the United Nations Economic Commission for Europe
Figure 3.2. The percent of microfibres, and triplicate (moss and sediment), surface trawl (mf km ⁻¹) and subsurface microfibre counts, observed across each of the five sampled media (ST= Surface trawl, SS= Subsurface, LSS= Lakeshore sediment, LS = Lake sediment, M = Moss) collected at each of the three lake catchments (GL = Glendalough, LM = Lough Maumwee, LV = Lough Veagh)
Figure 3.3. Microfibre lengths from media (ST= Surface trawl, SS= Subsurface, LSS= Lakeshore sediment, LS = Lake sediment, M = Moss) collected at each of the three headwater lake catchments (GL = Glendalough, LM = Lough Maumwee, LV = Lough Veagh. The black line indicates the median, the boxes represent the first and third quartiles, the whiskers represent the smallest and largest observations that fall within a distance of 1.5 times the box size and the dots represent values that are outside the 1.5 times distance
Figure 3.4. Colour distribution of microfibres collected from each media (ST= Surface trawl, SS= Subsurface, LSS= Lakeshore sediment, LS = Lake sediment, M = Moss) at the three lake catchments

List of Tables

Table 2.1. Latitude, longitude, elevation (EL) and annual rainfall (P) during the period of June 2017–May 2018 (Source: Met Éireann www.met.ie), for the four meteorological monitoring stations in the current study
Table 2.2. Annual sample volume, rainfall, microfibre count (mf) (coefficient of variation in parentheses), estimated mf deposition (mf m ⁻²), total and median fibre length (mm) for each precipitation chemistry monitoring station from June 2017–May 2018 29
Table 3.1. Latitude, longitude, elevation (EL), surface area (SA), lake volume (Vol), long-term (1981-2010) average annual air temperature (AT) and rainfall (P) were measured from the nearest meteorological station (Casement Aerodrome for Glendalough Upper, Mace Head for Lough Maumwee and Malin Head for Lough Veagh) for each headwater lake catchment
Table 3.2. The abundance of microfibres observed in water, sediment and moss from each headwater lake catchment from May 2018. Coefficient of variation [%] indicated in parenthesis for triplicate samples (i.e., sediment and moss)
Table 3.3. The median length (coefficient of variation between triplicates) of microfibres collected in the samples from each of the three headwater lake catchments
Table 3.4. Raman spectroscopy results for the subset of microfibres analysed, including the name (match %), and media where fibres were extracted

List of Appendices

Figure A2.1. Example image of area surrounding long term precipitation chemistry monitoring stations (Malin Head station depicted)
Table A2.1. The closest residential (distance away in parenthesis) and urban centres (pop. >10,000; distance away in parenthesis), with their respective populations, to each of the four precipitation chemistry stations
Table A2.2. List of criteria used to visually identify plastic microfibres following: (A) four criteria taken from Norén (2007) as cited by Hidalgo-Ruz (2010) and Löder and Gerdts (2015), and (B) eight criteria taken from Windsor et al. (2018), with a recommendation that a positive response for at least two of the eight criteria is required for identification of microplastic particles.
Table A2.3. Monthly sample volume, rainfall (P), microfibre count (mf), median, average and total fibre length, mf L ⁻¹ , and estimated mf deposition (mf m ⁻²)
Table A2.4. Pearson correlation coefficients for monthly meteorological and precipitation chemistry (temp = temperature, wetb = wet bulb temperature, dewpt = dew point temperature, vappr = vapor pressure, rhum = relative humidity, msl = mean sea level pressure, wdsp = wind speed, wddir = wind direction) against monthly microfibre counts from each of the four meteorological stations. (OP = Oak Park, JC = Johnstown Castle, VA = Valentia, MH = Malin Head)
Figure A2.2. Length (µm) distribution of microfibres across the four precipitation monitoring stations. Black line represents the median, boxplots represent the first quartile and third quartile, and the whiskers represent the minimum and maximum values.
Figure A2.3. Trajectory rose source-receptor plots showing the proportion (%) of air by direction and source (Republic of Ireland [red], Northern Ireland [orange], Great Britain [green] and Marine and other regions [blue]) arriving at the study sites (receptors; arrival height of 850 hPa) based on two-day back-trajectories estimated every six hours during the period 1989–2009 using historical wind fields (observed data and model output) smoothed onto a 3-dimensional grid with 16 pressure levels and a horizontal resolution of 1×1 degree obtained from the ECMWF ERA Interim data set. Lower: Close-up showing the proportion (%) of air by direction from three terrestrial source regions: Republic of Ireland (red), Northern Ireland (orange) and Great Britain (green) only
Figure A2.4. Raman spectral analysis reports from Bio Rad-KnowItAll online library for Mortonerm blue from a Johnstown Castle March microfibre

Figure A2.5. Multilinear regression analysis of principle components 2 and 6 (Predicted n) against monthly microfibre counts (Observed n) for the Oak Park precipitation chemistry monitoring station. Regression equation and R ² value for trendline included.
Table A3.1. The closest residential (distance away in parenthesis) and urban (pop. >10,000; distance away in parenthesis) areas, with their respective populations, to each of the three headwater lake catchments
Figure A3.1. Photographs (from top to bottom) of Glendalough, Lough Maumwee and Lough Veagh
Figure A3.2. Upper: Trajectory source-receptor rose plots showing the proportion (%) of air by direction and source (Republic of Ireland (red), Northern Ireland (orange), Great Britain (green) and marine and other regions (blue)) arriving at the study sites. Lower: Close-up of proportion (%) of air from Ireland, Northern Ireland and Great Britian source regions only. Source-receptor trajectory rose plots were based on two-day back trajectories (arrival height of 850 hPa) estimated every six hours during the period 1989–2009.
Table A3.2. List of criteria used to visually identify plastic microfibres following: (A) four criteria taken from Norén (2007) as cited by Hidalgo-Ruz (2010) and Löder and Gerdts (2015), and (B) eight criteria taken from Windsor et al. (2018), with a recommendation that a positive response for at least two of the eight criteria is required for identification of microplastic particles.
Table A3.3. The number of microfibres observed in triplicate moss, lake and lakeshore sediment samples from the three headwater lake catchments
Table A3.4. The total count of microfibres found in each media collected at the three headwater lake catchments
Figure A3.3A. Length distribution (µm) of microfibres in surface trawl samples from the three headwater lake catchments (Glendalough, Lough Maumwee and Lough Veagh). Black line represents the median, boxplots represent the first quartile and third quartile, whiskers represent the smallest and largest observations that fall within a distance of 1.5 times the box size and the dots represent values that are outside the 1.5 times distance.
Figure A3.4A. Raman spectral analysis report from Bio Rad-KnowItAll online library for Hostasol Green G-K identified from a Glendalough lake sediment microfibre
Table A3.5. Previous studies on microplastics, with the location, sample type, abundance (range in parentheses), and dominant type of microplastic

Chapter one: General introduction

1.1. Plastics in the environment

Since the 1950s the global production of plastic has increased from 1.5 million tonnes to 348 million tonnes in 2017 (PlasticsEurope, 2018). Despite increased efforts to recycle, 54% of plastic ends as waste (Horton et al., 2017). This is because the majority of plastics produced are for single use purposes (PlasticsEurope, 2016; Barrows et al., 2018). Plastic items are cheap, lightweight and manufactured to be durable, with various additives (e.g., stabilizers, antioxidants, and flame retardants) preventing deterioration or degradation (Barboza et al., 2015; Barrows et al., 2018; Franzellitti et al., 2019). As a result, plastic has been used for many domestic and industrial applications. However, these same characteristics have caused them to be an environmental concern. The most common types of plastics produced are polypropylene (PP), polystyrene, polyethylene, nylon (or polyamide), polyethylene terephthalate (PET), and polyvinyl chloride (PVC), constituting >80% of all plastics (Hidalgo-Ruz et al., 2012; Ivar do Sul and Costa, 2014; PlasticsEurope, 2016; Gago et al., 2018: Rios Mendoza and Balcer, 2019). These pose a high likelihood of being the most commonly found types of plastics in the environment (Andrady, 2011). Once in the environment, the additives in the waste plastics allow them to persist for years, with some plastics projected to take decades to degrade (Hidalgo-Ruz et al., 2012; Barboza et al., 2015). Over time this plastic waste can weather into smaller particles from larger debris (Thompson et al., 2004; Hidalgo-Ruz et al., 2012; Andrady, 2017). Plastic particles

that are smaller than 5 mm are referred to as microplastics (mp) and have been shown to be persistent and ubiquitous in the environment (Thompson et al., 2009; Rillig, 2012; Ivar do Sul and Costa, 2014). Microplastics are derived from primary and secondary sources. Primary sources are particles manufactured to be microscopic in size (e.g., personal care products, cosmetics etc.). The latter are fragmented from larger plastics items (e.g., bottles, bags, clothing, etc.), through UV radiation, physical abrasion and biodegradation (Cole et al., 2011; Hidalgo-Ruz et al., 2012; Eerkes-Medrano et al., 2015; Andrady, 2017). The most common form of microplastics found in the environment are plastic fibres (threadlike particles); these microfibres (mf) typically fragment from textiles, nets, fishing line and other plastic materials (Browne et al., 2011; Cole, 2016; Horton et al., 2017; Barrows et al., 2018; Gago et al., 2018).

1.2. Microfibres

Despite being reported as the dominant microplastic observed in the environment, plastics (e.g., PET, nylon, and PP) that are used for synthetic fibres have been excluded from estimates on the global production of plastics (PlasticsEurope, 2016; Obbard, 2018). This is notable as approximately 2 million tons of microfibres are estimated to be input into the aquatic environment each year with 150 million microfibres entering the Atlantic Ocean each day (Boucher and Friot, 2017; Mishra et al., 2019). The dominant kinds of microfibres found in the environment are polyester, polypropylene, nylon, polyamide, rayon, acrylic, wool, linen, cotton, and cellulose (Gago et al., 2018; Obbard, 2018; Mishra et al., 2019; Wang et al., 2019). Plastic fibres make up the majority (>60%)

of manufactured fibres (Obbard, 2018; Stanton et al., 2019; Mishra et al., 2019). The largest source of microfibres into the environment is from wastewater treatment plants (Gago et al., 2018; Barrows et al., 2018; Mishra et al., 2019). Microfibres are released from textiles throughout their life cycle, with the majority being released during washing, which ends up in wastewater treatment plants, prior to entering the aquatic environment (Boucher and Friot, 2017; Belzagui et al., 2019). Another lesser understood input of microfibres into the environment is through atmospheric deposition (Dris et al., 2016; Cai et al., 2017; Stanton et al., 2019; Allen et al., 2019). Some scientific studies on microplastics have excluded microfibres as they are considered to have the highest risk of laboratory contamination compared to other, less prominent microplastics (Foekema et al., 2013; Gago et al., 2018). This suggests that studies including microfibres need to have rigorous quality control methods to ensure that there is no contamination (Foekema et al., 2013; Gago et al., 2018; Barrows et al., 2018). There is also the risk of misidentifying natural fibres as being plastic (Barrows et al., 2018).

1.3. The sizes, shapes and colours of microfibres

There are three common characteristics that are used to identify and catalog microfibres in studies: shape, size and colour. Fibres are identified as long, slender and threadlike with the same width across the entire length. Microfibres can range in size from < 1 μ m to 5 mm (Gago et al., 2018; Frias and Nash, 2019). There is currently no defined convention on the ranges in size other than < 5 mm (Frias and Nash, 2019). Synthetic fibres have very characteristic colours which allow them to be easily identified

in environment samples. A variety of coloured fibres have been observed, as this is dependent on the colour of dyes used during the manufacturing of the textile (Gago et al., 2018).

1.4. Microfibres as pollutants

Microplastics have gained increasing attention over the last decade because of their ubiquity in the environment and the growing concern of their environmental impacts (Thompson et al., 2004; Ryan et al., 2009; Barboza and Gimenez, 2015; Belzagui et al., 2019). Their microscopic size allows them to be widely bioavailable to aquatic organisms (Franzellitti et al., 2019; Mishra et al., 2019). Aquatic organisms have been observed to ingest microfibres, through filter, suspension or deposition feeding (Moore, 2008; Franzellitti et al., 2019). Filter feeders have been suggested to be the most likely to ingest these particles, as they filter large quantities of water (Setala et al., 2016; Franzellitti et al., 2019). Filter feeders, especially bivalves, represent an important link between trophic levels as they connect the pelagic and benthic systems (Setala et al., 2016; Franzellitti et al., 2019). When ingested they can accumulate, and translocate into different tissues, which poses a risk of physical harm (blockage, and abrasion) (Cole et al., 2011; Zhao et al., 2014; Mathalon and Hill, 2014; Wagner et al., 2014). Fibrous materials (e.g. asbestos and nanotubes) have a higher likelihood of causing carcinogenesis and fibrosis compared to particles (e.g. fragments, films and beads) made from similar material, which are benign (Cole, 2016, Gago et al., 2018). Regular and prolonged exposure to microfibres may cause respiratory inflammation, pulmonary

fibrosis and potentially cancer (Carr, 2017). There is also the risk of chemical impacts from additives to the fibres (dyes, plasticizers, fillers, flame retardants and stabilizers) which can leach into the organism (Teuten et al., 2009; Vandermeersch et al., 2015; Hermabessiere et al., 2017). These chemical impacts are not exclusive to plastic fibres as natural microfibres can also contain similar additives (Remy et al., 2015; Obbard, 2018; Barrows et al., 2018). The leachates from different types of plastic have been studied to determine their toxicity under experimental conditions. Leachate from certain types of plastics (PVC, polyurethane and epoxy) have been shown to be toxic to the copepod Daphnia magna and the barnacle Amphibalanus amphitrite (Lithner et al., 2012; Li et al., 2016; Franzellitti et al., 2019). Additives to plastics such as bisphenol A, and phthalates, are known to be endocrine disrupters (Oehlmann et al., 2009; Vandermeersch et al., 2015; Franzellitti et al., 2019; Rochman et al., 2019). In addition, persistent organic pollutants, and trace metals can be absorbed and potentially transported by microplastics (Teuten et al., 2007; Teuten et al., 2009; Bakir et al., 2012; Rochman et al., 2014; Turner and Homes, 2015). These kinds of pollutants are absorbed onto the large hydrophobic surface area of microplastics (Teuten et al., 2007; Teuten et al., 2009), with the concentration of pollutants dependent on the type and age of the polymer (Müller et al., 2018; Wang and Wang, 2018; Zhang et al., 2018; Guo and Wang, 2019). In some cases, these chemicals have been shown to be up to six times higher in microfibres compared to ambient seawater (Mato et al., 2001; Taylor et al., 2016).

1.5. Microfibres in the environment

Microfibres have been found in a variety of environments (e.g., marine, freshwater, terrestrial, within densely populated and highly developed [urban] areas, and background natural environments [remote] with minimal anthropogenic infrastructure [undeveloped]) although the majority of studies have focused on marine systems (Wagner et al., 2014; Horton et al., 2017; Li et al., 2018). Marine studies have focused on surface waters (Thompson et al., 2004; Collignon et al., 2012; Lusher et al., 2014), beaches (Liebezeit and Dubaish, 2012; Stolte et al., 2015; Yu et al., 2016), and deep-sea sediments (Van Cauwenberghe et al., 2013; Woodall et al., 2014) across the globe from the Arctic (Obbard et al., 2014; Lusher et al., 2015) to Antarctica (Cincinelli et al., 2017; Munari et al., 2017).

Microfibres come from both ocean and land-based sources, with fishing activities, aquaculture and shipping estimated to contribute about 20% of total plastic debris observed in the marine environment and the remaining 80% coming from terrestrial sources (Andrady, 2011; GESAMP, 2016; Li et al., 2018). These terrestrial sources include landfills, agricultural application of sewage sludge and plastic mulch, domestic and industrial wastewater and manufacturing processes (Browne et al., 2011; Eerkes-Medrano et al., 2015; Huerta Lwanga et al., 2016; Mahon et al., 2016; Zhang et al., 2018; Corradini et al., 2019; Gatidou et al., 2019). Wastewater treatment effluent is considered one of the dominant sources of microfibre pollution into the freshwater environment as they are not targeted by current methodologies, so they are not

efficiently removed from treated water (Murphy et al., 2016; Estahbanati and Fahrenfeld, 2016; Li et al., 2018).

Although the majority of microfibres originate from the terrestrial environment, there are limited studies understanding the abundance, fate and ecological impacts (Horton et al., 2017; de Souze Machado et al., 2017). Similarly, microfibre pollution in freshwater environments reportedly represented < 4% of all studies (Lambert and Wagner, 2018; Li et al., 2018). Most of the studies on freshwater systems have focused on developed, densely populated areas, where there are higher abundances of microfibres (Cole et al., 2011; Free et al., 2014; Horton et al., 2017), with few studies on undeveloped, low densely populated areas (Free et al., 2014; Zhang et al., 2016). Recently several studies have assessed the atmospheric transport of microfibres (Dris et al., 2016; Cai et al., 2017; Stanton et al., 2019; Allen et al., 2019). These studies have focused predominately on urban centres, such as Paris, Nottingham, and Dongguan (Dris et al., 2015; Dris et al., 2016; Cai et al., 2017; Stanton et al., 2019); with only one study at a remote meteorological station in the Pyrenees mountains (Allen et al., 2019). As a result, the extent of transport via atmospheric deposition is not fully understood (Cai et al., 2017; Horton and Dixon, 2018).

1.6. Transboundary air pollution

Transboundary air pollution refers to pollutants, which are emitted into the atmosphere and can be carried long distances by the prevailing wind. This long-range transport,

carries air pollutants beyond their original boundaries, leading to impacts not just locally, but into environments far away (van Pul et al., 1998; Bull, 2003). Transboundary movement is not exclusive to anthropogenic pollutant emissions, as dust particles from the Saharan desert have been transported through prevailing winds to European countries like Great Britain and Ireland (Dall'Osto et al., 2010; Vieno et al., 2016). Areas that receive predominately clean air have been used as background or reference sites to determine the natural level of transboundary air pollutants. In order to reduce transboundary air pollutants, the United Nations Economic Commission for Europe (UNECE) established the Convention on Long-range Transboundary Air Pollution in 1979. This convention created legally binding principles for international cooperation to deal with air pollution problems and set up an institutional framework for research and policy. Since the Convention was created eight protocols regarding different air pollutants have been ratified by 34 different countries. Monitoring programs such as the European Monitoring and Evaluation Programme (precipitation chemistry) and the International Cooperative Programme on Assessment and Monitoring of Acidification of River and Lakes (water chemistry), have been created to further research and inform policy in order to comply with the principles and protocols created in the Convention on Long-range Transboundary Air Pollution.

Ireland is located on the western periphery of Europe and receives predominately unpolluted westerly winds from the Atlantic Ocean (Bowman, 1991). Due to its location limiting exposure to continental European anthropogenic air pollution, Ireland is

considered a background reference site for European transboundary air pollution (Biraud et al., 2000; Derwent, 2007). As a result, various anthropogenic air pollutants, such as mercury, carbon dioxide and ozone, have been monitored at the Mace Head Atmospheric Research Station on the west coast of Ireland (Biraud et al., 2000; Ebinghaus et al., 2002; Derwent et al., 2007). In addition, Ireland participates in the Convention on Long-range Transboundary Air Pollution, including the European Monitoring and Evaluation Programme, and International Cooperative Programme on Assessment and Monitoring Effects of Air Pollution on Rivers and Lakes.

1.7. Thesis objectives

The main objective of this thesis was to evaluate the level of anthropogenic microfibre contamination in background natural environments. To address this objective, the abundance and size of microfibres were measured in precipitation, moss, lake water and lake sediment from remote, undeveloped, and low populated areas in Ireland.

This thesis is written in manuscript style, and includes a general introduction (Chapter 1), two manuscript style chapters (Chapter 2 and 3) and a general conclusion (Chapter 4). Chapters 2 and 3 address the primary objective of the thesis. The methods are partially repeated across both chapters to facilitate stand-alone manuscripts.

Chapter 2, titled *Ambient atmospheric deposition of anthropogenic microfibres in Ireland*, quantified the abundance of microfibres in precipitation. Daily precipitation was

collected from wet-only and bulk collectors at four precipitation chemistry monitoring stations in collaboration with Met Éireann. The objectives of Chapter 2 were to estimate the deposition of microfibres and identify any relationships between meteorological variables and the amount of microfibres. Given that microfibres are ubiquitous in the environment, it was hypotheses that there would be no difference in the abundance and size of microfibres between the different stations. It was also hypothesized that rainfall and wind direction would be correlated with the amount of microfibres at each station.

Chapter 3, titled *Anthropogenic microfibres in headwater lake catchments in Ireland*, evaluated the abundance of microfibres in background headwater lake catchments.

Moss, lake water and lake sediment samples were collected from each catchment and analysed for microfibres. It was hypothesised that there would be no difference in microfibre abundance or length between moss, lake water and lake sediment samples collected at the three headwater lake catchments.

1.8. References

- Allen, S., Allen, D., Phoenix, V., Le Roux, G., Durántez Jiménez, P., Simonneau, A., Binet, S. and Galop, D. (2019). Atmospheric transport and deposition of microplastics in a remote mountain catchment. *Nature Geoscience*, 12(5), pp.339-344.
- Anderson, P., Warrack, S., Langen, V., Challis, J., Hanson, M. and Rennie, M. (2017).

 Microplastic contamination in Lake Winnipeg, Canada. *Environmental Pollution*, 225, pp.223-231.
- Andrady, A. (2011). Microplastics in the marine environment. *Marine Pollution Bulletin*, 62(8), pp.1596-1605.
- Andrady, A. (2017). The plastic in microplastics: A review. *Marine Pollution Bulletin*, 119(1), pp.12-22.
- Bakir, A., Rowland, S. and Thompson, R. (2012). Competitive sorption of persistent organic pollutants onto microplastics in the marine environment. *Marine Pollution Bulletin*, 64(12), pp.2782-2789.
- Baldwin, A., Corsi, S. and Mason, S. (2016). Plastic Debris in 29 Great Lakes Tributaries: Relations to Watershed Attributes and Hydrology. *Environmental Science & Technology*, 50(19), pp.10377-10385.
- Barboza, L. and Gimenez, B. (2015). Microplastics in the marine environment: Current trends and future perspectives. *Marine Pollution Bulletin*, 97(1-2), pp.5-12.
- Barletta, M., Lima, A. and Costa, M. (2019). Distribution, sources and consequences of nutrients, persistent organic pollutants, metals and microplastics in South American estuaries. *Science of The Total Environment*, 651, pp.1199-1218.
- Barrows, A.P., Cathey, S. and Peterson, C. (2018). Marine environment microfibre contamination: Global patterns and the diversity of microparticle origins. *Environmental Pollution*, 237, pp. 275-284.
- Belzagui, F., Crespi, M., Álvarez, A., Gutiérrez-Bouzán, C. and Vilaseca, M. (2019). Microplastics' emissions: Microfibers' detachment from textile garments. *Environmental Pollution*, 248, pp. 1028-1035.
- Biraud, S., Ciais, P., Ramonet, M., Simmonds, P., Kazan, V., Monfray, P., O'Doherty, S., Spain, T. and Jennings, S. (2000). European greenhouse gas emissions estimated from continuous atmospheric measurements and radon 222 at Mace Head, Ireland. *Journal of Geophysical Research: Atmospheres*, 105(D1), pp. 1351-1366.
- Blair, R., Waldron, S., Phoenix, V. and Gauchotte-Lindsay, C. (2019). Microscopy and elemental analysis characterisation of microplastics in sediment of a freshwater urban river in Scotland, UK. *Environmental Science and Pollution Research*, 26(12), pp. 12491-12504.
- Boucher, J. and Friot, D. (2017). Primary Microplastics in the Oceans: A Global Evaluation of Sources. Gland, Switzerland: IUCN, pp. 43.
- Bowman, J. (1991). Acid Sensitive Surface Waters in Ireland. Environmental Research Unit, Dublin, Ireland, pp. 32
- Browne, M., Crump, P., Niven, S., Teuten, E., Tonkin, A., Galloway, T. and Thompson, R. (2011). Accumulation of Microplastic on Shorelines Woldwide: Sources and Sinks. *Environmental Science & Technology*, 45(21), pp. 9175-9179.

- Bull, K. (2003) Protocol to the 1979 Convention on Long-Range Transboundary Air Pollution on Persistent Organic Pollutants: The 1998 Agreement for the UNECE Region. In: Fiedler H. (eds) Persistent Organic Pollutants. The Handbook of Environmental Chemistry (Vol. 3 Series: Anthropogenic Compounds), vol 3O. Springer, Berlin, Heidelberg
- Cai, L., Wang, J., Peng, J., Tan, Z., Zhan, Z., Tan, X. and Chen, Q. (2017). Characteristic of microplastics in the atmospheric fallout from Dongguan city, China: preliminary research and first evidence. *Environmental Scence andi Pollution Research*, 24(32), pp. 24928–24935.
- Carr, S. (2017). Sources and dispersive modes of micro-fibers in the environment. *Integrated Environmental Assessment and Management*, 13(3), pp. 466-469.
- Cincinelli, A., Scopetani, C., Chelazzi, D., Lombardini, E., Martellini, T., Katsoyiannis, A., Fossi, M. and Corsolini, S. (2017). Microplastic in the surface waters of the Ross Sea (Antarctica): Occurrence, distribution and characterization by FTIR. *Chemosphere*, 175, pp. 391-400.
- Cole, M., Lindeque, P., Halsband, C. and Galloway, T. (2011). Microplastics as contaminants in the marine environment: A review. *Marine Pollution Bulletin*, 62(12), pp. 2588-2597.
- Cole, M. (2016). A novel method for preparing microplastic fibres. *Scientific Reports*, 6(1).
- Collignon, A., Hecq, J., Glagani, F., Voisin, P., Collard, F. and Goffart, A. (2012). Neustonic microplastic and zooplankton in the North Western Mediterranean Sea. *Marine Pollution Bulletin*, 64(4), pp. 861-864.
- Corradini, F., Meza, P., Eguiluz, R., Casado, F., Huerta-Lwanga, E. and Geissen, V. (2019). Evidence of microplastic accumulation in agricultural soils from sewage sludge disposal. *Science of The Total Environment*, 671, pp. 411-420.
- Derwent, R., Simmonds, P., Manning, A. and Spain, T. (2007). Trends over a 20-year period from 1987 to 2007 in surface ozone at the atmospheric research station, Mace Head, Ireland. *Atmospheric Environment*, 41(39), pp. 9091–9098.
- de Souza Machado, A., Kloas, W., Zarfl, C., Hempel, S. and Rillig, M. (2017). Microplastics as an emerging threat to terrestrial ecosystems. *Global Change Biology*, 24(4), pp. 1405-1416.
- Dris, R., Gasperi, J., Rocher, V., Saad, M., Renault, N. and Tassin, B. (2015). Microplastic contamination in an urban area: a case study in Greater Paris. *Environmental Chemistry*, 12(5), pp. 592.
- Dris, R., Gasperi, J., Saad, M., Mirande, C. and Tassin, B. (2016). Synthetic fibres in atmospheric fallout: A source of microplastics in the environment?. *Marine Pollution Bulletin*. Elsevier Ltd, 104(1–2), pp. 290–293.
- Ebinghaus, R., Kock, H., Coggins, A., Spain, T., Jennings, S. and Temme, C. (2002). Longterm measurements of atmospheric mercury at Mace Head, Irish west coast, between 1995 and 2001. *Atmospheric Environment*, 36(34), pp. 5267-5276.

- Eerkes-Medrano, D., Thompson, R. and Aldridge, D. (2015). Microplastics in freshwater systems: A review of the emerging threats, identification of knowledge gaps and prioritisation of research needs. *Water Research*, 75, pp. 63-82.
- Eriksen, M., Mason, S., Wilson, S., Box, C., Zellers, A., Edwards, W., Farley, H. and Amato, S. (2013). Microplastic pollution in the surface waters of the Laurentian Great Lakes. *Marine Pollution Bulletin*, 77(1-2), pp. 177-182.
- Estahbanati, S. and Fahrenfeld, N. (2016). Influence of wastewater treatment plant discharges on microplastic concentrations in surface water. *Chemosphere*, 162, pp. 277-284.
- Fischer, E., Paglialonga, L., Czech, E. and Tamminga, M. (2016). Microplastic pollution in lakes and lake shoreline sediments A case study on Lake Bolsena and Lake Chiusi (central Italy). *Environmental Pollution*, 213, pp. 648-657.
- Foekema, E., De Gruijter, C., Mergia, M., van Franeker, J., Murk, A. and Koelmans, A. (2013). Plastic in North Sea Fish. *Environmental Science & Technology*, (47), pp. 8818-8824.
- Franzellitti, S., Canesi, L., Auguste, M., Wathsala, R. and Fabbri, E. (2019). Microplastic exposure and effects in aquatic organisms: A physiological perspective. *Environmental Toxicology and Pharmacology*, 68, pp. 37-51.
- Frias, J. and Nash, R. (2019). Microplastics: Finding a consensus on the definition. *Marine Pollution Bulletin*, 138, pp.145-147.
- Free, C., Jensen, O., Mason, S., Eriksen, M., Williamson, N. and Boldgiv, B. (2014). Highlevels of microplastic pollution in a large, remote, mountain lake. *Marine Pollution Bulletin*, 85(1), pp. 156-163.
- Gago, J., Carretero, O., Filgueiras, A. and Viñas, L. (2018). Synthetic microfibers in the marine environment: A review on their occurrence in seawater and sediments. *Marine Pollution Bulletin*, 127, pp. 365-376.
- Gatidou, G., Arvaniti, O. and Stasinakis, A. (2019). Review on the occurrence and fate of microplastics in Sewage Treatment Plants. *Journal of Hazardous Materials*, 367, pp. 504-512.
- GESAMP. (2016). Sources, fate and effects of microplastics in the marine environment: part two of a global assessment (eds Kershaw, P. J. & Rochman, C. M.). (IMO/FAO/UNESCO-IOC/UNIDO/WMO/IAEA/UN/UNEP/UNDP Joint Group of Experts on the Scientific Aspects of Marine Environmental Protection). *Rep. Stud. GESAMP*, 93, pp. 220.
- Guo, X. and Wang, J. (2019). The chemical behaviors of microplastics in marine environment: A review. *Marine Pollution Bulletin*, 142, pp. 1-14.
- Hermabessiere, L., Dehaut, A., Paul-Pont, I., Lacroix, C., Jezequel, R., Soudant, P. and Duflos, G. (2017). Occurrence and effects of plastic additives on marine environments and organisms: A review. *Chemosphere*, 182, pp. 781-793.
- Hidalgo-Ruz, V., Gutow, L., Thompson, R. C. and Thiel, M. (2012). Microplastics in the Marine Environment: A Review of the Methods Used for Identification and Quantification. *Environ. Sci. Technol.*, 46, pp. 3060–3075.
- Horton, A. A., Walton, A., Spurgeon, D. J., Lahive, E. and Svendsen, C. (2017).

 Microplastics in freshwater and terrestrial environments: Evaluating the current

- understanding to identify the knowledge gaps and future research priorities. *Science of the Total Environment*, 586, pp. 127–141.
- Horton, A. and Dixon, S. (2018). Microplastics: An introduction to environmental transport processes. *Wiley Interdisciplinary Reviews: Water*, 5(2), p.e1268.
- Huerta Lwanga, E., Gertsen, H., Gooren, H., Peters, P., Salánki, T., van der Ploeg, M., Besseling, E., Koelmans, A. and Geissen, V. (2016). Microplastics in the Terrestrial Ecosystem: Implications for Lumbricus terrestris (Oligochaeta, Lumbricidae). *Environmental Science & Technology*, 50(5), pp. 2685-2691.
- Ivar do Sul, J. and Costa, M. (2014). The present and future of microplastic pollution in the marine environment. *Environmental Pollution*, 185, pp. 352-364.
- Kosuth, M., Mason, S. and Wattenberg, E. (2018). Anthropogenic contamination of tap water, beer, and sea salt. *PLOS ONE*, 13(4), p.e0194970.
- Li, H., Getzinger, G., Ferguson, P., Orihuela, B., Zhu, M. and Rittschof, D. (2016). Effects of Toxic Leachate from Commercial Plastics on Larval Survival and Settlement of the Barnacle Amphibalanus amphitrite. *Environmental Science & Technology*, 50(2), pp. 924-931.
- Li, J., Liu, H. and Paul Chen, J. (2018). Microplastics in freshwater systems: A review on occurrence, environmental effects, and methods for microplastics detection. *Water Research*, 137, pp. 362-374.
- Li, L., Li, M., Deng, H., Cai, L., Cai, H., Yan, B., Hu, J. and Shi, H. (2018). A straightforward method for measuring the range of apparent density of microplastics. *Science of The Total Environment*, 639, pp. 367-373.
- Liebezeit, G. and Dubaish, F. (2012). Microplastics in Beaches of the East Frisian Islands Spiekeroog and Kachelotplate. *Bulletin of Environmental Contamination and Toxicology*, 89(1), pp. 213-217.
- Lithner, D., Nordensvan, I. and Dave, G. (2012). Comparative acute toxicity of leachates from plastic products made of polypropylene, polyethylene, PVC, acrylonitrile—butadiene—styrene, and epoxy to Daphnia magna. *Environmental Science and Pollution Research*, 19(5), pp. 1763-1772.
- Luo, W., Su, L., Craig, N., Du, F., Wu, C. and Shi, H. (2019). Comparison of microplastic pollution in different water bodies from urban creeks to coastal waters. *Environmental Pollution*, 246, pp. 174-182.
- Lusher, A., Burke, A., O'Connor, I. and Officer, R. (2014). Microplastic pollution in the Northeast Atlantic Ocean: Validated and opportunistic sampling. *Marine Pollution Bulletin*, 88(1-2), pp. 325-333.
- Lusher, A., Tirelli, V., O'Connor, I. and Officer, R. (2015). Microplastics in Arctic polar waters: the first reported values of particles in surface and sub-surface samples. *Scientific Reports*, 5(1).
- Mahon, A., O'Connell, B., Healy, M., O'Connor, I., Officer, R., Nash, R. and Morrison, L. (2016). Microplastics in Sewage Sludge: Effects of Treatment. *Environmental Science & Technology*, 51(2), pp. 810-818.
- Mathalon, A. and Hill, P. (2014). Microplastic fibers in the intertidal ecosystem surrounding Halifax Harbor, Nova Scotia. *Marine Pollution Bulletin*, 81(1), pp. 69-79.

- Mato, Y., Isobe, T., Takada, H., Kanehiro, H., Ohtake, C. and Kaminuma, T. (2001). Plastic Resin Pellets as a Transport Medium for Toxic Chemicals in the Marine Environment. *Environmental Science & Technology*, 35(2), pp. 318-324.
- Mishra, S., Rath, C. and Das, A. (2019). Marine microfiber pollution: A review on present status and future challenges. *Marine Pollution Bulletin*, 140, pp. 188-197.
- Moore, C. (2008). Synthetic polymers in the marine environment: A rapidly increasing, long-term threat. *Environmental Research*, 108(2), pp. 131-139.
- Müller, A., Becker, R., Dorgerloh, U., Simon, F. and Braun, U. (2018). The effect of polymer aging on the uptake of fuel aromatics and ethers by microplastics. *Environmental Pollution*, 240, pp. 639-646.
- Munari, C., Infantini, V., Scoponi, M., Rastelli, E., Corinaldesi, C. and Mistri, M. (2017). Microplastics in the sediments of Terra Nova Bay (Ross Sea, Antarctica). *Marine Pollution Bulletin*, 122(1-2), pp. 161-165.
- Murphy, F., Ewins, C., Carbonnier, F. and Quinn, B. (2016). Wastewater Treatment Works (WwTW) as a Source of Microplastics in the Aquatic Environment. *Environmental Science & Technology*, 50(11), pp. 5800-5808.
- Naidoo, T., Glassom, D. and Smit, A. (2015). Plastic pollution in five urban estuaries of KwaZulu-Natal, South Africa. *Marine Pollution Bulletin*, 101(1), pp. 473-480.
- Nel, H. and Froneman, P. (2015). A quantitative analysis of microplastic pollution along the south-eastern coastline of South Africa. *Marine Pollution Bulletin*, 101(1), pp. 274-279.
- Obbard, R., Sadri, S., Wong, Y., Khitun, A., Baker, I. and Thompson, R. (2014). Global warming releases microplastic legacy frozen in Arctic Sea ice. *Earth's Future*, 2(6), pp. 315-320.
- Obbard, R. (2018). Microplastics in Polar Regions: The role of long range transport. *Current Opinion in Environmental Science & Health*, 1, pp. 24-29.
- Oehlmann, J., Schulte-Oehlmann, U., Kloas, W., Jagnytsch, O., Lutz, I., Kusk, K., Wollenberger, L., Santos, E., Paull, G., Van Look, K. and Tyler, C. (2009). A critical analysis of the biological impacts of plasticizers on wildlife. *Philosophical Transactions of the Royal Society B: Biological Sciences*, 364(1526), pp. 2047-2062.
- Plastics Europe: Plastics the Facts 2016. (2016). An Analysis of European Latest Plastics Production, Demand and Waste Data. Plastics Europe: Association of Plastic Manufacturers, Brussels, p. 38
- Plastics Europe. 2018. Plastics—The facts 2017. (2017). An analysis of European plastics production, demand and waste data. Brussels, Belgium.
- Remy, F., Collard, F., Gilbert, B., Compère, P., Eppe, G. and Lepoint, G. (2015). When Microplastic Is Not Plastic: The Ingestion of Artificial Cellulose Fibers by Macrofauna Living in Seagrass Macrophytodetritus. *Environmental Science & Technology*, 49(18), pp. 11158-11166.
- Rillig, M. (2012). Microplastic in Terrestrial Ecosystems and the Soil?. *Environmental Science & Technology*, 46(12), pp. 6453-6454.

- Rios Mendoza, L. and Balcer, M. (2019). Microplastics in freshwater environments: A review of quantification assessment. *TrAC Trends in Analytical Chemistry*, 113, pp. 402-408.
- Rochman, C., Brookson, C., Bikker, J., Djuric, N., Earn, A., Bucci, K., Athey, S., Huntington, A., McIlwraith, H., Munno, K., De Frond, H., Kolomijeca, A., Erdle, L., Grbic, J., Bayoumi, M., Borrelle, S., Wu, T., Santoro, S., Werbowski, L., Zhu, X., Giles, R., Hamilton, B., Thaysen, C., Kaura, A., Klasios, N., Ead, L., Kim, J., Sherlock, C., Ho, A. and Hung, C. (2019). Rethinking microplastics as a diverse contaminant suite. *Environmental Toxicology and Chemistry*, 38(4), pp. 703-711.
- Rochman, C., Hentschel, B. and Teh, S. (2014). Long-Term Sorption of Metals Is Similar among Plastic Types: Implications for Plastic Debris in Aquatic Environments. *PLoS ONE*, 9(1), p.e85433.
- Ryan, P., Moore, C., van Franeker, J. and Moloney, C. (2009). Monitoring the abundance of plastic debris in the marine environment. *Philosophical Transactions of the Royal Society B: Biological Sciences*, 364(1526), pp. 1999-2012.
- Stanton, T., Johnson, M., Nathanail, P., MacNaughtan, W. and Gomes, R. (2019).

 Freshwater and airborne textile fibre populations are dominated by 'natural', not microplastic, fibres. *Science of The Total Environment*, 666, pp. 377-389.
- Stolte, A., Forster, S., Gerdts, G. and Schubert, H. (2015). Microplastic concentrations in beach sediments along the German Baltic coast. *Marine Pollution Bulletin*, 99(1-2), pp. 216-229.
- Su, L., Xue, Y., Li, L., Yang, D., Kolandhasamy, P., Li, D. and Shi, H. (2016). Microplastics in Taihu Lake, China. *Environmental Pollution*, 216, pp. 711-719.
- Taylor, M., Gwinnett, C., Robinson, L. and Woodall, L. (2016). Plastic microfibre ingestion by deep-sea organisms. *Scientific Reports*, 6(1).
- Teuten, E., Rowland, S., Galloway, T. and Thompson, R. (2007). Potential for Plastics to Transport Hydrophobic Contaminants. *Environmental Science & Technology*, 41(22), pp. 7759-7764.
- Teuten, E.L., Saquing, J.M., Knappe, D.R.U., Barlaz, M.A., Jonsson, S., BjÃrn, A., Rowland, S.J., Thompson, R.C., Galloway, T.S., Yamashita, R., Ochi, D., Watanuki, Y., Moore, C., Viet, P.H., Tana, T.S., Prudente, M., Boonyatumanond, R., Zakaria, M.P., Akkhavong, K., Ogata, Y., Hirai, H., Iwasa, S., Mizukawa, K., Hagino, Y., Imamura, A., Saha, M. and Takada, H. (2009). Transport and release of chemicals from plastics to the environment and to wildlife. *Philosophical Transactions of the Royal Society B: Biological Sciences*, 364, pp. 2027-2045.
- Thompson, R., Olsen, Y., Mitchell, R., Davis, A., Rowland, S., John, A., McGonigle, D. and Russell, A. (2004). Lost at Sea: Where Is All the Plastic?. *Science*, 304(5672), pp. 838-838.
- Thompson, R., Moore, C., vom Saal, F. and Swan, S. (2009). Plastics, the environment and human health: current consensus and future trends. *Philosophical Transactions of the Royal Society B: Biological Sciences*, 364(1526), pp. 2153-2166.
- Turner, A. and Holmes, L. (2015). Adsorption of trace metals by microplastic pellets in fresh water. *Environmental Chemistry*, 12(5), pp. 600.

- Van Cauwenberghe, L., Vanreusel, A., Mees, J. and Janssen, C. (2013). Microplastic pollution in deep-sea sediments. *Environmental Pollution*, 182, pp.495-499.
- Vandermeersch, G., Van Cauwenberghe, L., Janssen, C., Marques, A., Granby, K., Fait, G., Kotterman, M., Diogène, J., Bekaert, K., Robbens, J. and Devriese, L. (2015). A critical view on microplastic quantification in aquatic organisms. *Environmental Research*, 143, pp. 46-55.
- van Pul, W., de Leeuw, F., van Jaarsveld, J., van der Gaag, M. and Sliggers, C. (1998). The potential for long-range transboundary atmospheric transport. *Chemosphere*, 37(1), pp. 113-141.
- Wagner, M., Scherer, C., Alvarez-Muñoz, D., Brennholt, N., Bourrain, X., Buchinger, S., Fries, E., Grosbois, C., Klasmeier, J., Marti, T., Rodriguez-Mozaz, S., Urbatzka, R., Vethaak, A. D., Winther-Nielsen, M. and Reifferscheid, G. (2014). Microplastics in freshwater ecosystems: what we know and what we need to know. *Environ Sci Eur*, 26(12), pp. 1–9.
- Wang, J., Tan, Z., Peng, J., Qiu, Q. and Li, M. (2016). The behaviors of microplastics in the marine environment. *Marine Environmental Research*, 113, pp. 7-17.
- Wang, T., Zou, X., Li, B., Yao, Y., Zang, Z., Li, Y., Yu, W. and Wang, W. (2019). Preliminary study of the source apportionment and diversity of microplastics: Taking floating microplastics in the South China Sea as an example. *Environmental Pollution*, 245, pp. 965-974.
- Wang, W., Ndungu, A., Li, Z. and Wang, J. (2017). Microplastics pollution in inland freshwaters of China: A case study in urban surface waters of Wuhan, China. *Science of The Total Environment*, 575, pp. 1369-1374.
- Wang, W. and Wang, J. (2018). Different partition of polycyclic aromatic hydrocarbon on environmental particulates in freshwater: Microplastics in comparison to natural sediment. *Ecotoxicology and Environmental Safety*, 147, pp. 648-655.
- Watts, A., Urbina, M., Corr, S., Lewis, C. and Galloway, T. (2015). Ingestion of Plastic Microfibers by the Crab Carcinus maenas and Its Effect on Food Consumption and Energy Balance. *Environmental Science & Technology*, 49(24), pp. 14597-14604.
- Woodall, L., Sanchez-Vidal, A., Canals, M., Paterson, G., Coppock, R., Sleight, V., Calafat, A., Rogers, A., Narayanaswamy, B. and Thompson, R. (2014). The deep sea is a major sink for microplastic debris. *Royal Society Open Science*, 1(4), pp. 140317-140317.
- Yang, D., Shi, H., Li, L., Li, J., Jabeen, K. and Kolandhasamy, P. (2015). Microplastic Pollution in Table Salts from China. *Environmental Science & Technology*, 49(22), pp. 13622-13627.
- Yao, P., Zhou, B., Lu, Y., Yin, Y., Zong, Y., Chen, M. and O'Donnell, Z. (2019). A review of microplastics in sediments: Spatial and temporal occurrences, biological effects, and analytic methods. *Quaternary International*.
- Yu, X., Peng, J., Wang, J., Wang, K. and Bao, S. (2016). Occurrence of microplastics in the beach sand of the Chinese inner sea: the Bohai Sea. *Environmental Pollution*, 214, pp. 722-730.

- Yuan, W., Liu, X., Wang, W., Di, M. and Wang, J. (2019). Microplastic abundance, distribution and composition in water, sediments, and wild fish from Poyang Lake, China. *Ecotoxicology and Environmental Safety*, 170, pp. 180-187.
- Zhang, S., Yang, X., Gertsen, H., Peters, P., Salánki, T. and Geissen, V. (2018). A simple method for the extraction and identification of light density microplastics from soil. *Science of The Total Environment*, 616-617, pp. 1056-1065.
- Zhang, X., Zheng, M., Wang, L., Lou, Y., Shi, L. and Jiang, S. (2018). Sorption of three synthetic musks by microplastics. *Marine Pollution Bulletin*, 126, pp. 606-609.
- Zhang, K., Su, J., Xiong, X., Wu, X., Wu, C. and Liu, J. (2016). Microplastic pollution of lakeshore sediments from remote lakes in Tibet plateau, China. *Environmental Pollution*, 219, pp. 450-455.
- Zhao, S., Zhu, L., Wang, T. and Li, D. (2014). Suspended microplastics in the surface water of the Yangtze Estuary System, China: First observations on occurrence, distribution. *Marine Pollution Bulletin*, 86(1-2), pp. 562-568.

2.1. Abstract

Microfibres (mf), which are threadlike particles < 5 mm, are the most common type of microplastic in the environment. Few studies have focused on their abundance in atmospheric deposition in background natural environments. Rainfall was collected from four precipitation chemistry monitoring stations, representing wet-only and bulk deposition, from June 2017-May 2018; all stations were isolated from densely populated and industrial centres. Mf were observed in all precipitation samples; the annual average deposition of mf across the four precipitation monitoring stations was estimated to be ~28,800 mf m⁻². The annual average wet-only deposition of mf across three wet-only collectors was 26,300 mf m⁻². Meteorological variables were correlated with the abundance of microfibres in atmospheric deposition. Raman spectroscopic analysis verified that mf observed in rainfall were anthropogenic in origin as polyester and synthetic pigments were identified.

2.2. Introduction

Microplastics are waste plastics particles, smaller than 5 mm, which come from larger plastic objects (e.g., bottles, bags, clothing, etc.) that have broken down and fragmented through biodegradation, UV radiation and physical abrasion or are manufactured to be microscopic in size (Hidalgo-Ruz et al., 2012; Dris et al., 2015; Dris et al., 2016; Horton et al., 2017a; Peng et al., 2017). The most common type of microplastic reported in

environmental samples are microfibres, which enter the environment from textiles, nets, fishing line, and the fragmentation of other plastic material (Cole, 2016; Barrows, Cathey and Peterson, 2018; Cago et al., 2018). In 2016, nine million tons of fibres were produced globally with 40% being made from natural materials such as cotton, wool, or silk, the rest were made from plastic (Carr, 2017). The most common types of plastics used in microfibres are polypropylene, polystyrene, polyethylene (PE), nylon (or polyamide), and polyethylene terephthalate (PET) (PlasticsEurope, 2016; Gago et al., 2018). These represent some of the most common plastics found in the environment (Andrady, 2011). Microfibres have received international attention as an emerging and ubiquitous contaminant in the environment (Cole et al., 2011; Zhao et al., 2014). They are considered an environmental contaminant due to their chemical additives (e.g., dyes, plasticizers, fillers, flame retardants and stabilizers) and risk of physical harm (blockage, abrasion) to organisms when ingested (Cole et al., 2011; Zhao et al., 2014; Wagner et al., 2014). In addition, persistent organic pollutants, and trace elements can be absorbed and potentially transported by microfibres (Hidalgo-Ruz et al., 2012; Zhang et al., 2016; Horton et al., 2017a).

Numerous studies have focused on aquatic systems, and primarily on the marine environment (Hidalgo-Ruz et al., 2012; Wagner et al., 2014; Horton et al., 2017a). However, recent studies have observed that microfibres can also be transported through the atmosphere into terrestrial and aquatic environments (Liebezeit and Dubaish, 2012; Zhang et al., 2016; Peng et al., 2017; Anderson et al., 2017). However,

there has been limited research on the atmospheric deposition of microfibres, with the exception of studies in Paris, the Pyrenes mountains, Dongguan, and Nottingham (Dris et al., 2016; Cai et al., 2017; Stanton et al., 2019; Allen et al., 2019). Furthermore, the majority of these studies have focused only on collecting bulk deposition from densely populated, largely developed, urban (anthropogenic infrastructure) centres (Dris et al., 2016, Cai et al., 2017; Stanton et al., 2019); as such, the extent of transport via atmospheric deposition is not fully understood (Cai et al., 2017; Horton and Dixon, 2018). This is especially true for locations in remote regions, that have low populations and little anthropogenic infrastructure (undeveloped).

The objective of this study was to estimate the atmospheric deposition of anthropogenic microfibres in precipitation from remote regions and to identify any relationships between meteorological variables and the amount of microfibres.

Precipitation was collected from four precipitation chemistry monitoring stations in Ireland from June 2017 to May 2018. All monitoring stations were away from highly developed, densely populated, and industrial centres. Given that all sites are located in 'background' regions, it was hypothesised that there would not be a significant difference in the magnitude and size of microfibres between the four monitoring stations.

2.3. Materials and methods

2.3.1. Study sites

Ireland is situated on the western periphery of Europe and predominantly receives unpolluted air masses from the Atlantic Ocean (Derwent, 2007); as such, it is generally considered a background region for European transboundary air pollution (Derwent, 2007). In the current study, rainfall samples were collected from four precipitation chemistry monitoring stations, Oak Park (OP), Johnstown Castle (JC), Valentia (VA) and Malin Head (MH) (Figure 2.1). The four stations are part of the European Monitoring and Evaluation Programme, under the United Nations Economic Commission for Europe's Convention on Long-range Transboundary Air Pollution, which monitors long term chemical trends in air pollutants in background locations to support future air pollution protocols and policies. All monitoring stations were located away from point source influences of anthropogenic activity (see Figure A2.1). The closest residential area to the stations ranged from 1 to 3.1 km, with the closest town (pop. >10,000) ranging from 3.1 to 52 km (CSO, 2016; NISRA, 2013; see Table A2.1). Three of the monitoring stations (JC, VA, and MH) were located along the coast (< 10 km; Figure 2.1). During the study period (June 2017-May 2018), annual rainfall ranged from 840 mm (OP) to 1557 mm (VA) (Table 2.1). Daily rainfall samples were sent to the Met Éireann laboratories for chemical analysis and subsequently bulked by calendar month per station to a maximum of 2 L. The stations at OP, JC and VA had wet-only precipitation collectors whereas MH had a bulk collector (Table 2.1), which was continuously open (i.e., it collected wet deposition and a fraction of dry deposition).

Table 2.1. Latitude, longitude, elevation (EL) and annual rainfall (P) during the period of June 2017–May 2018 (source: Met Éireann www.met.ie), for the four meteorological monitoring stations in the current study.

Monitoring Station	Precipitation	Latitude	Longitude	EL	Р
	collector			(m)	(mm yr ⁻¹)
Oak Park	Wet-only	52.86120	-6.91495	61	840.2
Johnstown Castle	Wet-only	52.29766	-6.49677	49	1059.9
Valentia	Wet-only	51.93829	-10.24099	24	1557.4
Malin Head	Bulk	55.37175	-7.33945	23	1107.0



Figure 2.1. Location of the four precipitation chemistry monitoring stations in the current study. All stations are part of the European Monitoring and Evaluation Programme under the United Nations Economic Commission for Europe.

2.3.2. Microfibre extractions

All monthly samples were vacuum filtered onto glass-fibre papers (Fisherbrand™ G6 [09-804-42A]: 1.6 µm) and dyed with 1 mL of Rose Bengal (4,5,6,7-tetrachloro-2',4',5',7'-tetracodofluorescein, 200 mg L⁻¹) to help visually distinguish synthetic material from bioorganic matter following Liebezeit & Liebezeit (2014), i.e., the non-stained material was

assumed to be plastic. The dyed filter papers were transferred to petri dishes for storage and for assessment of microfibres.

2.3.3. Microscopy and microfibre identification

The filter papers were analysed for the presence of microfibres using a stereomicroscope (Leica EZ4W with EZ4W0170 camera), following a modified visual identification method from Norén (2007) and Windsor et al. (2018). Identification of microfibres following standardized criteria coordinated with strict examination can reduce the possibility of misidentification (Norén, 2007). Visual analyses for particles > 0.5 mm have been demonstrated to be suitable for identification (Löder and Gerdts, 2015). The five visual criteria were: (i) the fibre is unnaturally coloured (blue, red, green, purple, black, grey, white) compared to the majority of other particles / detritus; (ii) the fibre appears homogenous in material and texture with no visible cell structure or offshoots and is a consistent width throughout its entire length; (iii) the fibre remains intact and is not brittle when compressed, tugged or poked with fine tweezers; (iv) the fibre has a shiny or glossy appearance; and (v) there is limited fraying with no similarities to natural fibres (see Table A2.2). It is recommended that at least two of the criteria be met for a fibre to be classified as a microplastics (Windsor et al., 2018). Previous studies have classified all fibres not stained by Rose Bengal as microplastic (Liebezeit et al., 2014), while others have chosen to use the more general term 'anthropogenic debris' (Kosuth et al., 2018). In the current study microfibres that met at least two of the criteria, and were not stained by Rose Bengal, were considered anthropogenic. These

anthropogenic microfibres were photographed and then measured using the open source Image processing software ImageJ. Each microfibre was manually measured using a scale bar to convert the number of pixels measured to a known length.

2.3.4. Raman spectroscopy

In order to test the accuracy of the visual identification method, 48 fibres were randomly selected from each station and analysed using Raman spectroscopy (Renishaw inVia, operated by WiRE). Raman spectroscopy measurements were carried out using 5× 25× and 50× objectives and a 633 nm laser with adjustable laser power (ranging from 0.00001% to 100%). Due to fluorescence issues, lower laser power and longer accumulations were used to improve the raman signal. Raman spectra were recorded in the wavenumber range of 3,500–150 cm⁻¹. The spectrum of each fibre was identified using a commercial library (KnowltAll, Bio-Rad®).

2.3.5. Quality control

Contamination is a concern when dealing with microfibres (Wesch et al., 2017).

Throughout the sample processing and analysis, procedural open-air blanks were used to determine the amount of potential contamination; open-air blanks were exposed during filtering and inspection. Triplicate B-pure™ water blanks (1 L) were initially vacuum filtered and analysed following the same method as the rainfall samples to determine the level of microfibre contamination; the average number of microfibres was ~11 mf L⁻¹. As such, all B-pure™ water was filtered (Fisherbrand G6: 1.6 µm) prior to

use for cleaning and extraction (use in Rose Bengal) to avoid potential contamination.

Further, tin foil was used to cover samples during microfibre extractions (filtering) to prevent airborne contamination and all equipment was rinsed with filtered B-pure™. In total there were 22 blanks, which were analysed for contamination following the same methods as the rainfall samples. Finally, 100% cotton lab coats and nitrile gloves were worn when working with the samples.

2.3.6. Data analysis

Deposition (n m⁻²) was estimated using the number of microfibres from the monthly rainfall samples (mf L⁻¹), and the total rainfall volume (mm) from the corresponding month, at each meteorological station (see Equation below; NADP, 2019).

Deposition ($n m^{-2}$) = Concentration ($n L^{-1}$) x Precipitation (m m)

As noted above, bulk collectors measure wet deposition and a fraction of dry deposition, which depending on the pollutant can range from 20–40% (Cape et al., 2009). In order to estimate the fraction of dry deposition collected by bulk deposition in the current study, the average monthly deposition from the three wet-only collectors was subtracted from the monthly bulk deposition at MH. The long-term atmospheric source regions for each site were evaluated using source-receptor trajectory rose plots (arrival height of 850 hPa) based on two-day back trajectories estimated every six hours during the period 1989–2009 (see Figure A2.3). Monthly median values for length of microfibres were used in place of averages due to the data being skewed to smaller fibres. Microfibre lengths were categorized in size groupings similar to Dris et al., (2016;

i.e., a 200 µm size range). The coefficient of variation (or relative standard deviation) was used to assess the variation at each station throughout the 12 months. Monthly microfibre counts were tested for normality using Shapiro-Wilk's test in SPSS (IBM Corp., 2015). Repeated measures ANOVA were conducted in SPSS to determine if there was a significant difference between the monthly median fibre length, count and estimated deposition between each of the stations. Post Hoc Bonferroni tests, conducted using SPSS, were used to further evaluate any significant differences; Bonferroni corrections were used to account for multiple comparisons. The correlation between monthly meteorological and precipitation chemistry (sulphate and nitrogen as markers of anthropogenic pollution), and microfibre counts was evaluated using Person's Product-Moment Coefficient in SPSS (IMB Corp., 2015). In addition, the relationship between monthly meteorological variables and monthly microfibre counts was analysed using multiple linear regressions in Microsoft® Excel; the predicator (meteorological) variables were transformed into principal component in R Studio (R Core Team, 2013) prior to regression to remove collinearity. The loadings from the component that were significant predictors in the regression analysis, were used to determine what meteorological variables influenced the abundance of mf. Only statistical results that were found to be significant are described in the results.

2.4. Results

The potential contamination was approximately 0.31 mf L⁻¹ across all stations, i.e., less than 2 mf per sample. Due to the low potential contamination, samples were not blank

corrected. All rainfall samples contained microfibres; in total 1655 mf were observed in samples from the four sites, ranging from 349 mf at VA to 477 mf at MH (see Table A2.3). The annual average across all stations was 23.2 mf L⁻¹ (Table 2.2); this ranged monthly from 16-55 mf L^{-1} at OP, 11-39 mf L^{-1} JC, 8-28 mf L^{-1} VA, and 11-53 mf L^{-1} MH (Figure 2.2; see Table A2.3). The monthly average microfibre counts ranged from 16 (4%) in May to 52 (~13%) in July across the four stations, with the highest monthly microfibre count being 75 (18.4%) in April at JC (Figure 2.3; see Table A2.3). The monthly average microfibre counts were similar in summer (Jun, Jul, Aug) 40 mf (~10%) and autumn (Sept, Oct, Nov) 38 mf (~9%), compared to winter (Dec, Jan, Feb) 30 mf (~7%) and spring (Mar, Apr, May) 30 mf (~7%) (Figure 2.3). The monthly mf L⁻¹ were significantly lower at VA compared to OP and MH (p <0.05), whereas all other stations where not significantly different (p >0.05). The coefficient of variation for the number of microfibres per month was >30% in all stations with the highest being 53% (OP) (Table 2.2). The variation may suggest that the abundance of microfibres is correlated with the amount of rainfall, as they have similar variation (Table 2.2).

Table 2.2. Annual sample volume (Vol), rainfall amount, total microfibres (mf), microfibres per litre (coefficient of variation in parentheses), estimated mf deposition (mf m⁻²), total and median fibre length (mm) and fibre length deposition (m m⁻²) for each precipitation chemistry monitoring station from June 2017–May 2018.

Site	Vol	Rainfall	Total	mf	mf	Median	Total	Length
			mf		deposition	length	Length	Deposition
	(L)	(mm)	(count)	(n L ⁻¹)	(n m ⁻²)	(mm)	(mm)	(m m ⁻²)
OP	15.1	839 (36)	422	28 (53)	23,526 (40)	0.93 (121)	557	25.4
JC	18.2	1158 (45)	407	22 (44)	25,919 (46)	0.89 (108)	508.5	29.1
VA	21.7	1832 (31)	349	16 (30)	29,410 (28)	0.98 (128)	541.3	30.0
MH	16.3	1271 (45)	477	29 (51)	37,217 (52)	0.73 (105)	496.4	50.9
Average	17.8	1275	414	23.2	29,018	0.87*	525.8	33.9

^{*}Median value

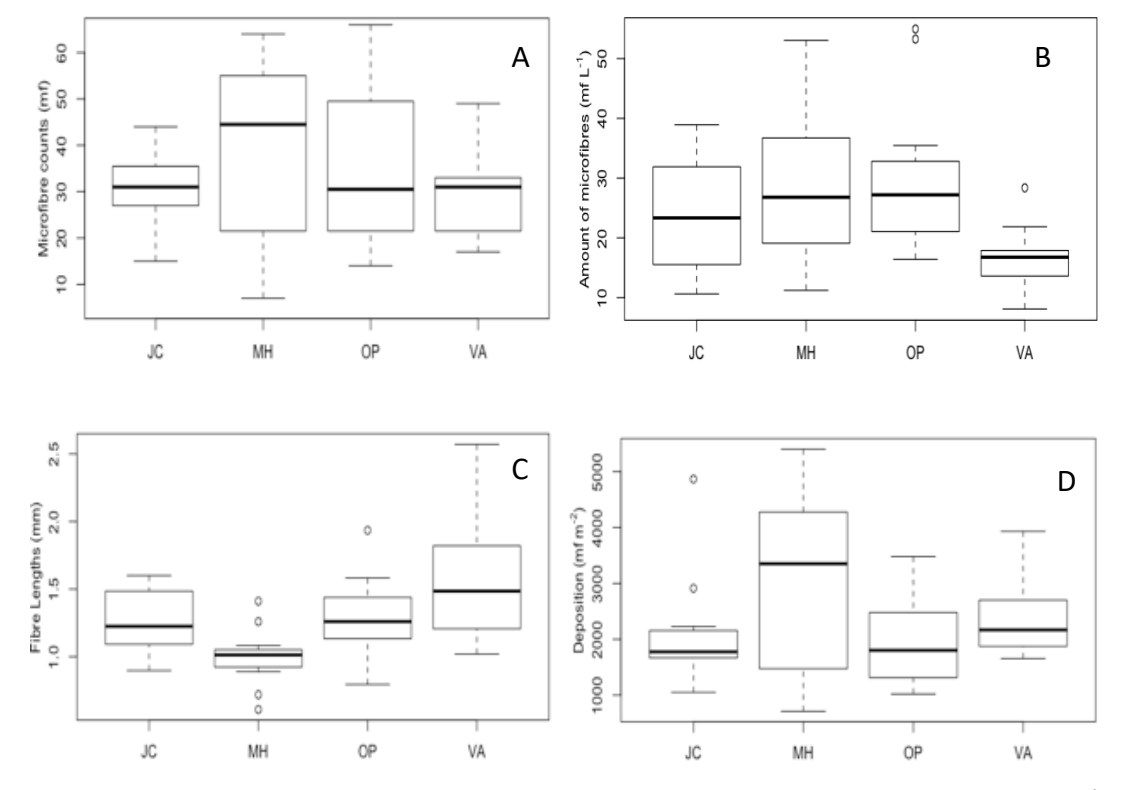


Figure 2.2A-2.2D. A) The monthly microfibre counts, B) microfibres per litre (mf L⁻¹), C) average microfibre length (mm) and D) estimated microfibre deposition (mf m⁻²) observed in rainfall collected from the four precipitation chemistry stations, Oak Park (OP), Johnstown Castle (JC), Valentia (VA), and Malin Head (MH) during June 2017–May 2018. The black line indicates the median, the box represents the first and third quartiles, the whiskers represent the smallest and largest observations that fall within a distance of 1.5 times the box size and the dots represent values that are outside the 1.5 times distance.

Monthly microfibre counts at MH were found to have a significant positive correlation with relative humidity (r = 0.72, p < 0.01), wind direction (r = 0.65, p < 0.05) and wind speed (r = 0.60, p < 0.05) (see Table A2.4). Monthly microfibre counts at OP were found to have a significant negative correlation with mean sea level pressure (r = -0.61, p < 0.05) (see Table A2.3). Further analysis using multilinear regressions showed that two PCAs loaded with meteorological variables (i.e., rain, wind speed, wind direction, pressure and relative humidity) were able to predict monthly microfibre counts at OP ($r^2 = 0.71$), VA ($r^2 = 0.56$) and MH ($r^2 = 0.73$) (see Tables A2.5A–E).

The length of the microfibres ranged from 0.04 mm to 19.75 mm with the largest at each station being 19.28 mm (OP), 11.50 mm (JC), 19.75 mm (VA), 11.39 mm (MH) (Figure 2.2 Panel C). The median microfibre size was 0.87 mm; with the median at each station being 0.93 mm (OP), 0.89 mm (JC), 0.98 mm (VA), and 0.73 mm (MH) (Table 2.2; Figure 2.2 Panel C). Smaller microfibres (e.g., in the 200-400 μ m and 400-600 μ m size ranges) were more predominant (58% < 1 mm) in rainfall compared to microfibres in the larger size ranges (7.5% > 3 mm) (see Figure A2.2). The coefficient of variation for the fibre lengths at each station was over 100% with a range of 105% (MH) to 128% (VA).

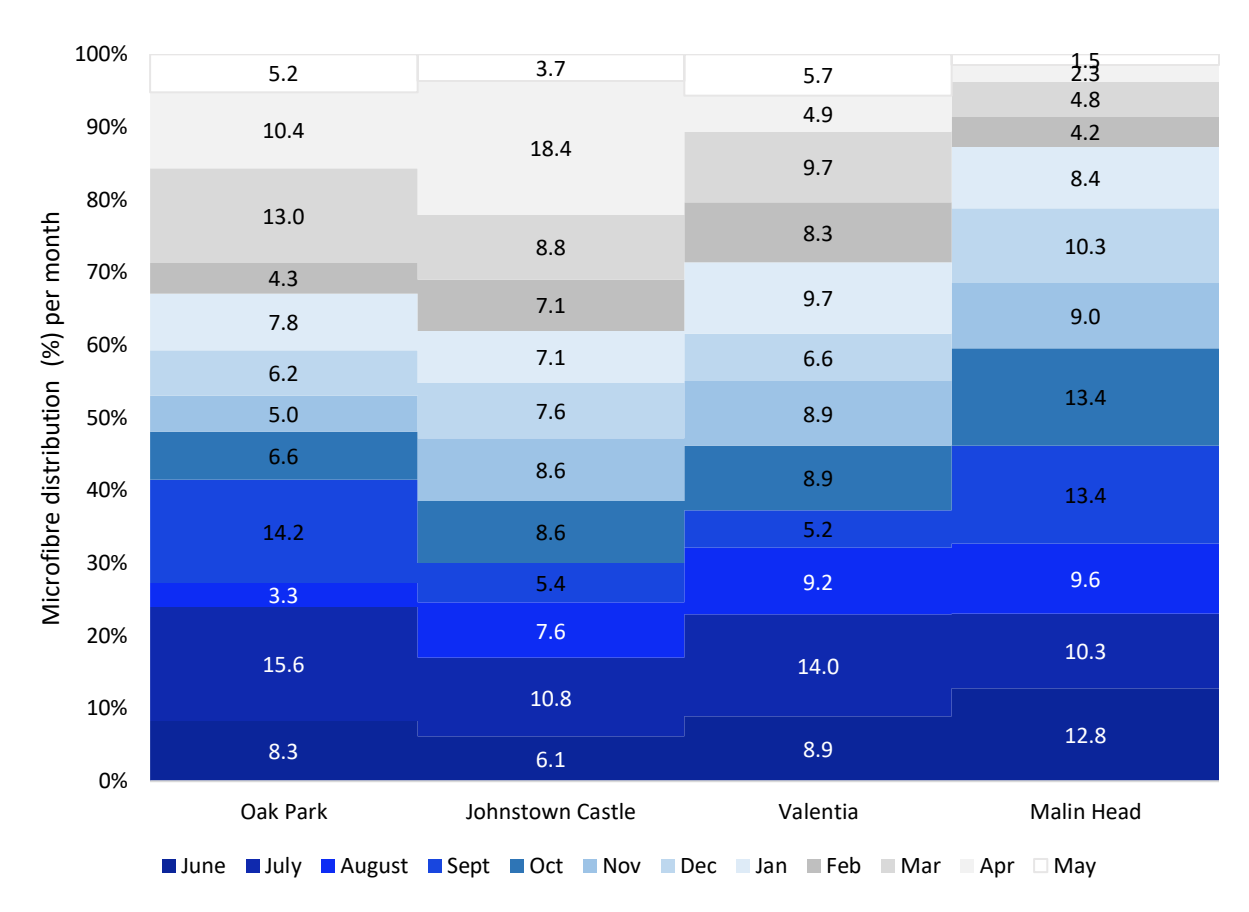


Figure 2.3. Monthly microfibre count as a percentage of the total number of microfibres at the four precipitation chemistry stations from June 2017–May 2018.

The average annual deposition of microfibres was estimated to be 28,769 mf m $^{-2}$ (length: 33.8 m m $^{-2}$) (Table 2.2). MH had the highest deposition (36,224 mf m $^{-2}$; length: 50.9 m m $^{-2}$), followed by VA (29,410 mf m $^{-2}$; length: 30.0 m m $^{-2}$), JC (25,919 mf m $^{-2}$; length: 29.1 m m $^{-2}$) and OP (23,526 mf m $^{-2}$; length: 25.4 m m $^{-2}$). The annual average wet deposition (wet-only stations) of microfibres was 26,285 mf m $^{-2}$ (length: 28.2 m m $^{-2}$). The average monthly deposition across the three wet-only collectors was 2,132 mf, compared to the bulk deposition collector which had a monthly average of 3,066 mf. The monthly average dry deposition in bulk collectors was estimated to be 943 mf which is ~30% of the monthly average deposition from MH.

The trajectory source receptor plots indicate the primary wind direction into the four precipitation monitoring stations is from the west indicating the dominant air source region to the stations is marine (~80%) (see Figure A2.3). However, the dominant terrestrial source of air and wind direction into each of the stations is different (see Figure A2.3). OP and JC receive the largest frequencies of terrestrial sourced air (<7%) from the west, VA receives dominant terrestrial air (<5%) from the north east, and MH receives terrestrial air from the south (<5%).

In total, 48 microfibres, 12 from each meteorological station, were analysed using Raman spectroscopy (Renishaw inVia). In total 31 of the tested fibres produced low signal to noise ratios that could be analysed through the Bio Rad-KnowItAll® library. The rest had spectra that were unidentifiable, due to high signal to noise ratios. The 31 different microfibres analysed were matched with six different synthetic materials. The two most common matches were with synthetic pigments indigo and Eriochrome blue. (see Figure A2.4). The other four synthetic materials were pigments; Levafix blue E-GRN, Drimarene turquoise x-2g and Mortoperm blue and Polyester film 2000 series (see Figure A2.4).

2.5. Discussion

Microfibres were observed in all rainfall samples collected from the precipitation chemistry monitoring stations. The monthly microfibre distribution across the four

stations suggests that the abundance of microfibres is higher in the summer and fall months, and lower in the winter and spring months (Figure 2.3). The driest time of year in Ireland is during the spring months, with higher amounts of rain throughout the rest of the year. The station with the highest amount of rainfall (VA), also had the highest wet deposition of microfibres (29,410 mf m⁻²), suggesting a relationship between rainfall and microfibre abundance (Table 2.2). The coefficients of variation in rainfall and microfibre deposition are similar suggesting that the variation in microfibres may be correlated to the variation of rainfall (Table 2.2). The only station that had a significant difference in the monthly abundance of microfibres was VA. On average the monthly abundance of microfibres at the wet-only collectors was 70% lower than at the bulk deposition collector, suggesting that there is a difference in the abundance depending on the type of collector. The annual microfibre abundance was found to be 1.2 to 1.5 times larger (range: 6,800-12,700 mf m⁻²) at the bulk deposition station compared to the wet-only collectors. This difference is estimated to be the annual fraction of dry deposition of microfibres collected by the bulk collector (~10,900 mf m⁻²). Previous studies used bulk collectors, which could include approximately 20-50% dry deposition (Dris et al., 2016; Cai et al., 2017; Stanton et al., 2019; Allen et al., 2019). The current study is the first such study to quantify wet deposition of microfibres, which had an annual average deposition of 26,285 mf m⁻² across three wet-only monitoring stations.

The annual average deposition (all stations) of microfibres observed in the current study (28,769 mf m $^{-2}$ [n=4]) was comparable to previous studies; Paris (~30,000 mf m $^{-2}$ [n=2]),

France, Dongguan city (~72,000 mf m⁻² [n=3]; estimated from three months), China, Nottingham (~27,000 mf m⁻² [n=4]), England, and the Pyrenees mountains (~16,000 mf m⁻² [n=1]; estimated from five months), France (Dris et al., 2016, Cai et al., 2017; Stanton et al., 2019; Allen et al., 2019). The European sites (Paris, Nottingham, Pyrenees mountains and the current study) have similar annual average microfibre abundances. This is further supported when looking at the range across sites in each study, with the highest abundances of microfibres (~47,000 mf m⁻² from Nottingham; ~40,000 mf m⁻² from Paris, and ~37,000 mf m⁻² from MH) and lowest abundances of microfibres (~19,000 mf m⁻² from Nottingham; ~19,000 mf m⁻² from Paris; ~16,000 mf m⁻² from Pyrenees mountains and ~23,000 mf m⁻² from the current study) in each of these studies. In general, there is a similar abundance of microfibres in atmospheric deposition between the four European studies despite being located in urban centres (Nottingham and Paris) or remote areas (the current study and Pyrenees mountains). The only difference between these studies is the proportion of the abundance that are confirmed to be plastic which ranges from 2% to 29% (Dris et al., 2016; Cai et al., 2017; Stanton et al., 2019). This suggests that the deposition of microfibres seen in the current study may be representative of ambient air abundances.

OP and MH were the only stations that had significant correlations between singular meteorological variables and the abundance of microfibres. Nonetheless, multiple linear regression analyses determined that PCA's loaded with meteorological variables (i.e., significant components were dominated by rain, wind speed, wind direction, mean sea

level pressure and relative humidity) were able to predict the amount of microfibres at OP, VA and MH (see Figures A2.5A–E and Tables A2.5A–E). Regression equations indicated that the abundance of microfibres at; OP increased with increasing rain and decreasing relative humidity and mean sea level pressure; VA increased with decreasing rain and increasing wind speed and wind direction; MH increased with increasing rain and wind speed (see Figure A2.5A–E). The varying importance of different variables between stations potentially reflects the relationship between meteorological variables and source air masses with higher mf abundance. The results from this study are similar to previous studies that found that meteorological variables were significantly correlated with the amount of microfibres observed in deposition (Allen et al., 2019; Liu et al., 2019).

Fibre lengths were predominantly in the ranges 0.2-0.4 mm (15%) and 0.4-0.6 mm (12%) (see Figure A2.2). In comparison, the study by Dris had a larger proportion of microfibres in the 0.2-0.4 mm (~17%) and 0.4-0.6 mm (~23%) size ranges. Fibre lengths in the range of 0.2-0.8 mm were observed (38%), which was comparable to previous studies by Dris et al. (2016), Cai et al. (2017) and Allen et al. (2019) which have ~40%, 30% and 47%. Although the current study had a smaller proportion of fibres in the lower size ranges compared with previous studies, there is still a similar distribution pattern between all studies (i.e., fibres are skewed towards the smaller size ranges) (Dris et al., 2016; Cai et al., 2017; Allen et al., 2019). This similar particle size distribution pattern supports that smaller fibres, or fragments from larger fibres, are more likely to be transported through

the atmosphere. Dris et al. (2016) and Cai et al. (2017) had the largest proportion of fibre lengths (~40-47%) observed to be <0.6-0.7 mm. The current study had a comparable proportion with fibres predominately < 0.8 mm (48%) (see Figure A2.2). The median length of bulk deposition (0.73 mm) in the current study was smaller than wet-only deposition (0.91 mm), which may be attributed to the fraction of dry deposition it receives.

The Raman spectroscopic analysis provided verification of synthetic pigments on microfibres and identified the types of pigment. The predominant pigment found in rainfall samples was Eriochrome blue, followed by Indigo, Levafix blue E-GRN, Drimarene turquoise x-2g and Mortoperm blue. All of the aforementioned dyes / pigments are used in the textile industry most commonly used with cotton and wool, and sometimes silk, nylon, and polyester. However, the presence of these pigments does not confirm whether the underlying fibres are natural (cotton or wool) or plastic (PE, PET, nylon, etc.), it does support that the fibres come from anthropogenic sources. Nonetheless, there was verification of plastic, as polyester film was identified. The high signal to noise ratio in the Raman spectra can be caused by dyes, pigments and biofouling (microorganisms that grow on the surface of the microfibres) as the signal can be either diluted by fluorescence (Fredericks, 2012; Araujo et al., 2018; Barrows et al., 2018) or completely blocked (Fredericks, 2012; Lenz et al., 2015). This required lowering the laser power, to reduce the fluorescence, which in turn increased the difficulty of acquiring spectra with adequate signal to noise to permit unambiguous

spectral interpretation (Zhao et al., 2017; Prata et al., 2019). This type of interference has been observed in previous studies, as dyes incorporated into polymers can override the polymer spectrum (Zhao et al., 2017; Horton et al., 2017b; Karami et al., 2017). Particles that have been identified with strong spectra of pigments have previously been inferred to be polymers and classified them as such (Van Cauwenberghe et al 2013; Horton et al., 2017b).

2.6. Conclusion

This study reported the presence of anthropogenic microfibres in rainfall collected from four precipitation chemistry monitoring stations in Ireland. Microfibres were determined to be anthropogenic in origin through visual identification methods supported by Raman spectral analysis. The average annual atmospheric deposition was approximately 28,800 mf m⁻² from June 2017-May 2018. This is also the first such study to characterise wet-only deposition, which had an annual average of approximately 26,300 mf m⁻². The abundance at the study sites may be more representative of ambient air, due to their similarity to previous European studies. Meteorological variables such as rain, wind speed, wind direction, mean sea level pressure, and relative humidity were able to predict the amount of microfibres in deposition.

2.7. References

- Anderson, P., Warrack, S., Langen, V., Challis, J., Hanson, M. and Rennie, M. (2017).

 Microplastic contamination in Lake Winnipeg, Canada. *Environmental Pollution*, 225, pp.223-231.
- Andrady, A. (2011). Microplastics in the marine environment. *Marine Pollution Bulletin*, 62(8), pp.1596-1605.
- Araujo, C., Nolasco, M., Ribeiro, A. and Ribeiro-Claro, P. (2018). Identification of microplastics using Raman spectroscopy: Latest developments and future prospects. *Water Research*, 142, pp.426-440.
- Barrows, A.P., Cathey, S. and Peterson, C. (2018). Marine environment microfibre contamination: Global patterns and the diversity of microparticle origins. *Environmental Pollution*, 237, pp. 275-284.
- Cago, J., Carretero, O., Filgueiras, A., Vinas, L. (2018). Synthetic microfibres in the marine environment: A review on their occurrence in seawater and sediments. *Marine Pollution Bulletin*, 127, pp. 365-376.
- Cai, L., Wang, J., Peng, J., Tan, Z., Zhan, Z., Tan, X. and Chen, Q. (2017). Characteristic of microplastics in the atmospheric fallout from Dongguan city, China: preliminary research and first evidence. *Environmental Scence andi Pollution Research*, 24(32), pp. 24928–24935. doi: 10.1007/s11356-017-0116-x.
- Cape, J., van Dijk, N. and Tang, Y. (2009). Measurement of dry deposition to bulk precipitation collectors using a novel flushing sampler. *J. Environ. Monit.*, 11(2), pp.353-358.
- Carr, S. (2017). Sources and dispersive modes of micro-fibers in the environment. *Integrated Environmental Assessment and Management*, 13(3), pp.466-469.
- Central Statistics Office (CSO). (2016). Census 2016. Central Statistics Office.
- Cole, M. (2016). A novel method for preparing microplastic fibres. *Scientific Reports*, 6(1).
- Cole, M., Lindeque, P., Halsband, C. and Galloway, T. S. (2011). Microplastics as contaminants in the marine environment: A review. *Marine Pollution Bulletin*, 62, pp. 2588–2597. doi: 10.1016/j.marpolbul.2011.09.025.
- Dris, R., Gasperi, J., Rocher, V., Saad, M., Renault, N. and Tassin, B. (2015). Microplastic contamination in an urban area: a case study in Greater Paris. *Environ. Chem.*, p. A-H. doi: 10.1071/EN14167.
- Dris, R., Gasperi, J., Saad, M., Mirande, C. and Tassin, B. (2016). Synthetic fibres in atmospheric fallout: A source of microplastics in the environment?. *Marine Pollution Bulletin*. Elsevier Ltd, 104(1–2), pp. 290–293. doi: 10.1016/j.marpolbul.2016.01.006.
- Derwent, R., Simmonds, P., Manning, A. and Spain, T. (2007). Trends over a 20-year period from 1987 to 2007 in surface ozone at the atmospheric research station, Mace Head, Ireland. *Atmospheric Environment*, 41(39), pp.9091–9098.
- Fredericks, P. (2012). Forensic analysis of fibres by vibrational spectroscopy. In: J. Chalmers, H. Edwards and M. Hargreaves, ed., *Infrared and Raman Spectroscopy*

- in Forensic Science. John Wiley & Sons.
- Hidalgo-Ruz, V., Gutow, L., Thompson, R. C. and Thiel, M. (2012). Microplastics in the Marine Environment: A Review of the Methods Used for Identification and Quantification. *Environ. Sci. Technol.*, 46, pp. 3060–3075. doi: 10.1021/es2031505.
- Horton, A. A., Walton, A., Spurgeon, D. J., Lahive, E. and Svendsen, C. (2017a).

 Microplastics in freshwater and terrestrial environments: Evaluating the current understanding to identify the knowledge gaps and future research priorities.

 Science of the Total Environment, 586, pp. 127–141. doi: 10.1016/j.scitotenv.2017.01.190.
- Horton, A., Svendsen, C., Williams, R., Spurgeon, D. and Lahive, E. (2017b). Large microplastic particles in sediments of tributaries of the River Thames, UK Abundance, sources and methods for effective quantification. *Marine Pollution Bulletin*, 114(1), pp.218-226.
- IMB Corp. Released 2015. IBM SPSS Statistics for Windows, Version 23.0. Armonk, NY: IBM Corp.
- Karami, A., Golieskardi, A., Ho, Y., Larat, V. and Salamatinia, B. (2017). Microplastics in eviscerated flesh and excised organs of dried fish. *Scientific Reports*, 7(1).
- Lenz, R., Enders, K., Stedmon, C., Mackenzie, D. and Nielsen, T. (2015). A critical assessment of visual identification of marine microplastic using Raman spectroscopy for analysis improvement. *Marine Pollution Bulletin*, 100(1), pp.82-91.
- Liebezeit, G. and Dubaish, F. (2012). Microplastics in Beaches of the East Frisian Islands Spiekeroog and Kachelotplate. *Bulletin of Environmental Contamination and Toxicology*, 89(1), pp.213-217.
- Liebezeit, G. and Liebezeit, E. (2014). Synthetic particles as contaminants in German beers. *Food Additives & Contaminants: Part A*, 31, pp. 1574-1578.
- Mishra, S., Rath, C. and Das, A. (2019). Marine microfiber pollution: A review on present status and future challenges. *Marine Pollution Bulletin*, 140, pp.188-197.
- National Atmospheric Deposition Program (NADP). (2019). Concentration vs. Deposition. Educational Resources. *National Atmospheric Deposition Program*.
- Northern Ireland Statistics and Research Agency (NISRA). (2011). Census 2011
 Population tables. Table P2: Usually resident population by single year of age and sex. Northern Ireland Statistics and Research Agency. pp. 28-29.
- Plastics Europe: Plastics the Facts 2016. (2016). An Analysis of European Latest Plastics Production, Demand and Waste Data. Plastics Europe: Association of Plastic Manufacturers, Brussels, p. 38
- R Core Team. (2013). R: A language and environment for statistical computing. R Foundation for Statistical Computing, Vienna, Austria.
- Stanton, T., Johnson, M., Nathanail, P., MacNaughtan, W. and Gomes, R. (2019).

 Freshwater and airborne textile fibre populations are dominated by 'natural', not microplastic, fibres. *Science of The Total Environment*, 666, pp.377-389.
- Peng, J., Wang, J. and Cai, L. (2017). Current Understanding of Microplastics in the Environment: Occurrence, Fate, Risks, and What We Should Do. *Integrated*

- Environmental Assessment and Management, 13(4), pp. 476–482.
- Prata, J., da Costa, J., Duarte, A. and Rocha-Santos, T. (2019). Methods for sampling and detection of microplastics in water and sediment: A critical review. *TrAC Trends in Analytical Chemistry*, 110, pp.150-159.
- Van Cauwenberghe, L., Vanreusel, A., Mees, J. and Janssen, C. (2013). Microplastic pollution in deep-sea sediments. *Environmental Pollution*, 182, pp.495-499.
- Wagner, M., Scherer, C., Alvarez-Muñoz, D., Brennholt, N., Bourrain, X., Buchinger, S., Fries, E., Grosbois, C., Klasmeier, J., Marti, T., Rodriguez-Mozaz, S., Urbatzka, R., Vethaak, A. D., Winther-Nielsen, M. and Reifferscheid, G. (2014). Microplastics in freshwater ecosystems: what we know and what we need to know. *Environ Sci Eur*, 26(12), pp. 1–9. doi: 10.1186/s12302-014-0012-7.
- Zhang, K., Su, J., Xiong, X., Wu, X., Wu, C. and Liu, J. (2016). Microplastic pollution of lakeshore sediments from remote lakes in Tibet plateau, China. *Environmental Pollution*, (219), pp. 450–455. doi: 10.1016/j.envpol.2016.05.048.
- Zhao, S., Zhu, L., Wang, T. and Li, D. (2014). Suspended microplastics in the surface water of the Yangtze Estuary System, China: First observations on occurrence, distribution. *Marine Pollution Bulletin*, 86, pp. 562–568. doi: 10.1016/j.marpolbul.2014.06.032.
- Zhao, S., Danley, M., Ward, J., Li, D. and Mincer, T. (2017). An approach for extraction, characterization and quantitation of microplastic in natural marine snow using Raman microscopy. *Analytical Methods*, 9(9), pp.1470-1478.

2.8. Appendix



Figure A2.1. Example image of area surrounding long term precipitation chemistry monitoring stations (Malin Head station depicted).

Table A2.1. The closest residential (distance away in parenthesis) and urban centres (pop. >10,000; distance away in parenthesis), with their respective populations, to each of the four precipitation chemistry stations.

Station	Nearest residential	Population	Nearest urban	Population
	area (km)		centre (km)	
Oak Park	Carlow (3.1)	24,272	Carlow (3.1)	24,272
Johnstown Castle	Murrin (2.4)	<500	Wexford (4.9)	20,188
Valentia	Cahersiveen (1.0)	1,168	Killarney (52)	14,504
Malin Head	Ballygorman (1.1)	<500	Derry (42)	107,877

Table A2.2. List of criteria used to visually identify plastic microfibres following: (A) four criteria taken from Norén (2007) as cited by Hidalgo-Ruz (2010) and Löder and Gerdts (2015), and (B) eight criteria taken from Windsor et al. (2018), with a recommendation that a positive response for at least two of the eight criteria is required for identification of microplastic particles.

	Source: Löder and Gerdts (2015) and Hidalgo-Ruz (2010) following Norén (2007)
1	No (cellular) structures of organic origin should be visible in the plastic particle or
	fibre.
2	Fibres should be equally thick throughout their entire length and have a three-
	dimensional bending to exclude a biological origin.
3	Particles should be clear and homogeneously coloured.
4	Transparent or whitish particles must be examined under high magnification and
	with the help of fluorescence microscopy to exclude a biological origin.
В	Source: Windsor et al. (2018) following Löder and Gerdts (2015)
1	Unnaturally coloured compared to the majority of other particles/detritus in the
	sample, e.g., red, bright blue and yellow.
2	Appears homogenous in material or texture, e.g., no cell structure.
3	Unnatural shape or structure, e.g. perfectly spherical, smooth or sharp edges.
4	Fibres that remain intact with a firm tug or poke with fine tweezers.
5	Shiny or glassy in appearance.
6	Flexible and can be compressed without being brittle.
7	Share similar surface characteristics to reference plastic material.

Table A2.3. Monthly sample volume, rainfall (P), microfibre count (mf), median, average and total fibre length, mf L^{-1} , and estimated mf deposition (mf m^{-2}).

OP Jul 1.201 52.7 66 0.6 1.2 78.94 55.0 289 OP Aug 0.853 62.3 14 0.94 1.23 17.29 16.4 102 OP Sept 2.058 91.3 60 0.93 1.02 60.98 29.2 266 OP Oct 0.928 62.9 28 1.21 1.29 36.15 30.2 188 OP Dec 1.473 84.2 26 1.25 1.57 40.92 17.7 148 OP Jan 1.96 108.1 33 1.04 1.58 52.21 16.8 182 OP Jan 1.96 108.1 33 1.04 1.58 52.21 16.8 182 OP Jan 1.87 1.8 0.64 0.80 14.31 30.0 116 OP Apr 1.8 1.3 44 1.02 1.30 57.3 <	Site	Month	Vol (L)	P (mm)	mf	Median (mm)	Average (mm)	Total (mm)	mf L ⁻¹	mf m ⁻²
OP Aug 0.853 62.3 14 0.94 1.23 17.29 16.4 102 OP Sept 2.058 91.3 60 0.93 1.02 60.98 29.2 266 OP Oct 0.928 62.9 28 1.21 1.29 36.15 30.2 129 OP Nov 0.832 52.8 21 1.02 1.30 27.29 25.2 133 OP Jan 1.96 108.1 33 1.04 1.58 52.21 16.8 182 OP Jan 1.96 108.1 33 1.04 1.58 52.21 16.8 182 OP Mar 1.551 98.1 55 0.87 193 106.4 35.5 347 OP Mar 1.537 44 1.02 1.30 57.36 24.4 178 OP Mar 1.537 60.2 44 1.06 1.00 1.01	OP	Jun	1.388	91	35	0.78	1.19	41.5	25.2	2295
OP Aug 0.853 62.3 14 0.94 1.23 17.29 16.4 102 OP Sept 2.058 91.3 60 0.93 1.02 60.98 29.2 266 OP Oct 0.928 62.9 28 1.21 1.29 36.15 30.2 129 OP Nov 0.832 52.8 21 1.02 1.30 27.29 25.2 133 OP Jan 1.96 108.1 33 1.04 1.58 55.2.1 16.8 182 OP Jan 1.96 108.1 33 1.04 1.58 55.2.1 16.8 182 OP Mar 1.551 98.1 55 0.87 193 106.4 35.5 347 OP Apr 1.8 73 44 1.02 1.30 57.36 24.4 178 OP Mar 1.517 53.3 129 1.33 1.52	OP	Jul	1.201	52.7	66	0.6	1.2	78.94	55.0	2896
OP Sept 2.058 91.3 60 0.93 1.02 60.98 29.2 266 OP Oct 0.928 62.9 28 1.21 1.29 36.15 30.2 189 OP Nov 0.832 52.8 21 1.02 1.30 27.29 25.2 133 OP Dec 1.473 84.2 26 1.25 1.57 40.92 1.77 148 OP Jan 1.96 108.1 33 1.04 1.58 52.21 16.8 182 OP Mar 1.551 98.1 55 0.87 1.93 106.4 35.5 347 OP Mar 1.88 73 44 1.02 1.30 57.36 24.4 178 OP May 0.413 24.3 22 0.84 1.08 23.7 53.3 129 IC Jun 1.81 124.8 25 1.43 1.60	OP	Aug	0.853	62.3		0.94	1.23	17.29	16.4	1023
OP Nov 0.832 52.8 21 1.02 1.30 27.29 25.2 133 OP Dec 1.473 84.2 26 1.25 1.57 40.92 17.7 148 OP Ian 1.96 108.1 33 1.04 1.58 52.21 16.8 182 OP Mar 1.551 98.1 55 0.87 1.93 106.4 35.5 347 OP May 0.413 24.3 22 0.84 1.08 23.7 53.3 129 IC Jun 1.8 124.8 25 1.43 1.60 40.02 13.9 173 IC Jul 1.537 60.2 44 0.69 1.02 44.73 28.6 172 IC Aug 1.281 75.2 31 0.92 1.13 35.15 24.2 182 IC Aug 1.281 1.50 0.5 1.57 1.21	OP	_	2.058	91.3	60	0.93	1.02	60.98	29.2	2662
OP Dec 1.473 84.2 26 1.25 1.57 40.92 17.7 148 OP Jan 1.96 108.1 33 1.04 1.58 52.21 116.8 182 OP Feb 0.6 38.7 18 0.64 0.80 14.31 30.0 116 OP Mar 1.551 98.1 55 0.87 1.93 106.4 35.5 347 OP Apr 1.8 73 44 1.02 1.30 57.36 22.4 178 JC Jun 1.8 124.8 25 1.43 1.60 40.02 13.9 173 JC Jul 1.537 60.2 44 0.69 1.02 44.73 28.6 172 JC Aug 1.281 75.2 31 0.92 1.13 35.15 24.2 182 JC Aug 1.281 75.2 31 0.92 1.13 <td< td=""><td>OP</td><td>Oct</td><td>0.928</td><td>62.9</td><td>28</td><td>1.21</td><td>1.29</td><td>36.15</td><td>30.2</td><td>1898</td></td<>	OP	Oct	0.928	62.9	28	1.21	1.29	36.15	30.2	1898
OP Dec 1.473 84.2 26 1.25 1.57 40.92 17.7 148 OP Jan 1.96 108.1 33 1.04 1.58 52.21 116.8 182 OP Feb 0.6 38.7 18 0.64 0.80 14.31 30.0 116 OP Mar 1.551 98.1 55 0.87 1.93 106.4 35.5 347 OP Apr 1.8 73 44 1.02 1.30 57.36 22.4 178 JC Jun 1.8 124.8 25 1.43 1.60 40.02 13.9 173 JC Jul 1.537 60.2 44 0.69 1.02 44.73 22.6 172 JC Aug 1.281 75.2 31 0.92 1.13 35.15 24.2 182 JC Aug 1.281 75.2 31 0.92 1.13 <td< td=""><td>OP</td><td>Nov</td><td>0.832</td><td>52.8</td><td>21</td><td>1.02</td><td>1.30</td><td>27.29</td><td>25.2</td><td>1333</td></td<>	OP	Nov	0.832	52.8	21	1.02	1.30	27.29	25.2	1333
OP Jan 1.96 108.1 33 1.04 1.58 52.21 16.8 182 OP Feb 0.6 38.7 18 0.64 0.80 14.31 30.0 116 OP Mar 1.551 98.1 55 0.87 1.93 106.4 35.5 347 OP Apr 1.8 73 44 1.02 1.30 57.36 24.4 178 OP May 0.413 22.3 22 0.84 1.08 23.7 53.3 129 JC Jul 1.537 60.2 44 0.69 1.02 44.73 28.6 172 JC Aug 1.281 75.2 31 0.92 1.13 35.15 24.2 182 JC Aug 1.281 75.2 31 0.99 1.975 10.6 170.6 JC Oct 1.089 64.8 35 1.15 1.50 52.57 <	OP	Dec	1.473			1.25	1.57	40.92	17.7	1486
OP Feb 0.6 38.7 18 0.64 0.80 14.31 30.0 116 OP Mar 1.551 98.1 55 0.87 1.93 106.4 35.5 347 OP Apr 1.8 73 44 1.02 1.30 57.36 24.4 178 OP May 0.413 24.3 22 0.84 1.08 23.7 53.3 129 IC Jul 1.537 60.2 44 0.69 1.02 44.73 28.6 172 IC Aug 1.281 75.2 31 0.92 1.13 35.15 24.2 182 IC Aug 1.281 75.2 31 0.92 1.13 35.15 24.2 182 IC Aug 1.281 75.2 31 0.92 1.13 35.15 24.2 182 IC Or0 1.089 64.8 35 1.15 1.50	OP	Jan	1.96	108.1		1.04	1.58	52.21	16.8	1820
OP May 1.8 73 44 1.02 1.30 57.36 24.4 178 OP May 0.413 24.3 22 0.84 1.08 23.7 53.3 129 JC Jun 1.8 124.8 25 1.43 1.60 40.02 13.9 173 JC Jul 1.537 60.2 44 0.69 1.02 44.73 28.6 172 JC Aug 1.281 75.2 31 0.92 1.13 35.15 24.2 182 JC Oct 1.089 64.8 35 1.15 1.50 52.57 32.1 208 JC Nov 1.557 72.4 35 0.59 1.05 36.77 22.5 162 JC Nov 1.557 72.4 35 0.59 1.05 36.77 22.5 162 JC Dec 1.497 107.6 31 1.15 1.53 47.58 20.7		Feb								1161
OP Apr 1.8 73 44 1.02 1.30 57.36 24.4 178 OP May 0.413 24.3 22 0.84 1.08 23.7 53.3 129 JC Jun 1.8 124.8 25 1.43 1.60 40.02 13.9 173 JC Jul 1.537 60.2 44 0.69 1.02 44.73 28.6 172 JC Aug 1.281 75.2 31 0.92 1.13 35.15 24.2 182 JC Aug 1.281 75.2 31 0.92 1.13 35.15 24.2 182 JC Oct 1.089 64.8 35 1.15 1.50 52.57 32.1 208 JC Nov 1.557 72.4 35 0.59 1.05 36.77 22.5 162 JC Dec 1.497 107.6 31 1.15 1.53 47.58 20.7	OP	Mar	1.551	98.1	55	0.87	1.93	106.4	35.5	3479
OP May 0.413 24.3 22 0.84 1.08 23.7 53.3 129 JC Jun 1.8 124.8 25 1.43 1.60 40.02 13.9 173 JC Jul 1.537 60.2 44 0.69 1.02 44.73 28.6 172 JC Aug 1.281 75.2 31 0.92 1.13 35.15 24.2 182 JC Aug 1.281 75.2 31 0.92 1.13 35.15 24.2 182 JC Nov 1.557 72.4 35 0.59 1.05 36.77 22.5 162 JC Nov 1.557 72.4 35 0.59 1.05 36.77 22.5 162 JC Dec 1.497 107.6 31 1.15 1.53 47.58 20.7 222 JC Jan 2.09 109.8 29 0.87 1.47	OP	Apr	1.8	73	44	1.02	1.30	57.36	24.4	1784
JC Jul 1.537 60.2 44 0.69 1.02 44.73 28.6 172 JC Aug 1.281 75.2 31 0.92 1.13 35.15 24.2 182 JC Sept 2.073 160.8 22 0.61 0.90 19.75 10.6 170 JC Oct 1.089 64.8 35 1.15 1.50 52.57 32.1 208 JC Nov 1.557 72.4 35 0.59 1.05 36.77 22.5 162 JC Dec 1.497 107.6 31 1.15 1.53 47.58 20.7 222 JC Jan 2.09 109.8 29 0.087 1.47 42.54 13.9 152 JC Mar 2.099 169.8 36 0.78 1.26 45.26 17.2 291 JC Mar 1.927 125 75 0.8 1.20	OP	=	0.413	24.3	22	0.84	1.08	23.7	53.3	1294
JC Jul 1.537 60.2 44 0.69 1.02 44.73 28.6 172 JC Aug 1.281 75.2 31 0.92 1.13 35.15 24.2 182 JC Sept 2.073 160.8 22 0.61 0.90 19.75 10.6 170 JC Oct 1.089 64.8 35 1.15 1.50 52.57 32.1 208 JC Nov 1.557 72.4 35 0.59 1.05 36.77 22.5 162 JC Dec 1.497 107.6 31 1.15 1.53 47.58 20.7 222 JC Jan 2.09 109.8 29 0.087 1.47 42.54 13.9 152 JC Mar 2.099 169.8 36 0.78 1.26 45.26 17.2 291 JC Mar 1.927 125 75 0.8 1.20	JC	Jun	1.8	124.8	25	1.43	1.60	40.02	13.9	1733
JC Aug 1.281 75.2 31 0.92 1.13 35.15 24.2 182 JC Sept 2.073 160.8 22 0.61 0.90 19.75 10.6 170 JC Oct 1.089 64.8 35 1.15 1.50 52.57 32.1 208 JC Nov 1.557 72.4 35 0.59 1.05 36.77 22.5 162 JC Dec 1.497 107.6 31 1.15 1.53 47.58 20.7 22.2 JC Jan 2.09 109.8 29 0.87 1.47 42.54 13.9 152 JC Mar 2.099 169.8 36 0.78 1.26 45.26 17.2 291 JC Mar 1.9297 125 75 0.8 1.20 90.29 38.9 486 JC Mar 1.929 18.8 17.2 291 JA JUL 1.7261 31										1723
JC Sept 2.073 160.8 22 0.61 0.90 19.75 10.6 170 JC Oct 1.089 64.8 35 1.15 1.50 52.57 32.1 208 JC Nov 1.557 72.4 35 0.59 1.05 36.77 22.5 162 JC Dec 1.497 107.6 31 1.15 1.53 47.58 20.7 222 JC Jan 2.09 109.8 29 0.87 1.47 42.54 13.9 152 JC Feb 0.76 54.3 29 1.05 1.25 36.20 38.2 207 JC Mar 2.099 169.8 36 0.78 1.26 45.26 17.2 291 JC Mar 0.474 33.2 15 0.82 1.17 17.61 31.6 105 VA Jul 1.727 108.4 49 0.67 1.13										1820
JC Oct 1.089 64.8 35 1.15 1.50 52.57 32.1 208 JC Nov 1.557 72.4 35 0.59 1.05 36.77 22.5 162 JC Dec 1.497 107.6 31 1.15 1.53 47.58 20.7 222 JC Jan 2.09 109.8 29 0.87 1.47 42.54 13.9 152 JC Feb 0.76 54.3 29 1.05 1.25 36.20 38.2 207 JC Mar 2.099 169.8 36 0.78 1.26 45.26 17.2 291 JC Apr 1.927 125 75 0.8 1.20 90.29 38.9 486 JC May 0.474 33.2 15 0.82 1.17 17.61 31.6 105 VA Jul 1.727 108.4 49 0.67 1.13		_								1707
JC Nov 1.557 72.4 35 0.59 1.05 36.77 22.5 162 JC Dec 1.497 107.6 31 1.15 1.53 47.58 20.7 222 JC Jan 2.09 109.8 29 0.87 1.47 42.54 13.9 152 JC Feb 0.76 54.3 29 1.05 1.25 36.20 38.2 207 JC Mar 2.099 169.8 36 0.78 1.26 45.26 17.2 291 JC Mar 1.927 125 75 0.8 1.20 90.29 38.9 486 JC May 0.474 33.2 15 0.82 1.17 17.61 31.6 105 VA Jul 1.727 108.4 49 0.67 1.13 55.15 28.4 307 VA Aug 1.904 102.8 32 0.92 1.18		-								2083
JC Dec 1.497 107.6 31 1.15 1.53 47.58 20.7 222 JC Jan 2.09 109.8 29 0.87 1.47 42.54 13.9 152 JC Feb 0.76 54.3 29 1.05 1.25 36.20 38.2 207 JC Mar 2.099 169.8 36 0.78 1.26 45.26 17.2 291 JC Apr 1.927 125 75 0.8 1.20 90.29 38.9 486 JC May 0.474 33.2 15 0.82 1.17 17.61 31.6 105 VA Jul 1.727 108.4 49 0.67 1.13 55.15 28.4 307 VA Aug 1.904 102.8 32 0.92 1.18 37.89 16.8 172 VA Sept 2.034 204.4 18 0.7 1.50										1627
JC Jan 2.09 109.8 29 0.87 1.47 42.54 13.9 152 JC Feb 0.76 54.3 29 1.05 1.25 36.20 38.2 207 JC Mar 2.099 169.8 36 0.78 1.26 45.26 17.2 291 JC Apr 1.927 125 75 0.8 1.20 90.29 38.9 486 JC May 0.474 33.2 15 0.82 1.17 17.61 31.6 105 VA Jun 1.854 141.5 31 1.22 1.36 42.31 16.7 236 VA Jul 1.727 108.4 49 0.67 1.13 55.15 28.4 307 VA Aug 1.904 102.8 32 0.92 1.18 37.89 16.8 172 VA Sept 2.034 204.4 18 0.7 1.50	JC	Dec		107.6				47.58		2228
JC Feb 0.76 54.3 29 1.05 1.25 36.20 38.2 207. JC Mar 2.099 169.8 36 0.78 1.26 45.26 17.2 291. JC Apr 1.927 125 75 0.8 1.20 90.29 38.9 486 JC May 0.474 33.2 15 0.82 1.17 17.61 31.6 105 VA Jul 1.854 141.5 31 1.22 1.36 42.31 16.7 236 VA Jul 1.727 108.4 49 0.67 1.13 55.15 28.4 307 VA Aug 1.904 102.8 32 0.92 1.18 37.89 16.8 172 VA Sept 2.034 204.4 18 0.7 1.50 27.06 8.8 180 VA Oct 1.975 162.2 31 1.21 2.03										1524
JC Mar 2.099 169.8 36 0.78 1.26 45.26 17.2 291. JC Apr 1.927 125 75 0.8 1.20 90.29 38.9 486. JC May 0.474 33.2 15 0.82 1.17 17.61 31.6 105 VA Jun 1.854 141.5 31 1.22 1.36 42.31 16.7 236 VA Jul 1.727 108.4 49 0.67 1.13 55.15 28.4 307 VA Aug 1.904 102.8 32 0.92 1.18 37.89 16.8 172 VA Sept 2.034 204.4 18 0.7 1.50 27.06 8.8 180 VA Oct 1.975 162.2 31 1.21 2.03 63.08 15.7 254 VA Nov 1.717 107.4 31 1.2 1.47										2072
JC Apr 1.927 125 75 0.8 1.20 90.29 38.9 486. JC May 0.474 33.2 15 0.82 1.17 17.61 31.6 105 VA Jun 1.854 141.5 31 1.22 1.36 42.31 16.7 236 VA Jul 1.727 108.4 49 0.67 1.13 55.15 28.4 307 VA Aug 1.904 102.8 32 0.92 1.18 37.89 16.8 172 VA Sept 2.034 204.4 18 0.7 1.50 27.06 8.8 180 VA Oct 1.975 162.2 31 1.21 2.03 63.08 15.7 254 VA Nov 1.717 107.4 31 1.2 1.47 45.48 18.1 193 VA Dec 1.997 198.8 23 1.37 1.53										2912
JC May 0.474 33.2 15 0.82 1.17 17.61 31.6 105 VA Jun 1.854 141.5 31 1.22 1.36 42.31 16.7 236 VA Jul 1.727 108.4 49 0.67 1.13 55.15 28.4 307 VA Aug 1.904 102.8 32 0.92 1.18 37.89 16.8 172 VA Sept 2.034 204.4 18 0.7 1.50 27.06 8.8 180 VA Oct 1.975 162.2 31 1.21 2.03 63.08 15.7 254 VA Nov 1.717 107.4 31 1.2 1.47 45.48 18.1 193 VA Dec 1.997 198.8 23 1.37 1.53 35.13 11.5 229 VA Jan 2.06 238.2 34 1.93 2.57										4865
VA Jun 1.854 141.5 31 1.22 1.36 42.31 16.7 236 VA Jul 1.727 108.4 49 0.67 1.13 55.15 28.4 307 VA Aug 1.904 102.8 32 0.92 1.18 37.89 16.8 172 VA Sept 2.034 204.4 18 0.7 1.50 27.06 8.8 180 VA Oct 1.975 162.2 31 1.21 2.03 63.08 15.7 254 VA Nov 1.717 107.4 31 1.2 1.47 45.48 18.1 193 VA Dec 1.997 198.8 23 1.37 1.53 35.13 11.5 229 VA Jan 2.06 238.2 34 1.93 2.57 87.27 16.5 393 VA Feb 1.69 119.1 29 1 1.23		=								1051
VA Jul 1.727 108.4 49 0.67 1.13 55.15 28.4 307 VA Aug 1.904 102.8 32 0.92 1.18 37.89 16.8 172 VA Sept 2.034 204.4 18 0.7 1.50 27.06 8.8 180 VA Oct 1.975 162.2 31 1.21 2.03 63.08 15.7 254 VA Nov 1.717 107.4 31 1.2 1.47 45.48 18.1 193 VA Dec 1.997 198.8 23 1.37 1.53 35.13 11.5 229 VA Jan 2.06 238.2 34 1.93 2.57 87.27 16.5 393 VA Feb 1.69 119.1 29 1 1.23 35.55 17.2 204 VA Mar 1.555 130.6 34 0.7 1.77										2366
VA Aug 1.904 102.8 32 0.92 1.18 37.89 16.8 172 VA Sept 2.034 204.4 18 0.7 1.50 27.06 8.8 180 VA Oct 1.975 162.2 31 1.21 2.03 63.08 15.7 254 VA Nov 1.717 107.4 31 1.2 1.47 45.48 18.1 193 VA Dec 1.997 198.8 23 1.37 1.53 35.13 11.5 229 VA Jan 2.06 238.2 34 1.93 2.57 87.27 16.5 393 VA Feb 1.69 119.1 29 1 1.23 35.55 17.2 204 VA Mar 1.555 130.6 34 0.7 1.77 60.25 21.9 285 VA Apr 2.1 204.5 17 0.64 1.87		Jul								3076
VA Sept 2.034 204.4 18 0.7 1.50 27.06 8.8 180 VA Oct 1.975 162.2 31 1.21 2.03 63.08 15.7 254 VA Nov 1.717 107.4 31 1.2 1.47 45.48 18.1 193 VA Dec 1.997 198.8 23 1.37 1.53 35.13 11.5 229 VA Jan 2.06 238.2 34 1.93 2.57 87.27 16.5 393 VA Feb 1.69 119.1 29 1 1.23 35.55 17.2 204 VA Mar 1.555 130.6 34 0.7 1.77 60.25 21.9 285 VA Apr 2.1 204.5 17 0.64 1.87 31.75 8.1 165 VA May 1.129 114.3 20 0.63 1.02		Aug								1728
VA Oct 1.975 162.2 31 1.21 2.03 63.08 15.7 2544 VA Nov 1.717 107.4 31 1.2 1.47 45.48 18.1 193 VA Dec 1.997 198.8 23 1.37 1.53 35.13 11.5 229 VA Jan 2.06 238.2 34 1.93 2.57 87.27 16.5 393 VA Feb 1.69 119.1 29 1 1.23 35.55 17.2 204 VA Mar 1.555 130.6 34 0.7 1.77 60.25 21.9 285 VA Apr 2.1 204.5 17 0.64 1.87 31.75 8.1 165 VA May 1.129 114.3 20 0.63 1.02 20.43 17.7 202 MH Jun 1.728 114.6 49 0.74 1.02	VA	_	2.034	204.4		0.7	1.50	27.06		1809
VA Nov 1.717 107.4 31 1.2 1.47 45.48 18.1 193 VA Dec 1.997 198.8 23 1.37 1.53 35.13 11.5 229 VA Jan 2.06 238.2 34 1.93 2.57 87.27 16.5 393 VA Feb 1.69 119.1 29 1 1.23 35.55 17.2 204 VA Mar 1.555 130.6 34 0.7 1.77 60.25 21.9 285 VA Apr 2.1 204.5 17 0.64 1.87 31.75 8.1 165 VA May 1.129 114.3 20 0.63 1.02 20.43 17.7 202 MH Jun 1.15 77.7 61 0.8 0.99 60.61 53.0 412 MH Jul 1.728 114.6 49 0.74 1.02 <	VA	-	1.975	162.2		1.21	2.03	63.08		2546
VA Dec 1.997 198.8 23 1.37 1.53 35.13 11.5 229 VA Jan 2.06 238.2 34 1.93 2.57 87.27 16.5 393 VA Feb 1.69 119.1 29 1 1.23 35.55 17.2 204 VA Mar 1.555 130.6 34 0.7 1.77 60.25 21.9 285 VA Apr 2.1 204.5 17 0.64 1.87 31.75 8.1 165 VA May 1.129 114.3 20 0.63 1.02 20.43 17.7 202 MH Jun 1.15 77.7 61 0.8 0.99 60.61 53.0 412 MH Jul 1.728 114.6 49 0.74 1.02 50.02 28.4 325 MH Aug 1.469 172.5 46 0.73 1.02	VA	Nov	1.717	107.4		1.2	1.47	45.48	18.1	1939
VA Jan 2.06 238.2 34 1.93 2.57 87.27 16.5 393 VA Feb 1.69 119.1 29 1 1.23 35.55 17.2 204 VA Mar 1.555 130.6 34 0.7 1.77 60.25 21.9 285 VA Apr 2.1 204.5 17 0.64 1.87 31.75 8.1 165 VA May 1.129 114.3 20 0.63 1.02 20.43 17.7 202 MH Jun 1.15 77.7 61 0.8 0.99 60.61 53.0 412 MH Jul 1.728 114.6 49 0.74 1.02 50.02 28.4 325 MH Aug 1.469 172.5 46 0.73 1.02 46.79 31.3 540 MH Sept 1.672 90.2 64 0.64 0.96	VA	Dec	1.997			1.37	1.53	35.13	11.5	2290
VA Feb 1.69 119.1 29 1 1.23 35.55 17.2 204 VA Mar 1.555 130.6 34 0.7 1.77 60.25 21.9 285 VA Apr 2.1 204.5 17 0.64 1.87 31.75 8.1 165 VA May 1.129 114.3 20 0.63 1.02 20.43 17.7 202 MH Jun 1.15 77.7 61 0.8 0.99 60.61 53.0 412 MH Jul 1.728 114.6 49 0.74 1.02 50.02 28.4 325 MH Aug 1.469 172.5 46 0.73 1.02 46.79 31.3 540 MH Sept 1.672 90.2 64 0.64 0.96 61.23 38.3 345 MH Nov 1.223 137.5 43 1.07 1.41										3931
VA Mar 1.555 130.6 34 0.7 1.77 60.25 21.9 285 VA Apr 2.1 204.5 17 0.64 1.87 31.75 8.1 165 VA May 1.129 114.3 20 0.63 1.02 20.43 17.7 202 MH Jun 1.15 77.7 61 0.8 0.99 60.61 53.0 412 MH Jul 1.728 114.6 49 0.74 1.02 50.02 28.4 325 MH Aug 1.469 172.5 46 0.73 1.02 46.79 31.3 540 MH Sept 1.672 90.2 64 0.64 0.96 61.23 38.3 345 MH Oct 1.617 111.9 64 0.68 1.08 69.31 39.6 442 MH Nov 1.223 137.5 43 1.07 1.41	VA							35.55		2044
VA Apr 2.1 204.5 17 0.64 1.87 31.75 8.1 165 VA May 1.129 114.3 20 0.63 1.02 20.43 17.7 202 MH Jun 1.15 77.7 61 0.8 0.99 60.61 53.0 412 MH Jul 1.728 114.6 49 0.74 1.02 50.02 28.4 325 MH Aug 1.469 172.5 46 0.73 1.02 46.79 31.3 540 MH Sept 1.672 90.2 64 0.64 0.96 61.23 38.3 345 MH Oct 1.617 111.9 64 0.68 1.08 69.31 39.6 442 MH Nov 1.223 137.5 43 1.07 1.41 60.68 35.2 483 MH Dec 1.942 117 49 0.91 1.26	VA					0.7				2856
VA May 1.129 114.3 20 0.63 1.02 20.43 17.7 202. MH Jun 1.15 77.7 61 0.8 0.99 60.61 53.0 412 MH Jul 1.728 114.6 49 0.74 1.02 50.02 28.4 325 MH Aug 1.469 172.5 46 0.73 1.02 46.79 31.3 540 MH Sept 1.672 90.2 64 0.64 0.96 61.23 38.3 345 MH Oct 1.617 111.9 64 0.68 1.08 69.31 39.6 442 MH Nov 1.223 137.5 43 1.07 1.41 60.68 35.2 483 MH Dec 1.942 117 49 0.91 1.26 61.57 25.2 295 MH Jan 2.085 203.7 40 0.44 0.89								31.75		1655
MH Jun 1.15 77.7 61 0.8 0.99 60.61 53.0 412 MH Jul 1.728 114.6 49 0.74 1.02 50.02 28.4 3250 MH Aug 1.469 172.5 46 0.73 1.02 46.79 31.3 540 MH Sept 1.672 90.2 64 0.64 0.96 61.23 38.3 345 MH Oct 1.617 111.9 64 0.68 1.08 69.31 39.6 442 MH Nov 1.223 137.5 43 1.07 1.41 60.68 35.2 483 MH Dec 1.942 117 49 0.91 1.26 61.57 25.2 295 MH Jan 2.085 203.7 40 0.44 0.89 35.66 19.2 390	VA	•		114.3	20	0.63		20.43		2025
MH Jul 1.728 114.6 49 0.74 1.02 50.02 28.4 3250 MH Aug 1.469 172.5 46 0.73 1.02 46.79 31.3 5400 MH Sept 1.672 90.2 64 0.64 0.96 61.23 38.3 3450 MH Oct 1.617 111.9 64 0.68 1.08 69.31 39.6 4420 MH Nov 1.223 137.5 43 1.07 1.41 60.68 35.2 4830 MH Dec 1.942 117 49 0.91 1.26 61.57 25.2 2950 MH Jan 2.085 203.7 40 0.44 0.89 35.66 19.2 3900										4121
MH Aug 1.469 172.5 46 0.73 1.02 46.79 31.3 540.0 MH Sept 1.672 90.2 64 0.64 0.96 61.23 38.3 345.0 MH Oct 1.617 111.9 64 0.68 1.08 69.31 39.6 442.0 MH Nov 1.223 137.5 43 1.07 1.41 60.68 35.2 483.0 MH Dec 1.942 117 49 0.91 1.26 61.57 25.2 295.0 MH Jan 2.085 203.7 40 0.44 0.89 35.66 19.2 390.0										3250
MH Sept 1.672 90.2 64 0.64 0.96 61.23 38.3 345.5 MH Oct 1.617 111.9 64 0.68 1.08 69.31 39.6 442.5 MH Nov 1.223 137.5 43 1.07 1.41 60.68 35.2 483.6 MH Dec 1.942 117 49 0.91 1.26 61.57 25.2 295.6 MH Jan 2.085 203.7 40 0.44 0.89 35.66 19.2 390.6										5402
MH Oct 1.617 111.9 64 0.68 1.08 69.31 39.6 442 MH Nov 1.223 137.5 43 1.07 1.41 60.68 35.2 483 MH Dec 1.942 117 49 0.91 1.26 61.57 25.2 295 MH Jan 2.085 203.7 40 0.44 0.89 35.66 19.2 3900		_								3453
MH Nov 1.223 137.5 43 1.07 1.41 60.68 35.2 483-4 MH Dec 1.942 117 49 0.91 1.26 61.57 25.2 295-7 MH Jan 2.085 203.7 40 0.44 0.89 35.66 19.2 390-7										4429
MH Dec 1.942 117 49 0.91 1.26 61.57 25.2 295. MH Jan 2.085 203.7 40 0.44 0.89 35.66 19.2 3908										4834
MH Jan 2.085 203.7 40 0.44 0.89 35.66 19.2 3908										2952
										3908
MH Feb 1.06 74.2 20 0.62 0.61 12.23 18.9 140			1.06				0.61			1400
										1547
										711
		=								789

Table A2.4. Pearson correlation coefficients for monthly meteorological and precipitation chemistry (temp = temperature, wetb = wet bulb temperature, dewpt = dew point temperature, vappr = vapor pressure, rhum = relative humidity, msl = mean sea level pressure, wdsp = wind speed, wddir = wind direction) against monthly microfibre counts from each of the four meteorological stations. (OP = Oak Park, JC = Johnstown Castle, VA = Valentia, MH = Malin Head)

OP	JC	VA	MH
0.403	-0.354	-0.407	0.418
0.216	-0.077	0.165	0.494
0.214	-0.088	0.168	0.522
0.204	-0.110	0.16	0.549
0.208	-0.097	0.201	0.554
-0.503	-0.327	0.057	0.723**
-0.611*	0.399	-0.036	-0.089
-0.048	-0.223	-0.062	0.188
-0.317	0.349	0.125	0.652*
0.416	-0.327	-0.418	0.417
0.286	-0.398	-0.225	0.43
-0.132	-0.051	-0.305	0.257
-0.225	-0.295	0.227	0.087
-0.241	-0.324	0.333	0.603*
-0.168	-0.323	0.218	0.578*
-0.020	-0.250	-0.197	0.222
NA	-0.153	NA	0.193
-0.124	-0.120	0.116	0.006
-0.054	-0.221	-0.062	0.188
0.042	0.269	0.177	-0.486
0.027	0.013	0.063	-0.442
	0.403 0.216 0.214 0.204 0.208 -0.503 -0.611* -0.048 -0.317 0.416 0.286 -0.132 -0.225 -0.241 -0.168 -0.020 NA -0.124 -0.054 0.042	0.403 -0.354 0.216 -0.077 0.214 -0.088 0.204 -0.110 0.208 -0.097 -0.503 -0.327 -0.611* 0.399 -0.048 -0.223 -0.317 0.349 0.416 -0.327 0.286 -0.398 -0.132 -0.051 -0.225 -0.295 -0.241 -0.324 -0.168 -0.323 -0.020 -0.250 NA -0.153 -0.124 -0.120 -0.054 -0.221 0.042 0.269	0.403 -0.354 -0.407 0.216 -0.077 0.165 0.214 -0.088 0.168 0.204 -0.110 0.16 0.208 -0.097 0.201 -0.503 -0.327 0.057 -0.611* 0.399 -0.036 -0.048 -0.223 -0.062 -0.317 0.349 0.125 0.416 -0.327 -0.418 0.286 -0.398 -0.225 -0.132 -0.051 -0.305 -0.225 -0.295 0.227 -0.241 -0.324 0.333 -0.168 -0.323 0.218 -0.020 -0.250 -0.197 NA -0.153 NA -0.124 -0.120 0.116 -0.054 -0.221 -0.062 0.042 0.269 0.177

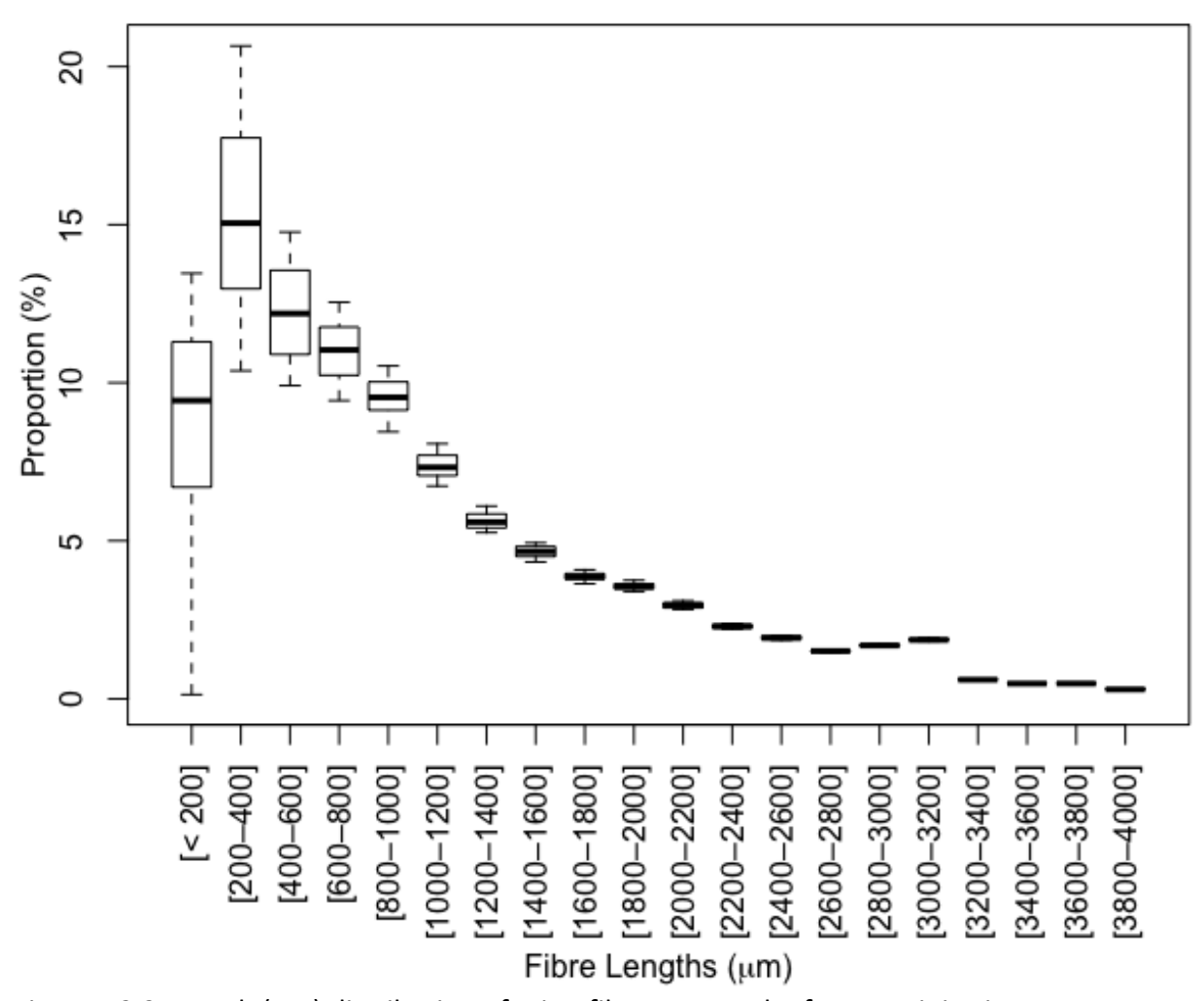


Figure A2.2. Length (μ m) distribution of microfibres across the four precipitation monitoring stations. Black line represents the median, boxplots represent the first quartile and third quartile, and the whiskers represent the minimum and maximum values.

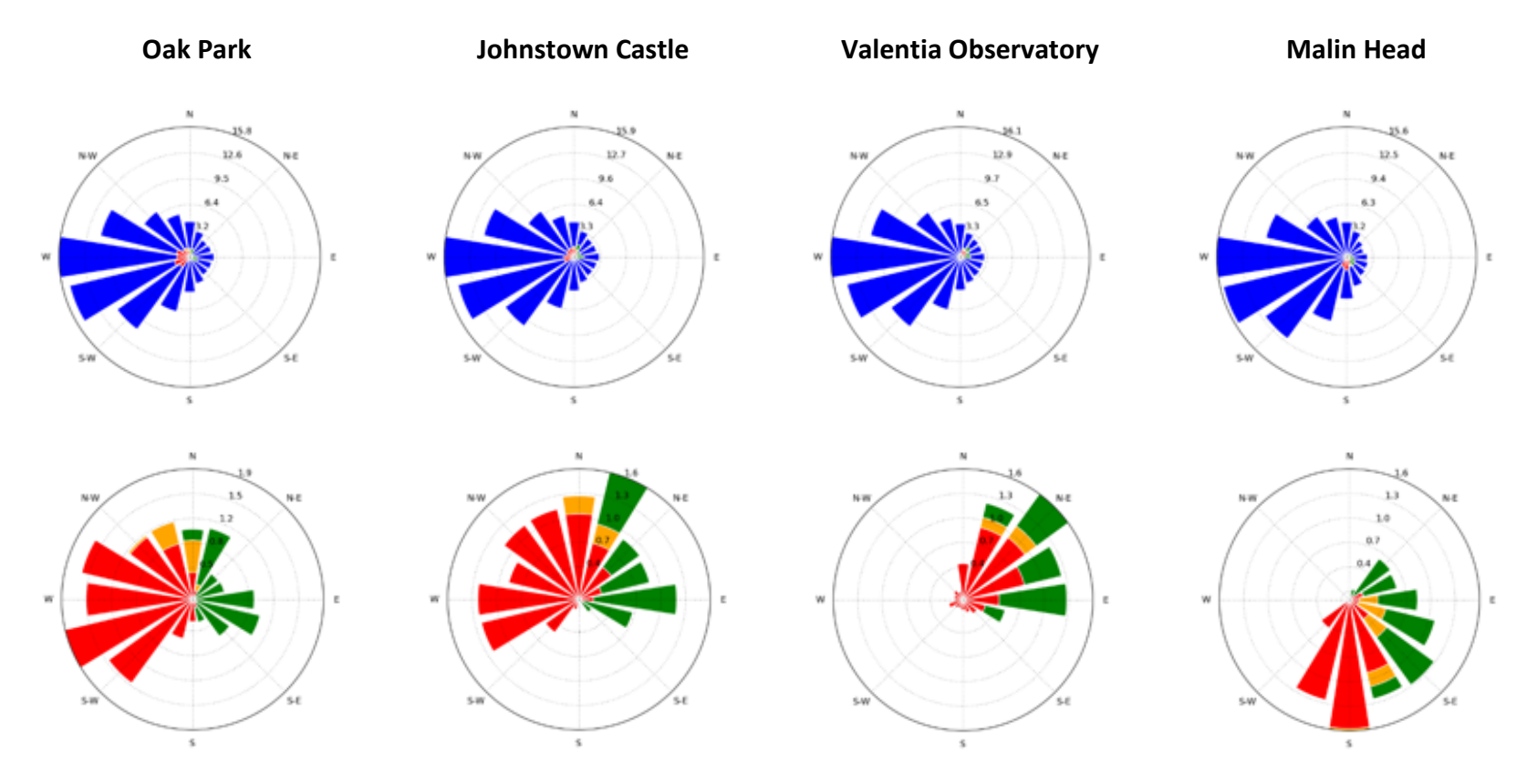


Figure A2.3. Trajectory rose source-receptor plots showing the proportion (%) of air by direction and source (Republic of Ireland [red], Northern Ireland [orange], Great Britain [green] and Marine and other regions [blue]) arriving at the study sites (receptors; arrival height of 850 hPa) based on two-day back-trajectories estimated every six hours during the period 1989–2009 using historical wind fields (observed data and model output) smoothed onto a 3-dimensional grid with 16 pressure levels and a horizontal resolution of 1 × 1 degree obtained from the ECMWF ERA Interim data set. Lower: Close-up showing the proportion (%) of air by direction from three terrestrial source regions: Republic of Ireland (red), Northern Ireland (orange) and Great Britain (green) only.

Appendix 2.4. Raman spectral analysis reports from Bio Rad-KnowltAll online library for media collected from precipitation chemistry monitoring stations.

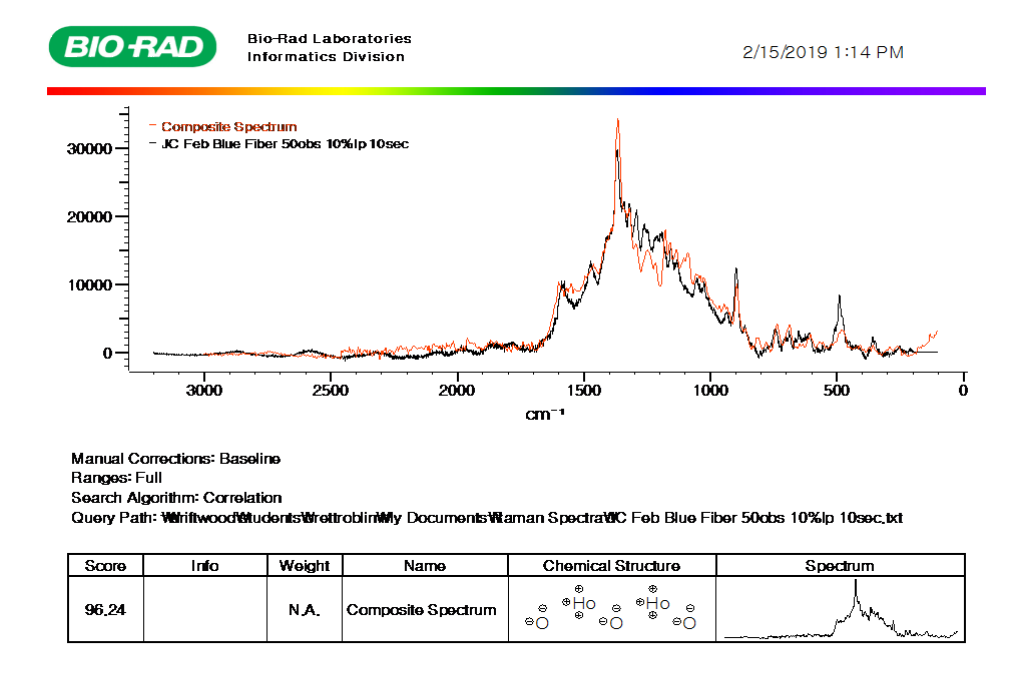
Figure A2.4A. Levafix blue E-GRN pigment

Figure A2.4B. Eriochrome blue pigment

Figure A2.4C. Polyester Film plastics

Figure A2.4D. Drimaren Turquoise X-2G pigment

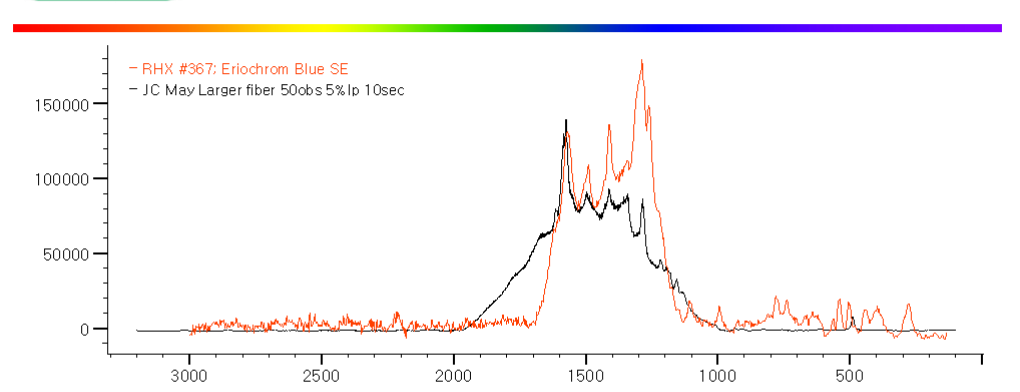
Figure A2.4E. Mortoperm blue pigment



Score: 86,8%

Composite spectra score: 96,24% with Levafix Blue E-GRN and Holmium (III) Oxide

Figure A2.4A. Raman spectral analysis reports from Bio Rad-KnowltAll online library for Levafix blue E-GRN from a Johnstown Castle February microfibre.



cm-1

Manual Corrections: Baseline

Ranges: Full

Search Algorithm: Correlation

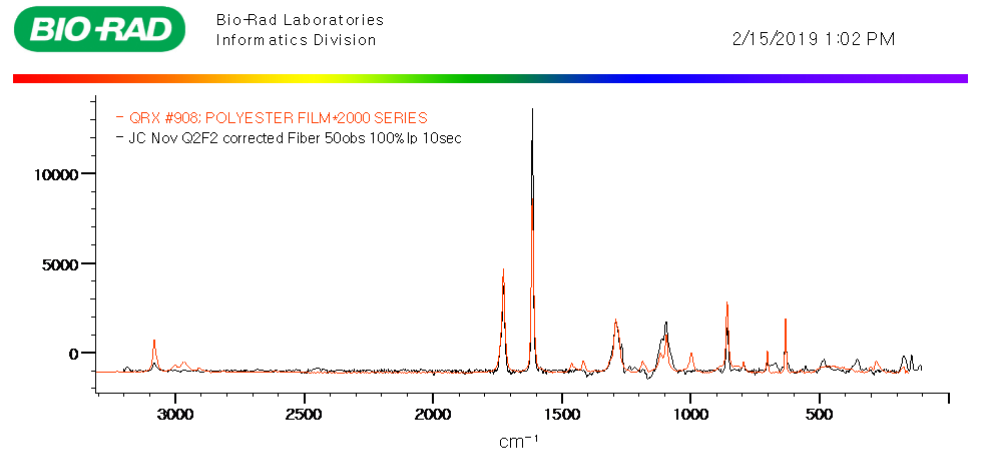
Query Path: \##riftwood\#tudents\#prettroblin\#y Documents\#aman Spectra\#C May Larger fiber 50obs 5%lp 10sec.txt

Name	Value
Resulting HQI	84.36
Database Abbreviation	RHX
Database Title	Raman -Forensic -HORIBA
Record ID	367
Name	Eriochrom Blue SE
CAS Registry Number	1058-92-0
Classification	dyestuff, stain
Comments	Merck 285
Formula	C16H9CIN2O9S2Na8
InChl	InChl=1S/C16H11CIN2O9S2.2Na/c
InChlKey	LNXMAD NIU WFTPP-
Instrument Name	HORIBA LabRAM Infinity-
Laser Power	632.8
Source of Sample	LKA Berlin
Source of Spectrum	HORIBA Scientific
Synonyms	C.I. Generic name: Mordant Blue 13; MB13; C.I. Constitution No:

Score: 84.36%

Figure A2.4B. Raman spectral analysis reports from Bio Rad-KnowltAll online library for Eriochrome blue from a Johnstown Castle May microfibre.





Manual Corrections: Noise

Ranges: Full

Search Algorithm: Correlation

Query Path: \text{\text{\text{Wiriftwood\text{\text{\text{troblin\text{\text{W}}}}}} Documents\text{\text{\text{\text{\text{W}}}} aman Spectra\text{\text{\text{\text{UC}}} Nov Q2F2 corrected Fiber 50obs 100\text{\text{\text{\text{\text{troblin\text{\texi}\text{\texi}\text{\tex{\text{\text{\text{\text{\text{\text{\text{\text{\text{\text{\tex 10sec,txt

Name	Value
Resulting HQI	88,35
Database Abbreviation	QRX
Database Title	Raman -Polymers & Monomers (Basic) -Bio-Rad Sadtler
Record ID	908
Name	POLYESTER FILM*2000 SERIES
Classification	POLYESTERS
Instrument Name	Bio-Rad FTS 175C with Raman accessory
Raman Corrections	Referenced to internal white light source; Baseline subtracted
Raman Laser Source	Nd:YAG
Raman Laser Wavelength	1064
Source of Sample	Celanese Corporation, Celanese Engineering Resins Division
Synonyms	CELANAR POLYESTER FILM*2000 SERIES
Technique	FT-Raman

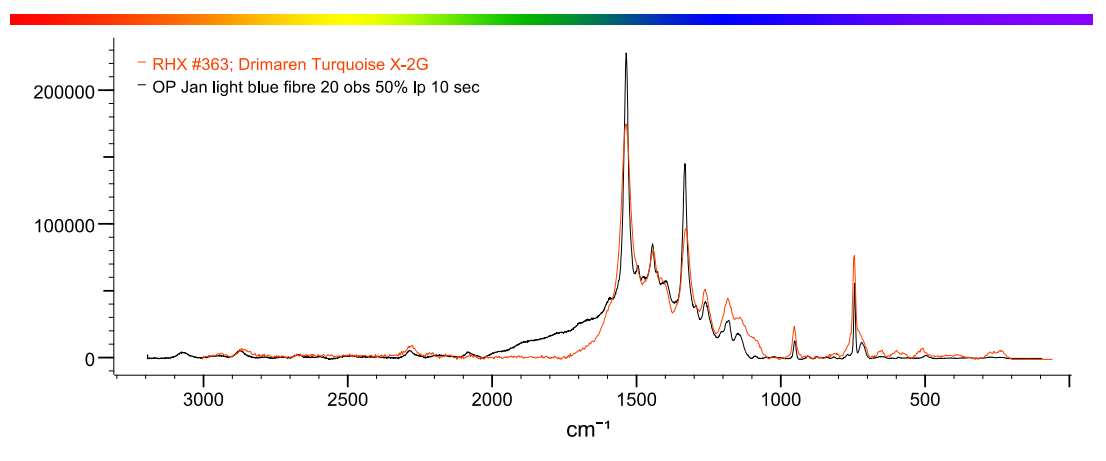
Score: 88,35%

Figure A2.4C. Raman spectral analysis reports from Bio Rad-KnowItAll online library for Polyester film from a Johnstown Castle November microfibre.



7/10/2019 11:04 AM

1



Manual Corrections: Baseline

Ranges: Full

Search Algorithm: Correlation

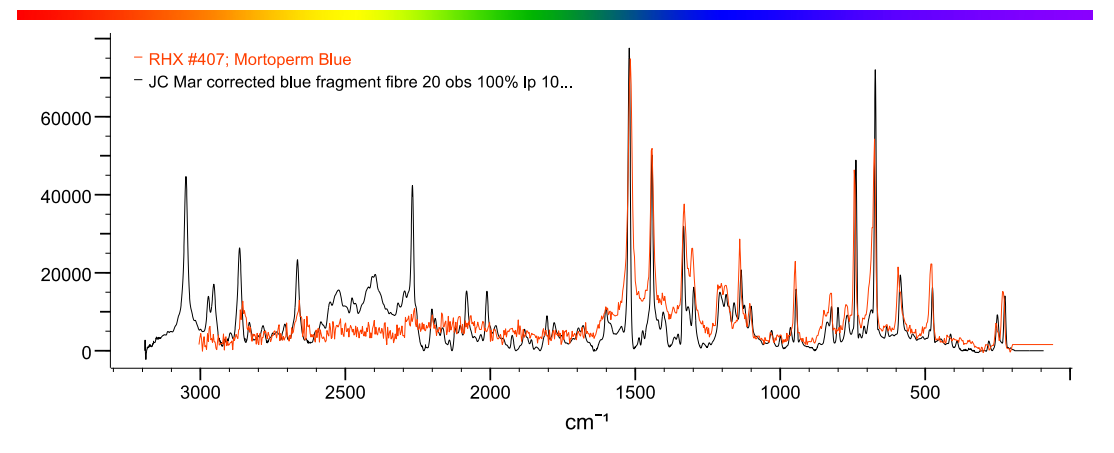
Query Path: \\driftwood\students\brettroblin\My Documents\Raman Spectra\OP Jan light blue fibre 20 obs 50% lp 10 sec.txt

Name	Value
Resulting HQI	90.76
Database Abbreviation	RHX
Database Title	Raman - Forensic - HORIBA
Record ID	363
Name	Drimaren Turquoise X-2G
Classification	dyestuff
Comments	Sandoz 194; Reactive
Instrument Name	HORIBA LabRAM Infinity-
Laser Power	632.8
Source of Sample	LKA Berlin
Source of Spectrum	HORIBA Scientific

Match of 90.76% with Drimaren Turquoise X-2G

Figure A2.4D. Raman spectral analysis reports from Bio Rad-KnowltAll online library for Drimaren Turquoise X-2G from an Oak Park January microfibre.





Manual Corrections: Baseline, Noise

Ranges: Full

Search Algorithm: Correlation

Query Path: \\driftwood\students\brettroblin\My Documents\Raman Spectra\JC Mar corrected blue fragment fibre 20 obs

100% lp 10 sec.txt

Name	Value
Resulting HQI	64.94
Database Abbreviation	RHX
Database Title	Raman - Forensic - HORIBA
Record ID	407
Name	Mortoperm Blue
CAS Registry Number	574-93-6
Classification	dyestuff
Comments	Chemical class: Cu-Phthalocyanin
InChI	InChI=1S/C32H18N8/c1-2-10-18-
InChlKey	IEQIEDJGQAUEQZ-
Instrument Name	HORIBA LabRAM Infinity-
Laser Power	632.8
Source of Sample	LKA Berlin
Source of Spectrum	HORIBA Scientific
Synonyms	C.I. Generic name: Pigment Blue
	16:4; PB 16:4; C.I. Constitution No:
	74100; Phthalocyanine

Match of 65% with Mortoperm blue

.

Figure A2.4E. Raman spectral analysis reports from Bio Rad-KnowltAll online library for Mortoperm blue from a Johnstown Castle March microfibre.

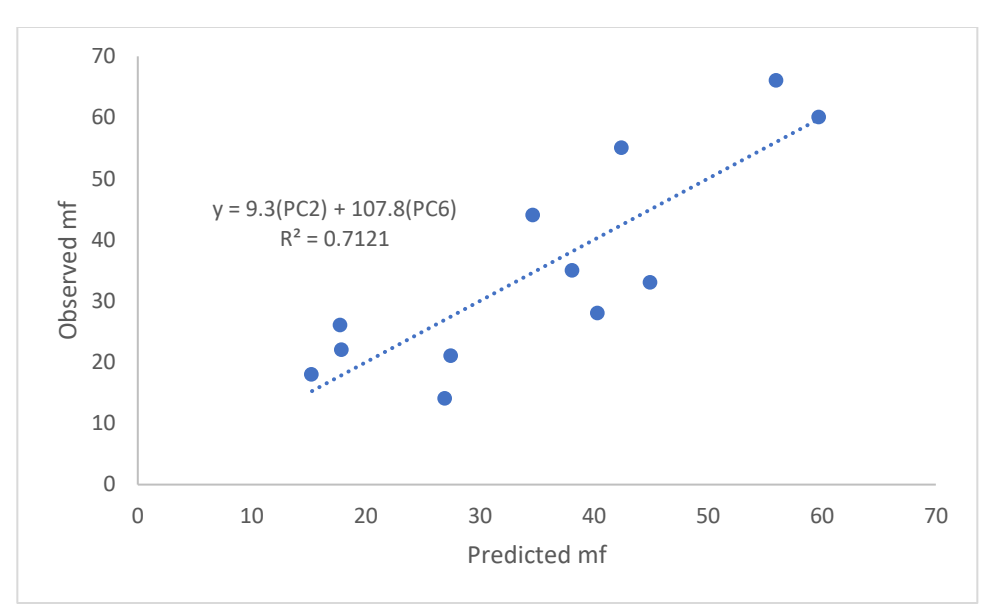


Figure A2.5A. Multilinear regression analysis of principle components 2 and 6 (predicted mf) against monthly microfibre counts (observed mf) for the Oak Park precipitation chemistry monitoring station. Regression equation and R² value for trendline included.

Table A2.5A. Loadings for principle components, including meteorological variables and the proportion of variation, from Oak Park precipitation chemistry monitoring station.

Variable	PC1	PC2	PC3	PC4	PC5	PC6
rain	-0.336919	0.512709	0.393838	-0.076019	0.283652	-0.598723
temp	0.472665	0.370113	-0.007291	0.373375	-0.114297	-0.225563
vappr	0.473631	0.379748	0.089557	0.332195	-0.078391	0.213287
rhum	-0.174839	-0.478289	0.291698	0.769121	0.230419	-0.099425
msl	0.410711	-0.445175	0.194719	-0.223722	-0.395265	-0.594827
wdsp	-0.381737	0.143566	0.418939	0.105703	-0.771340	0.214538
wddir	0.306222	-0.091566	0.733692	-0.302798	0.309899	0.368005
Variance	43%	24%	16%	10%	8%	0%

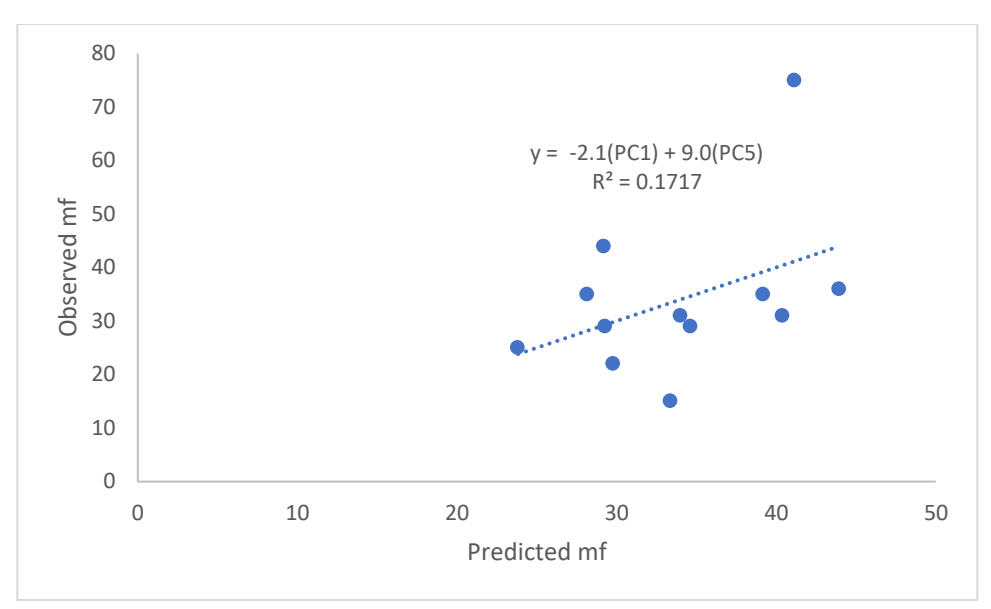


Figure A2.5B. Multilinear regression analysis of principle components 1 and 5 (predicted mf) against monthly microfibre counts (observed mf) for Johnstown Castle precipitation chemistry monitoring station. Regression equation and R² value for trendline included.

Table A2.5B. Loadings for principle components, including meteorological variables and the proportion of variation, from Johnstown Castle precipitation chemistry monitoring station.

Variable	PC1	PC2	PC3	PC4	PC5
rain	-0.381264	0.468767	-0.077425	-0.535511	-0.155828
temp	0.465443	0.393172	-0.153818	0.079623	-0.314517
vappr	0.453861	0.426934	-0.110833	0.061350	-0.297848
rhum	-0.100413	0.571403	0.378745	0.469825	0.536624
msl	0.435422	-0.337141	0.349437	0.144990	-0.074795
wdsp	-0.446838	0.008993	0.353421	0.422862	-0.702603
wddir	0.180752	0.0561526	0.753392	-0.531558	-0.029531
Variation	43%	26%	6%	4%	1%

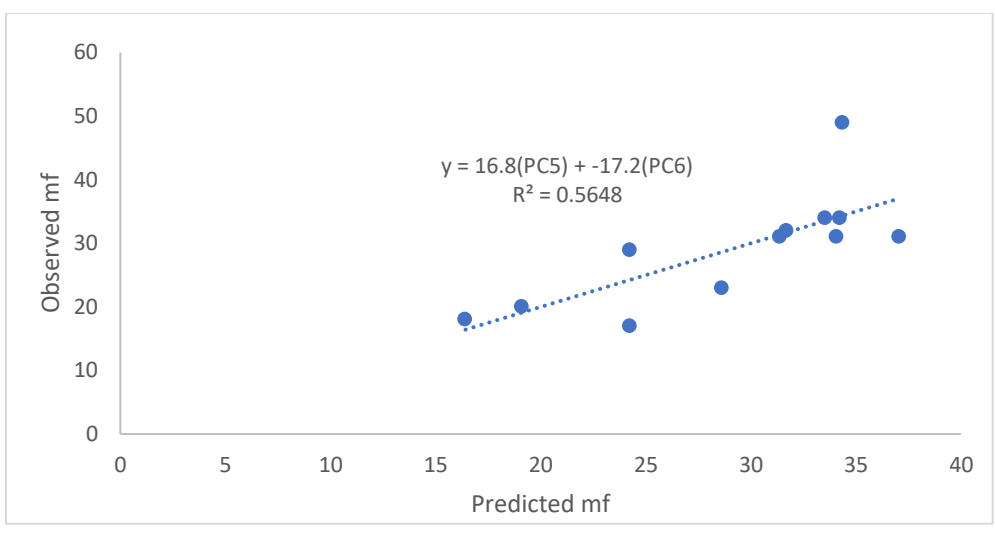


Figure A2.5C. Multilinear regression analysis of principle components 5 and 6 (predicted mf) against monthly microfibre counts (observed mf) for Valentia precipitation chemistry monitoring station. Regression equation and R² value for trendline included.

Table A2.5C. Loadings for principle components, including meteorological variables and the proportion of variation, from Valentia precipitation chemistry monitoring station.

		,				
Variable	PC1	PC2	PC3	PC4	PC5	PC6
rain	0.151399	0.641181	-0.354456	0.159991	-0.622627	0.146623
temp	-0.496652	-0.029409	-0.193432	-0.395969	-0.170849	0.231328
vappr	-0.499788	-0.006389	-0.219978	-0.244788	0.113328	0.417369
rhum	-0.414244	0.226063	-0.363144	0.628176	0.435854	-0.199524
msl	-0.308478	0.064824	0.707284	0.442634	-0.209162	0.398031
wdsp	0.236471	0.625852	0.207825	-0.277786	0.567514	0.302995
wddir	-0.397432	0.375479	0.336509	-0.299991	-0.120475	-0.678783
Variation	53%	25%	17%	4%	2%	1%

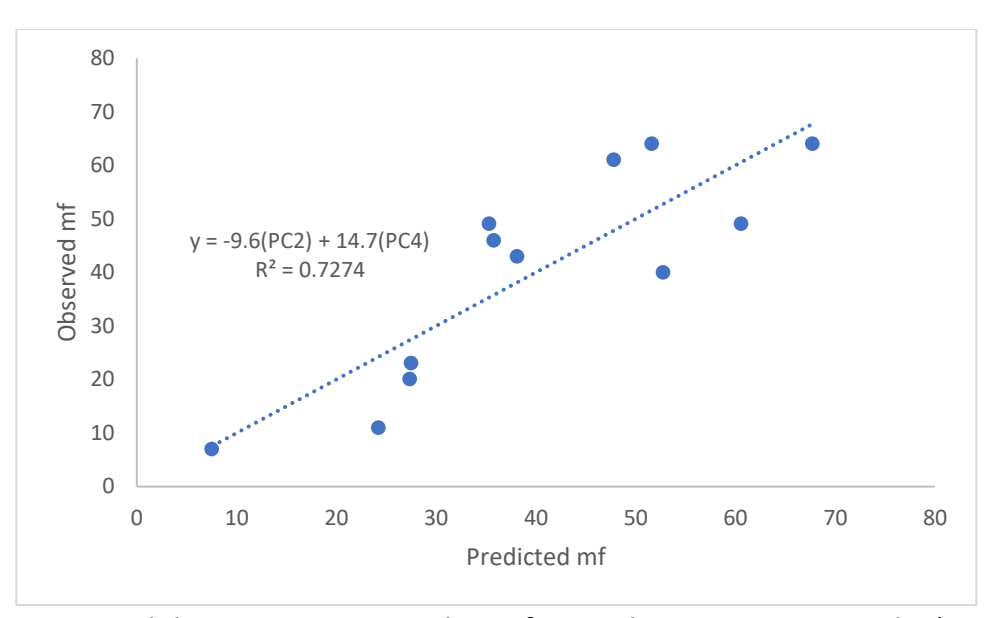


Figure A2.5D. Multilinear regression analysis of principle components 2 and 4 (Predicted mf) against monthly microfibre counts (Observed mf) for Malin Head precipitation chemistry monitoring station. Regression equation and R² value for trendline included.

Table A2.5D. Loadings for principle components, including meteorological variables and the proportion of variation, from Malin Head precipitation chemistry monitoring station.

Variable	PC1	PC2	PC3	PC4
rain	0.010968	-0.580915	0.095132	-0.758038
temp	-0.570013	-0.043682	-0.157969	0.113554
vappr	-0.561908	-0.098216	-0.181457	0.116775
rhum	-0.157053	-0.555312	-0.316974	0.321626
msl	-0.316105	0.232231	0.668565	0.033025
wdsp	0.467589	-0.306526	0.098476	0.489917
wddir	-0.126469	-0.441272	0.613123	0.233009
Variation	41%	32%	17%	5%

Chapter 3: Presence of anthropogenic microfibres in headwater lake catchments in Ireland

3.1. Abstract

Microfibres (mf), which are threadlike particles < 5 mm, are the most common form of microplastic reported in the environment. However, few studies have focused on their abundance in background environments. Headwater lakes are widely used in environmental programs as they integrate impacts on the surrounding catchment area, especially atmospheric deposition, as the main influence on these lakes is through deposition. Moss (Hylocomium splendens), lake water, and lake sediment samples were collected from three headwater lake catchments in Ireland. All lake catchments are remote from anthropogenic disturbance and emission sources. Microfibres were observed in all samples; across the three headwater lake catchments the estimated average microfibres were 24 mf g⁻¹ dry weight in moss (range: 6-34 mf g⁻¹ dry weight), 0.70 mf m⁻³ in surface trawl (range: 0.52-0.86 mf m⁻³), 9,690 m m⁻³ in subsurface (range: 9,030-10,190 mf m⁻³), 910 mf kg⁻¹ in lake sediment (range: 619-1396 mf kg⁻¹), and 576 mf kg⁻¹ in lakeshore sediment samples (range: 249-1014 mf kg⁻¹). Mf were visual identified using modified methods supported by Raman spectroscopic analysis. The Raman analysis verified the visual identification by determining mf were anthropogenic in origin by identifying synthetic pigments.

3.2. Introduction

Microplastics, which are plastic particles < 5 mm, have gained attention during the last decade owing to their ubiquity in natural environments. These waste plastics are either manufactured to be microscopic in size or come from the breakdown of bottles, bags, clothing etc., through UV radiation, physical abrasion or biodegradation (Hidalgo-Ruz et al., 2012; Dris et al., 2015; Dris et al., 2016; Peng, Wang and Cai, 2017). The most reported type of microplastics are microfibres (mf) (Wesch et al., 2017), which come from textiles, nets, fishing line and the fragmentation of larger plastic materials (Barrows, Cathey and Peterson, 2018; Cago et al., 2018). In 2016, nine million tons of fibres were produced globally with 40% being made from natural materials such as cotton, wool, or silk, the rest were made from plastic (Carr, 2017). The most common types of microfibres produced are polypropylene, polystyrene, polyethylene (PE), nylon (or polyamide), and polyethylene terephthalate (PET) (PlasticsEurope, 2016; Gago et al., 2018). These also represent some of the most common plastics found in the environment (Andrady, 2011). Microfibres are considered an environmental contaminant due to their chemical additives (dyes, corrosion resistance, enhanced durability) and risk of physical harm (blockage, abrasion) to organisms when ingested (Cole et al., 2011; Zhao et al., 2014; Wagner et al., 2014). In addition, persistent organic pollutants and trace elements can be absorbed and potentially transported by microfibres (Hidalgo-Ruz et al., 2012; Zhang et al., 2016; Horton et al., 2017a). The majority of microfibre studies have focused on aquatic systems, especially marine systems, which act as a sink for point source anthropogenic pollution (e.g., microplastics and microfibres), primarily from highly developed areas (Wagner et al., 2014; Horton et al., 2017a). Studies that focus on freshwater systems, such as lakes and rivers, are conducted similarly in highly developed areas, with large populations, industry and agriculture and typically downstream of wastewater treatment plants (Hidalgo-Ruz et al., 2012; Eriksen et al., 2013; Free et al., 2014; Li et al., 2018).

Lakes are widely included in environmental monitoring programs as they integrate impacts on the surrounding catchment area, which can influence the composition and quantity of water entering and leaving the lake (Cardille et al., 2004). This can indicate impacts that may be occurring in the lake and the surrounding area. Accordingly, headwater lakes have been referred to as sentinels of change. Headwater lakes typically receive smaller hydraulic inputs (e.g., first-order creeks, and streams) from the surrounding catchment area and therefore the majority of their water budget comes from precipitation (Cardille et al., 2004). In general, headwater lakes in background regions are considered to be pristine and free of direct anthropogenic inputs; as a result, they have commonly been used to assess long-range atmospheric transport of contaminants, such as persistent organic pollutants (Carrera, Fernandez and Grimalt, 2002), mercury (Swain et al., 1992), nitrogen (Holtgrieve et al., 2011), and trace metals (Tarvainen et al., 1997). There is limited knowledge about microplastic and microfibre inputs into headwater lakes (i.e., lakes that are not downstream of wastewater treatment plants) (Imhof et al., 2013). Recent studies have reported microfibres in atmospheric deposition, which suggests that microfibres could be transported to

background natural (pristine), headwater lakes (Dris et al., 2016; Cai et al., 2017; Roblin and Aherne, 2019; Allen et al., 2019).

The objective of this study was to evaluate the abundance of microfibres in three headwater lake catchments in Ireland. All lake catchments were considered pristine (background natural environments), and remote (i.e., in areas away from large population centres, anthropogenic infrastructures and industrial emissions). Moss, water, and sediment samples were collected from each headwater lake catchment to assess relative atmospheric input, current environmental levels and historic input of microfibres.

3.3. Materials and methods

3.3.1. Study sites

Ireland is situated on the western periphery of Europe and predominantly receives unpolluted air masses from the Atlantic Ocean (Derwent, 2007); as such, it is generally considered a background region for European transboundary air pollution (Derwent, 2007). The dominant land cover and land use in Ireland is agriculture, primarily grassland (EPA, 2012). The annual average air temperature and rainfall (based on annual averages from 1981–2010) is 9–10°C and ~1230 mm, respectively (Walsh, 2012). The three headwater lake catchments used in this study were remote from point source influences of anthropogenic activity and located in National Parks, or protected areas far from urban centres, with no anthropogenic sources upstream (e.g., agricultural runoff,

wastewater treatment plants, etc.). The three lakes, Glendalough, Lough Maumwee and Lough Veagh, have been part of the International Cooperative Programme on Assessment and Monitoring Effects of Air Pollution on Rivers and Lakes since the 1980s, under the Convention on Long-range Transboundary Air Pollution, which monitors long term trends in air pollutants in remote water bodies to support future air pollution protocols and policies. The main land use in the catchments was mainly recreational (e.g., hiking and fishing). The closest residential areas to the headwater lake catchments range from 2 km to 8.6 km away, with the closest urban centre (pop. >10,000) ranging from 17.5 km to 39.3 km (CSO, 2016; see Table A3.1). Glendalough, located in the Wicklow Mountains National Park, is in the valley of two mountain ranges with native woodland along the northern and southern edges, and shoreline on the east side (Figure 3.1; see Figure A3.1). On the western side of the lake catchment there was a small historic lead and silver mine, which ended operations in 1957 (Beining and Otte, 1996; Benning and Otte, 1997). There are three main inflows, Glenealo River and Lugduff River, that drain the catchment into the headwater lake and one smaller inflow (Bowman, 1991). Lough Maumwee, a private lake for recreational fishing managed by the Corrnamona Angling Club, is surrounded by peatland (Figure 3.1; see Figure A3.1) and has three small inflows (Bowman, 1991). Lough Veagh, located in Glenveagh National Park, is in a mountain valley with native woodland on the southern and eastern shores (Figure 3.1; see Figure A3.1). This headwater lake has five inflows draining the surrounding catchment area, with the two main ones being the Owenveagh River and the Glenlackburn River (Bowman, 1991). The lake catchments have similar annual

average air temperatures but vary in annual rainfall (Table 3.1). A previous study determined the presence of microfibres in rainfall collected from precipitation chemistry monitoring stations in Ireland; annual average deposition of microfibres was estimated to be ~28,800 mf m⁻² (Roblin and Aherne, 2019). The primary wind direction into the headwater lake catchments is from the west and west southwest (see Figure A3.2). The largest headwater lake in terms of surface area (km²) and volume (m³) is Lough Veagh, followed by Glendalough and Lough Maumwee (see Table 3.1). Water, sediment, and moss was collected from each headwater lake catchment during May 2018. Moss has been widely used as a biomonitor of atmospheric deposition, surface water has been used to indicate current inputs into lakes, and sediments have been used to determine historic inputs.

Table 3.1. Latitude, longitude, elevation (EL), surface area (SA), lake volume (Vol), long-term (1981-2010) average annual air temperature (AT) and rainfall (P) were measured from the nearest meteorological station (Casement Aerodrome for Glendalough Upper, Mace Head for Lough Maumwee and Malin Head for Lough Veagh) for each headwater lake catchment.

Lake Catchment	Latitude	Longitude	EL (m ASL)	SA (km²)	Vol (m³ x10 ⁶)	AT (°C)	P (mm yr ⁻¹)
Glendalough Upper	53.00280	-6.36805	133	0.38	6.37	9.6	754
Lough Maumwee	53.47675	-9.54091	50	0.27	0.6	10.7	1340
Lough Veagh	55.03822	-7.97269	43	2.3	47.8	9.7	1093



Figure 3.1. Location of the three headwater lake catchments: Glendalough, Lough Maumwee and Lough Veagh. All lake catchments are part of International Cooperative Programme on Assessment and Monitoring of Effects of Air Pollution on Rivers and Lakes under the United Nations Economic Commission for Europe.

3.3.2. Field sampling

Water sampling

Surface trawl and subsurface samples were collected from each headwater lake catchment, surface trawl samples were collected using a plankton tow net (~100 μ m mesh, 94 cm circumference, 15 cm radius), which was pulled alongside the boat for approximately 1 km and subsequently rinsed into 500 mL glass jars using filtered ultrapure water (18.2 megaohm). Subsurface samples were collected using a Van Dorn sampler, at ~1.5 m depths, following a modified method from Ng and Obbard (2006), from three different locations for an approximate 4 L composite sample at each lake.

The plankton tow net and Van Dorn samples were rinsed between each lake with filtered ultra-pure water.

Sediment sampling

Lake sediments were collected using an Ekman dredge (15 cm × 15 cm × 15 cm) from three locations, which were combined into one composite sample for each lake.

Lakeshore sediment was collected from the shoreline using a stainless-steel trowel from three locations, which were also combined into one composite sample by lake.

Composite sediment samples were thoroughly mixed before being poured into respective 500 mL glass jars. Sampling equipment was triple rinsed between sites using filtered B-pure™.

Moss sampling

The moss species *Hylocomium splendens* was collected from each headwater lake catchment following survey protocols recommended by ICP Vegetation (ICPV, 2015). *Hylocomium splendens* commonly grows on soil, humus, rotten logs and rock in both coniferous and deciduous forests (McKnight et al., 2013). The living green portion of *hylocomium splendens* is considered to represent the last 2–3 years of growth. At each study site, a composite sample of moss was collected from > 5 locations by hand (with nitrile gloves) from three 50 m² plots per lake catchment; samples were collected away from tree canopy cover, trails, and roads or any anthropogenic activity. The samples (~ 5

g wet weight) were stored in 500 mL HDPE jars that were triple rinsed with filtered Bpure™ water prior to sampling.

3.3.3. Microfibre extraction

Water samples

Surface trawl and subsurface samples were vacuum filtered onto glass-fibre filter papers (Fisherbrand™ G6 [09-804-42A]: 1.6 µm) and dyed using 1 mL of Rose Bengal (4,5,6,7-tetrachloro-2',4',5',7'-tetraiodofluorescein, 200 mg L⁻¹) to help visually distinguish synthetic material from bio-organic matter following Liebezeit & Liebezeit (2014). Filter papers were placed into individual petri dishes for storage after being dyed.

Sediment samples

Sediment samples were dried at 50°C for 72 hrs. Triplicate 20 g samples for each site were placed into a portable density separating apparatus (Cappock et al., 2013) and separated using zinc chloride (ZnCl₂; density of 1.5 g cm⁻³). The apparatus used a stir rod to shake up the material and allow lighter material, such as microfibres, to float to the top. This top portion was then decanted, and vacuum filtered following the same procedure as the water samples; depending on the amount of visible bio-organic matter, the sample was digested using a wet peroxide oxidation (WPO) method (Masura et al., 2015; Herrera et al., 2018). Digestion was carried out by adding 40 mL of Fe (II) solution to each sediment sample and 40 mL of 30% hydrogen peroxide (H₂O₂) was subsequently added and the mixture was left at room temperature for 5 minutes. The

digestate was heated between $40-50^{\circ}\text{C}$ to increase the reaction rate, and further 20 mL aliquots of H_2O_2 were added when the reaction slowed down (reduced bubbling and temperature), or if organic matter was still visible. At least two H_2O_2 aliquots were added to each sample, which were then vacuum filtered, dyed and stored following the same methods as the water samples.

Moss samples

In the laboratory, moss samples were dried at 50°C for 48 hrs. Triplicate 1 g moss samples for each site (and the remaining mass as a fourth sample per site) were digested following the same WPO method as the sediment samples. Samples were then vacuum filtered, dyed and stored following the same procedure as the water samples.

3.3.4. Microscopy and microfibre identification

The filter papers were analysed for the presence of microfibres using a stereomicroscope (Leica EZ4W with EZ4W0170 camera), following a modified visual identification method from Norén (2007) and Windsor et al. (2018). Identification of microfibres following standardized criteria coordinated with strict examination can reduce the possibility of misidentification (Norén, 2007). Visual analyses for particles > 0.5 mm have been demonstrated to be suitable for identification (Löder and Gerdts, 2015). The five visual criteria were: (i) the fibre is unnaturally coloured (blue, red, green, purple, black, grey, white) compared to the majority of other particles / detritus; (ii) the fibre appears homogenous in material and texture with no visible cell structure or

offshoots and is a consistent width throughout its entire length; (iii) the fibre remains intact and is not brittle when compressed, tugged or poked with fine tweezers; (iv) the fibre has a shiny or glossy appearance; and (v) there is limited fraying with no similarities to natural fibres (see Table A3.2). It is recommended that at least two of the criteria be met for a fibre to be classified as a microplastics (Windsor et al., 2018). Previous studies have classified all fibres not stained by Rose Bengal as microplastic (Liebezeit et al., 2014), while others have chosen to use the more general term 'anthropogenic debris' (Kosuth et al., 2018). In the current study microfibres that met at least two of the criteria, and were not stained by Rose Bengal, were considered anthropogenic. These anthropogenic microfibres were photographed and then measured using the open source Image processing software ImageJ. Each microfibre was manually measured using a scale bar to convert the number of pixels measured to a known length.

3.3.5. Raman spectroscopy

In order to test the accuracy of the visual identification method, a number of fibres were randomly selected from the media at each lake catchment and analysed using Raman spectroscopy (Renishaw inVia, operated by WiRE). Raman spectroscopy measurements were carried out using 5× 25× and 50× objectives and a 633 nm laser with adjustable laser power (ranging from 0.00001% to 100%). Due to fluorescence issues, lower laser power and longer accumulations were used to improve the raman signal. Raman spectra were recorded in the wavenumber range of 3,500–150 cm⁻¹. The spectrum of each fibre was identified using a commercial library (KnowltAll, Bio-Rad®).

3.3.6. Quality control and data analysis

Throughout sample processing and analysis, procedural open-air blanks were used to determine the amount of potential contamination; open-air and digestion blanks were used during filtering, digesting and oven drying (35 blanks in total). Digestion blanks were completed by using filtered B-pure™ in place of sample media during the digestion process. Triplicate B-pure™ water blanks (1 L) were initially vacuum filtered and analysed following the same method as the water samples to determine the level of microfibre contamination; the average number of microfibres was > 11 mf L⁻¹. As such, all B-pure™ water was filtered (Fisherbrand G6: 1.6 µm) prior to use for cleaning and extraction (used in FE(II), Rose Bengal and zinc chloride) to avoid potential contamination. Further, during microfibre extraction (digesting and filtering), the samples were covered with tin foil to prevent airborne contamination and all equipment was rinsed with filtered B-pure™ water prior to use. After each sediment sample, but also if the apparatus was sitting too long (although covered with tin foil), the apparatus were cleaned and the zinc chloride solution was filtered until filter papers came back free of material. Peroxide blanks (1 L in total) were also vacuum filtered and analysed following the same method as the water samples to determine the level of microfibre contamination. Finally, 100% cotton clothes were worn during sample collection, and 100% cotton laboratory coats were worn when extracting and analysing the samples.

Triplicate samples were analysed for lake and lakeshore sediments, as well as moss samples for each headwater lake catchment. The quantity of microfibres in sediment and moss samples were calculated using the dry weight for each triplicate sample (see Table A3.3). The coefficient of variation (or relative standard deviation) was used to assess the variation in triplicate samples. The number of microfibres per g of dry moss were scaled to atmospheric deposition using published values for the biomass of moss, i.e., 2 kg dry weight/m² (Forman, 1969: Singh et al., 2005). The abundance of microfibres in surface trawl samples was calculated by dividing the mf km⁻¹ by the diameter of the plankton net (3.0x10⁻⁴ km) which was then expressed as mf km⁻² (see Equation 3.1).

Equation 3.1

Surface trawl estimate
$$\frac{mf \ km^{-1}}{Diameter \ (3.0 \ x \ 10^{-4} km)} = mf \ km^{-2}$$

The abundance of microfibres in surface trawl samples was also converted into mf m⁻³ by dividing the number of microfibres observed at each lake catchment by the volume sampled (45.9 m⁻³) (see Equation 3.2).

Equation 3.2 Surface trawl estimate
$$\frac{mf}{Volume\ of\ water\ trawled\ (m^3)} = mf\ m^{-3}$$

The abundance of microfibres in each headwater lake was calculated by multiplying the amount of mf m⁻³ by the volume (m³) of water trawled at each lake.

The long-term atmospheric source regions for each site were evaluated using source-receptor trajectory rose plots (arrival height of 850 hPa) based on two-day back trajectories estimated every six hours during the period 1989–2009 (see Figure A3.2).

Median values for length of microfibres were used in place of averages due to the data being skewed to smaller fibres. Microfibre lengths were categorized in size groupings similar to Dris et al., 2016, (i.e., a 200 µm size range). Repeated measures ANOVA were conducted in SPSS (IBM Corp., 2015) to compare microfibre abundance and length of triplicate samples from sediment and moss between the lake catchments. Statistical analysis that were found to be significantly different are described in the results. Previously published studies were compared to the current study based on having similar methods, and sample media, and reporting primarily microfibres.

3.4. Results

3.4.1. Microfibre abundance in headwater lake catchments

In total there were 35 filter banks used to estimate the potential contamination of microfibres from open air exposure, water, and H_2O_2 . The average potential contamination per lake catchment was estimated to be 2.7 mf. This represented 0.56 mf per moss sample, 0.08 mf per surface trawl sample, 0.67 mf per subsurface sample, 0.38 mf per lake sediment sample and 1 mf per lakeshore sediment sample. Digestion blanks found contamination of 0.33 mf per sample. Samples were not blank corrected due to the low microfibre contamination.

In the current study, microfibres were found in all moss, water and sediment samples collected from the three headwater lake catchments (Table 3.1; see Table A3.4). In total, there were 749 microfibres observed across five different sampling media from the lake

catchments. The average proportions of microfibres across the three lake catchments ranged from 14% (surface trawl and lakeshore sediment) to 38% (moss) (Figure 3.2). The largest proportion (38%) was observed in moss, which had 300 mf in 12.47 g dw moss. This was broken down into 162 mf (54%) at Glendalough, 56 mf (29%) at Lough Maumwee, and 82 mf (32%) at Lough Veagh (see Table A3.4). There was an average of 24 mf g⁻¹ per lake catchment, which ranged in triplicate (1 g) samples from 13–34 mf g⁻¹ at Glendalough, 6–19 mf g⁻¹ at Lough Maumwee, and 8–33 mf g⁻¹ at Lough Veagh (see Table A3.3). The coefficient of variation for moss samples was > 45% (range: 46%-85%) (Table 3.2). The atmospheric deposition of microfibres observed in moss from the three lake catchments was estimated to be ~47,700 mf m⁻² (Table 3.2). Glendalough had the highest estimated deposition at 58,900 mf m⁻² followed by Lough Veagh (48,000 mf m⁻²) and Lough Maumwee (30,600 mf m⁻²). Surface trawl samples had an average of 82,288 mf km⁻² per lake catchment; this ranged from 61,533 mf km⁻² (Glendalough) to 100,899 mf km⁻² (Lough Maumwee) (Table 3.2). This was also converted to an average of 0.70 mf m⁻³, which ranged from 0.52 mf m⁻³ (Glendalough) to 0.86 mf m⁻³ (Lough Maumwee) to compare with the subsurface samples. Subsurface samples had an average of 9,690 mf m⁻³ (9.69 mf L⁻¹) per lake catchment (Table 3.2). This ranged from 9,030 mf m⁻³ (9.03 mf L⁻¹) (Lough Veagh) to 10,190 mf m⁻³ (10.19 mf L⁻¹) (Lough Maumwee). Lake sediment samples had an average of 910 mf kg⁻¹ dw across all lake catchments, which ranged from 619 mf kg⁻¹ (Lough Veagh) to 1,396 mf kg⁻¹ (Lough Maumwee). Lakeshore sediment samples had an average of 576 mf kg⁻¹ per lake. The abundance of microfibres ranged from 249 mf kg⁻¹ dw (Lough Maumwee) to 1,014 mf kg⁻¹ dw (Lough Veagh). In general,

the abundance of microfibres in lake sediment was ~2 times larger than the lakeshore sediment (Table 3.2). Lakeshore sediment had a coefficient of variation >40% (range: 40%-71%) and lake sediment had a coefficient of variation >25% (range: 25%-92%).

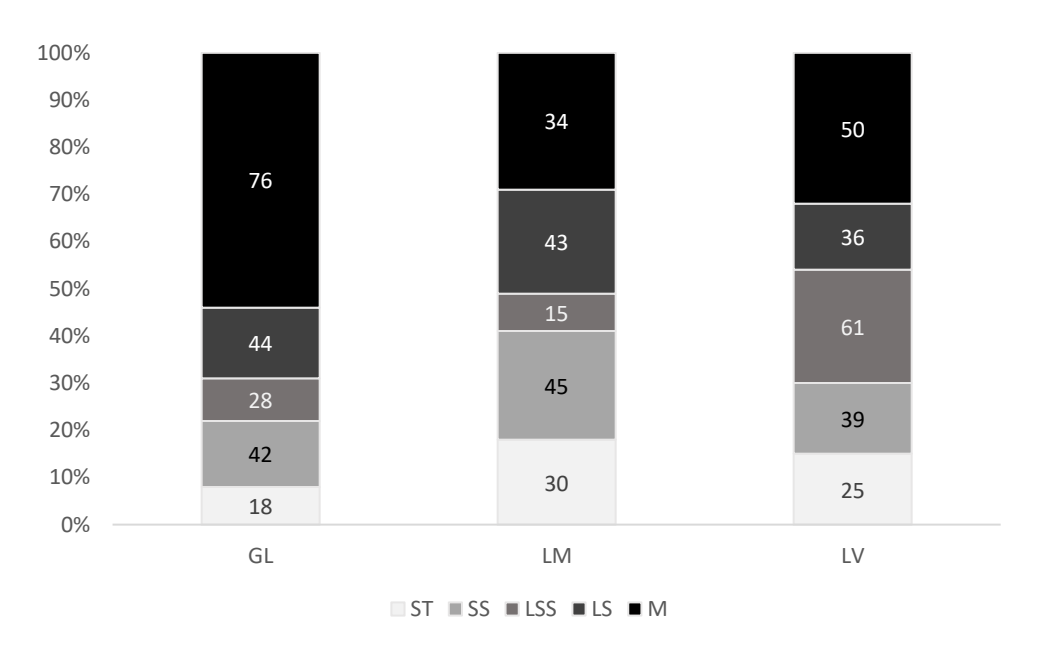


Figure 3.2. The percent of microfibres, and triplicate (moss and sediment), surface trawl (mf km⁻¹) and subsurface microfibre counts, observed across each of the five sampled media (ST= Surface trawl, SS= Subsurface, LSS= Lakeshore sediment, LS = Lake sediment, M = Moss) collected at each of the three lake catchments (GL = Glendalough, LM = Lough Maumwee, LV = Lough Veagh).

Table 3.2. The abundance of microfibres observed in water, sediment and moss from each headwater lake catchment from May 2018. Coefficient of variation [%] indicated in parenthesis for triplicate samples (i.e., sediment and moss).

Sample Site	Surface Trawl	Subsurface	Lake Sediment	Lakeshore Sediment	Moss
	$mf m^{-3} (mf km^{-2})$	$mf L^{-1} (mf m^{-3})$	mf kg ⁻¹ dw*	mf kg ⁻¹ dw*	$mf g^{-1} dw* (mf m^{-2})$
Glendalough	0.52 (61,533)	9.86 (9,860)	1,090 [92%]	464 [71%]	29.5 (58,900) [46%]
Lough Maumwee	0.86 (100,899)	10.19 (10,190)	1,690 [25%]	249 [40%]	15.3 (30,600) [60%]
Lough Veagh	0.72 (84,433)	9.03 (9,030)	946 [29%]	1,014 [47%]	24.0 (48,000) [85%]
Average	0.70 (82,288)	9.69 (9,690)	1,242	576	23.9 (47,700)

^{*}Dry weight = dw

3.3.2. Size and colour of microfibres

The size of microfibres observed in this study were predominately <1 mm with the proportion of microfibres ranging from 58% (surface trawl) to 71% (moss) (Figure 3.3). The largest frequencies of fibre lengths across all lake catchments were between 0.2–0.4 mm, which ranged from 15.5% (lake sediment) to 22% (subsurface) (Figure 3.3; see Figure A3.3). The largest fibre lengths found in this study were > 2.6 mm, with the longest fibre observed being ~30 mm (Glendalough Moss) (Figure 3.3; see Figure A3.3).

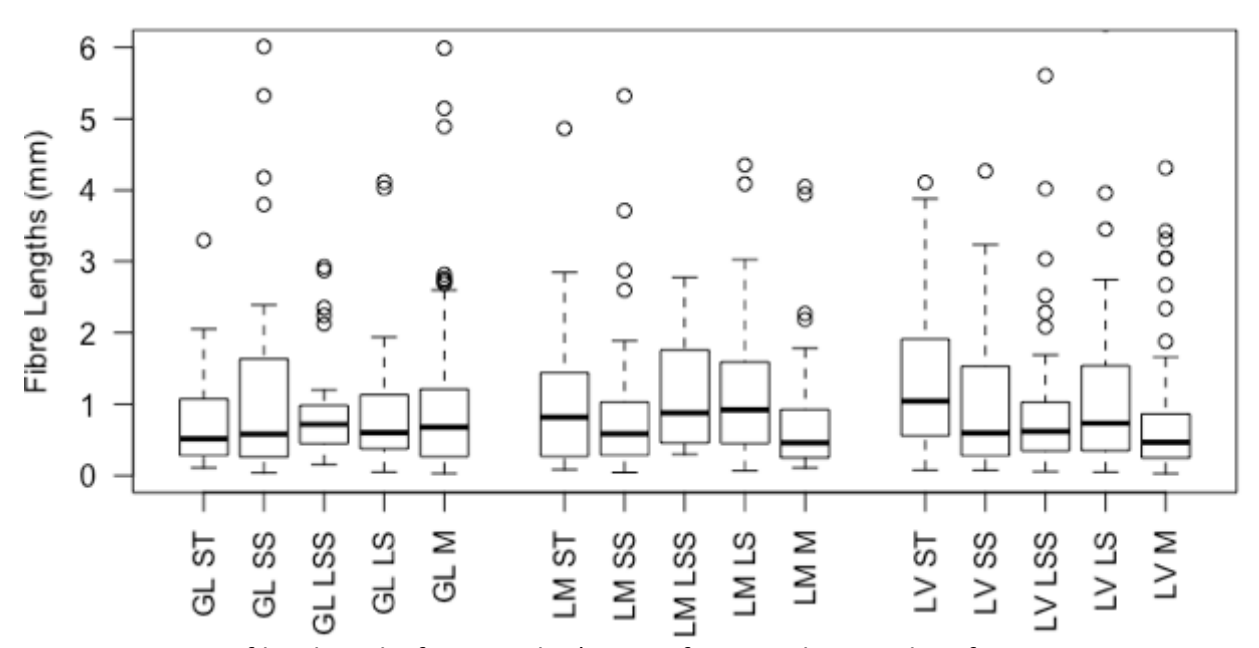


Figure 3.3. Microfibre lengths from media (ST= Surface trawl, SS= Subsurface, LSS= Lakeshore sediment, LS = Lake sediment, M = Moss) collected at each of the three headwater lake catchments (GL = Glendalough, LM = Lough Maumwee, LV = Lough Veagh. The black line indicates the median, the boxes represent the first and third quartiles, the whiskers represent the smallest and largest observations that fall within a distance of 1.5 times the box size and the dots represent values that are outside the 1.5 times distance.

The median mf length found associated with the moss samples was 0.55 mm which ranged from 0.46 mm (Lough Maumwee) to 0.68 mm (Glendalough) (Table 3.3). The

coefficient of variation in moss ranged from 31% (Lough Veagh) to 42% (Lough Maumwee). This indicates that the moss samples had a similar degree of variation. The median lengths in water samples were 0.85 mm (surface trawl) and 0.59 mm (subsurface); this ranged from 0.52 mm (Glendalough) to 1.04 mm (Lough Veagh) in surface trawl and 0.58 mm (Glendalough) to 0.60 mm (Lough Veagh) in subsurface (Table 3.3). Sediment samples had the same median length of 0.71 mm (Table 3.3). This ranged from 0.60 mm at Glendalough to 0.92 mm at Lough Maumwee in lake sediment, and 0.62 mm at Lough Veagh to 0.88 mm at Lough Maumwee in lakeshore sediment (Table 3.3).

Table 3.3. The median length (coefficient of variation between triplicates) of microfibres collected in the samples from each of the three headwater lake catchments.

Sample Site	Surface Trawl	Subsurface	Lake Sediment	Lakeshore Sediment	Moss
	mm	mm	mm	mm	mm
Glendalough	0.52	0.58	0.72 (38%)	0.60 (14%)	0.68 (36%)
Lough Maumwee	0.82	0.59	0.88 (47%)	0.92 (99%)	0.46 (42%)
Lough Veagh	1.04	0.60	0.62 (6%)	0.73 (10%)	0.47 (31%)
Median	0.85	0.59	0.71	0.71	0.55

The dominant mf colour observed in this study was blue (Figure 3.4), which ranged from 53% (lake sediment) to 76% (Moss) (Figure 3.4). The next dominant colours were grey, (3% lake sediment to 22% surface trawl) and black, (1% surface trawl to 19% lake sediment). Green was the only other colour of microfibre observed to be >10% of a sample (lake sediment).

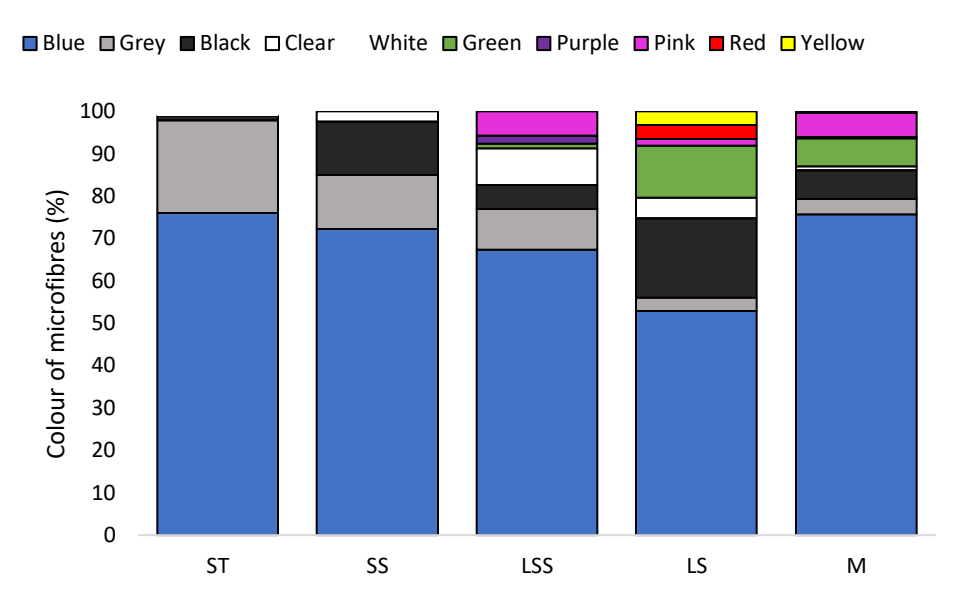


Figure 3.4. Colour distribution of microfibres collected from each media (ST= Surface trawl, SS= Subsurface, LSS= Lakeshore sediment, LS = Lake sediment, M = Moss) at the three lake catchments.

3.4.3 Trajectory source receptor plot analysis

The two-day trajectory source receptor plots indicated the primary wind direction into the four precipitation monitoring stations was from the west (see Figure A3.2).

However, the dominant terrestrial source regions into each of the lake catchments was different owing to their predominant coastal locations (Figure 3.1). Glendalough received the largest frequencies of terrestrial wind (<15%) from the west, Lough Maumwee, received terrestrial air (<7%) from the east, and Lough Veagh received terrestrial winds (<9%) from the south (see Figure A3.2).

3.4.4. Raman analysis

A subset of 30 microfibres were analysed using Raman spectroscopy (Renishaw inVia). In total 15 fibres were matched to synthetic pigments; Indigo, Eriochrome blue, Cobalt

Phthalocyanine, Hostasol green, and Hostopen violet (Table 3.4; see Figure A3.4). These pigments were identified with match percentages that ranged from 73%–96% (Table 3.4). Surface trawl and subsurface samples produced 10 of the 15 identified spectra, with the dominant pigment being identified as indigo (Table 3.4). Moss samples produced the least identifiable spectra with only one tested fibre being matched with indigo (Table 3.4).

Table 3.4. Raman spectroscopy results for the subset of microfibres analysed, including the name (match %), and media where fibres were extracted.

Media	Site	Identity (% match)
Moss	Lough Maumwee	Indigo (73%)
Lakeshore	Lough Maumwee	Indigo
	Lough Veagh	Indigo
Lake sediment	Glendalough	Hostasol Green G-K (96%)
	Lough Veagh	Hostopen Violet (89%)
Surface trawl	Glendalough	Indigo, and Eriochrome Blue (74%)
	Lough Maumwee	Indigo (x2)
	Lough Veagh	Phthalocyanine (83%)
Subsurface	Glendalough	Indigo (x2)
	Lough Maumwee	Indigo and Eriochrome Blue
	Lough Veagh	Eriochrome Blue

3.5. Discussion

3.5.1. Abundance of microfibres in headwater lake catchments

The results of this study observed the presence of microfibres in moss, water, and sediment at each of the three background headwater lake catchments. The lake catchments are not downstream of major influences of microfibres and are considered natural environments, with two sources of microfibres into these catchments being, visitors, e.g., two of the study sites are in national parks, and / or atmospheric

deposition. The number of visitors is the highest in the Wicklow Mountains National Park, where Glendalough is located, as approximately 1 million people each year visit the park, whereas 80,000 a year visit Glenveagh National Park, where Lough Veagh is located. The closest densely populated and industrial areas (population >10,000), which are likely sources of mf emissions, are Wicklow (20.5 km; pop. 10,584) (Glendalough), Galway (39.3 km; pop. 79,934) (Lough Maumwee), and Letterkenny (17.5 km; pop. 19,274) (Lough Veagh). However, these population centres are not predominately upwind of the lake catchments, which may suggest that the abundance of microfibres observed in this study are background levels.

Based on published estimates for the biomass of moss, the average atmospheric deposition of microfibres collected on moss was ~47,700 mf m⁻² across the three headwater lake catchments. Previous estimates of atmospheric deposition in the area (28,769 mf m⁻²) are ~1.7 times lower than the estimates from moss. This difference may be explained by the life characteristics of *Hylocomium splendens*, as the current growth of the moss can represent a cumulative 2–3 years of deposition. This suggests that the abundance of microfibres estimated from moss, is representative of approximately 2 years of atmospheric deposition. However, moss biomass can vary greatly by site and species of moss; as such, further measurements are needed to accurately scale-up microplastic observations on moss to regional deposition. The use of moss in this study suggests that moss may be a suitable biomonitor for the atmospheric deposition of microfibres.

Previous studies with surface trawl samples observed microfibre abundances ranging from 10,000 – 6.5x10⁶ mf km⁻² (see Table A3.5). Similarly, previously reported bulk samples ranged from 3.4 – 34 mf L⁻¹ (see Table A3.5). However, due to differing methodologies (i.e., nets with different mesh size or different sampling depths) it is difficult to compare the current study to previous studies. The estimated amount of microfibres per kg for lake sediment and lakeshore sediment was 915 mf kg⁻¹ dw and 576 mf kg⁻¹ dw. The abundance of microfibres reported in previous studies ranged from 11–506 mf kg⁻¹ (see Table A3.5). However, a number of the previous studies reported microfibre abundance based on visual identification corrected according to Raman and FT-IR results (Su et al., 2016; Yuan et al., 2019), making it difficult to compare the current study to previous studies.

3.5.2. Size and colour of microfibres

The median length of fibres observed in the surface trawl samples were predominately (~59%) < 1 mm (see Figure A3.3). Similarly, the largest proportion of fibre lengths reported in previous studies ranged from 0.333-1 mm (Su et al., 2016; Fischer et al., 2016). Subsurface samples had a median length of 0.59 mm with fibre lengths being predominantly (82%) < 2 mm (see Figure A3.3). Previous studies, collecting bulk samples, observed fibre lengths being predominantly (range from 70% - 85%) < 2 mm (Su et al., 2016; Wang et al., 2017; Wang et al., 2018; Yuan et al., 2019). Sediment samples had median microfibre lengths of 0.71 mm with 58% (Lakeshore) and 55%

(lake) of fibres predominantly being <0.8 mm (see Figure 3.3). Previous studies reported the largest proportion of microfibres ranging from 0.5-1 mm (Fischer et al., 2016; Su et al., 2016; Yuan et al., 2019). The small size range of microfibres found in these different media suggest that the microfibres observed in the environment come from secondary sources (are fragmented from larger fibres). When comparing the fibre size in the current study, all the media collected across the three lake catchments have similar median lengths. This suggests that the microfibres may be coming from a similar source, i.e., atmospheric deposition.

The dominant colour found in the current study was blue. This is comparable to Lake Taihu which observed 63% of fibres in surface trawl and 50% in bulk water being blue (Su et al., 2016). In Dongting and Hong lake bulk water samples, transparent fibres were the dominantly observed (28.7% and 22%) followed by blue (Wang et al., 2018). In contrast, the authors of studies done on Lake Taihu and Lake Poyang observed white (44%) and coloured (~40%) as being the dominant colours in sediment samples (Su et al., 2016; Yuan et al., 2019).

3.5.3. Raman analysis

Raman spectroscopic analysis verified the presence of synthetic pigments on the microfibres (see Figure A3.4). These pigments were identified as Indigo, Eriochrome blue, Copper Phthalocyanine, Hostasol green, and Hostopen violet. The dominant pigment found in the lake catchment samples was Indigo, followed by Eriochrome blue.

All of the aforementioned pigments are used in the textile industry most commonly being used with cotton and wool, with use on silk, nylon, polyester and other synthetic polymers. Indigo, phthalocyanine and hostasol green have been identified in previous microplastic studies (Zhao et al., 2017; Karami et al., 2017). Indigo is dominantly associated with natural fabrics (Wiesheu et al., 2016), whereas phthalocyanine, and hostasol green, are known to be used with different plastic polymers (Zhao et al., 2017). However, the presence of these synthetic additives (pigments) does not confirm whether the fibres are plastic; nonetheless it confirms that these fibres are anthropogenic in origin (Remy et al., 2015; Zhao et al., 2017).

The number of clean spectra obtained were limited due to high signal to noise ratios. The high signal to noise ratio in the Raman spectra can be caused by dyes, pigments and biofouling (microorganisms that grow on the surface of the microfibres) as the signal can be either diluted by fluorescence (Fredericks, 2012; Araujo et al., 2018; Barrows et al., 2018) or completely blocked (Fredericks, 2012; Lenz et al., 2015). This required lowering the laser power, to reduce the fluorescence, which in turn increases the difficulty of interpreting the spectra (Zhao et al., 2017; Prata et al., 2019). This type of interference has been observed in previous studies, as dyes incorporated into polymers can override the polymer spectrum (Zhao et al., 2017; Horton et al., 2017b; Karami et al., 2017). Particles that have been identified with strong spectrum of pigments were inferred to be polymers and classified them as such (Van Cauwenberghe et al 2013; Horton et al., 2017b).

3.6. Conclusion

The present study reported the presence of anthropogenic microfibres in three background headwater lake catchments. Microfibres were observed in all moss, water and sediment samples collected from these lake catchments. Microfibres were determined to be anthropogenic in origin through visual identification methods supported by Raman spectral analysis. Synthetic pigments, Indigo, Eriochrome blue and Hostasol Green, were identified by Raman spectroscopy from a subset of microfibres. Similar sized microfibres found between the different media at all lakes indicate they may come from a similar source, i.e., atmospheric deposition.

3.7. References

- Anderson, P., Warrack, S., Langen, V., Challis, J., Hanson, M. and Rennie, M. (2017).

 Microplastic contamination in Lake Winnipeg, Canada. *Environmental Pollution*, 225, pp.223-231.
- Andrady, A. (2017). The plastic in microplastics: A review. Marine Pollution Bulletin, 119(1), pp.12-22.
- Beining, B. A., & Otte, M. L. (1996). Retention of Metals Originating From An Abandoned Lead: Zinc Mine by a Wetland at Glendalough, Co. Wicklow. In Biology and Environment: Proceedings of the Royal Irish Academy (pp. 117-126). Royal Irish Academy.
- Beining, B. and Otte, M. (1997). Retention of metals and longevity of a wetland receiving mine leachate. *Journal American Society of Mining and Reclamation*, 1997(1), pp.43-48.
- Cardille, J., Coe, M. and Vano, J. (2004). Impacts of Climate Variation and Catchment Area on Water Balance and Lake Hydrologic Type in Groundwater-Dominated Systems: A Generic Lake Model. *Earth Interactions*, 8(13), pp.1-24.
- Carrera, G., Fernández, P., Grimalt, J., Ventura, M., Camarero, L., Catalan, J., Nickus, U., Thies, H. and Psenner, R. (2002). Atmospheric Deposition of Organochlorine Compounds to Remote High Mountain Lakes of Europe. *Environmental Science & Technology*, 36(12), pp.2581-2588.
- Central Statistics Office (CSO). (2016). Census 2016. Central Statistics Office.
- Fischer, E., Paglialonga, L., Czech, E. and Tamminga, M. (2016). Microplastic pollution in lakes and lake shoreline sediments A case study on Lake Bolsena and Lake Chiusi (central Italy). *Environmental Pollution*, 213, pp.648-657.
- Forman, R. (1969). Comparison of Coverage, Biomass, and Energy as Measures of Standing Crop of Bryophytes in Various Ecosystems. *Bulletin of the Torrey Botanical Club*, 96(5), pp. 582.
- Holtgrieve, G., Schindler, D., Hobbs, W., Leavitt, P., Ward, E., Bunting, L., Chen, G., Finney, B., Gregory-Eaves, I., Holmgren, S., Lisac, M., Lisi, P., Nydick, K., Rogers, L., Saros, J., Selbie, D., Shapley, M., Walsh, P. and Wolfe, A. (2011). A Coherent Signature of Anthropogenic Nitrogen Deposition to Remote Watersheds of the Northern Hemisphere. *Science*, 334(6062), pp. 1545-1548.
- Horton, A. A., Walton, A., Spurgeon, D. J., Lahive, E. and Svendsen, C. (2017a).

 Microplastics in freshwater and terrestrial environments: Evaluating the current understanding to identify the knowledge gaps and future research priorities.

 Science of the Total Environment, 586, pp. 127–141. doi: 10.1016/j.scitotenv.2017.01.190.
- Horton, A., Svendsen, C., Williams, R., Spurgeon, D. and Lahive, E. (2017b). Large microplastic particles in sediments of tributaries of the River Thames, UK Abundance, sources and methods for effective quantification. *Marine Pollution Bulletin*, 114(1), pp.218-226.

- Imhof, H., Ivleva, N., Schmid, J., Niessner, R. and Laforsch, C. (2013). Contamination of beach sediments of a subalpine lake with microplastic particles. *Current Biology*, 23(19), pp. R867-R868.
- Irish Environmental Protection Agency (EPA). (2012). Corine 2012.
- Jiang, C., Yin, L., Wen, X., Du, C., Wu, L., Long, Y., Liu, Y., Ma, Y., Yin, Q., Zhou, Z. and Pan, H. (2018). Microplastics in Sediment and Surface Water of West Dongting Lake and South Dongting Lake: Abundance, Source and Composition. *International Journal of Environmental Research and Public Health*, 15(10), p.2164.
- Karami, A., Golieskardi, A., Ho, Y., Larat, V. and Salamatinia, B. (2017). Microplastics in eviscerated flesh and excised organs of dried fish. *Scientific Reports*, 7(1).
- Koelmans, A., Mohamed Nor, N., Hermsen, E., Kooi, M., Mintenig, S. and De France, J. (2019). Microplastics in freshwaters and drinking water: Critical review and assessment of data quality. *Water Research*, 155, pp.410-422.
- Li, J., Liu, H. and Paul Chen, J. (2018). Microplastics in freshwater systems: A review on occurrence, environmental effects, and methods for microplastics detection. *Water Research*, 137, pp.362-374.
- Lusher, A., McHugh, M. and Thompson, R. (2013). Occurrence of microplastics in the gastrointestinal tract of pelagic and demersal fish from the English Channel. *Marine Pollution Bulletin*, 67(1-2), pp.94-99.
- Lusher, A., Welden, N., Sobral, P. and Cole, M. (2017). Sampling, isolating and identifying microplastics ingested by fish and invertebrates. *Analytical Methods*, 9(9), pp.1346-1360.
- McKnight, K., Rohrer, J., and Perdrizet, W. (2013). Common mosses of the Northeast and Appalachians. Princeton University Press. Princeton, NJ. pp. 391.
- Ng, K. and Obbard, J. (2006). Prevalence of microplastics in Singapore's coastal marine environment. *Marine Pollution Bulletin*, 52(7), pp.761-767.
- Obbard, R. (2018). Microplastics in Polar Regions: The role of long range transport. Current Opinion in Environmental Science & Delta, 1, pp.24-29.
- Remy, F., Collard, F., Gilbert, B., Compère, P., Eppe, G. and Lepoint, G. (2015). When Microplastic Is Not Plastic: The Ingestion of Artificial Cellulose Fibres by Macrofauna Living in Seagrass Macrophytodetritus. *Environmental Science & Technology*, 49(18), pp.11158-11166.
- Singh, M., Juhász, A., Csintalan, Z., Kaligaric, M., Marek, M., Urban, O. and Tuba, Z. (2005). Preliminary estimation of bryophyte biomass and carbon pool from three contrasting different vegetation types. *Cereal Research Communications*, 33(1), pp. 267-270.
- Su, L., Xue, Y., Li, L., Yang, D., Kolandhasamy, P., Li, D. and Shi, H. (2016). Microplastics in Taihu Lake, China. *Environmental Pollution*, 216, pp.711-719.
- Swain, E., Engstrom, D., Brigham, M., Henning, T. and Brezonik, P. (1992). Increasing Rates of Atmospheric Mercury Deposition in Midcontinental North America. *Science*, 257(5071), pp.784-787.
- Tarvainen, T., Lahermo, P. and Mannio, J. (1997). Sources of trace metals in streams and headwater lakes in Finland. *Water, Air, and Soil Pollution*, 94(1-2), pp.1-32.

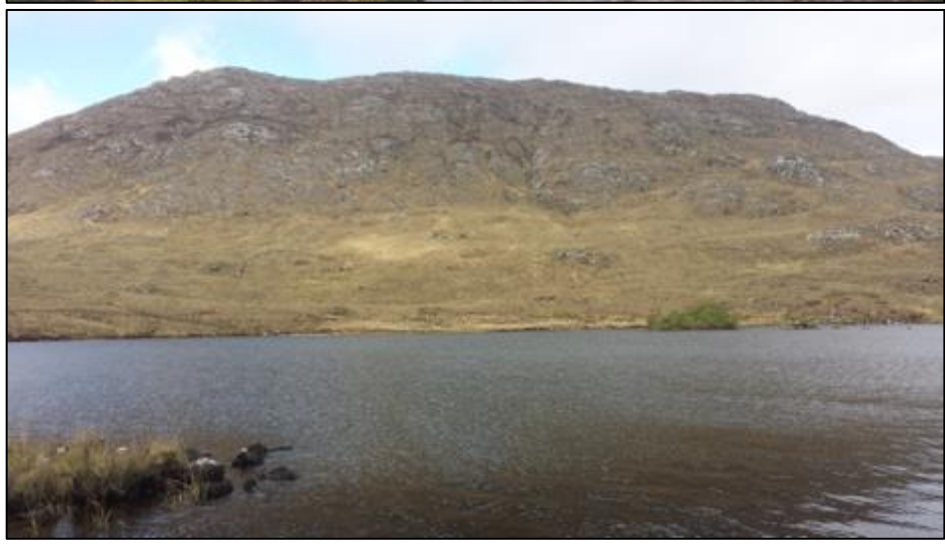
- Van Cauwenberghe, L., Vanreusel, A., Mees, J. and Janssen, C. (2013). Microplastic pollution in deep-sea sediments. *Environmental Pollution*, 182, pp.495-499.
- Van Metre, P.C., Wilson, J.T., Fuller, C.C., Callender, Edward, and Mahler, B.J. (2004) Collection, analysis, and agedating of sediment cores from 56 U.S. lakes and reservoirs sampled by the U.S. Geological Survey, 1992–2001: *U.S. Geological Survey Scientific Investigations Report*, 2004–5184, pp. 180
- Wang, W., Ndungu, A., Li, Z. and Wang, J. (2017). Microplastics pollution in inland freshwaters of China: A case study in urban surface waters of Wuhan, China. *Science of The Total Environment*, 575, pp.1369-1374.
- Wang, W., Yuan, W., Chen, Y. and Wang, J. (2018). Microplastics in surface waters of Dongting Lake and Hong Lake, China. *Science of The Total Environment*, 633, pp.539-545.
- Walsh, S. (2012). A summary of climate averages for Ireland 1981-2010. Met Eireann Climatology Note: 14. U.D.C 551.582 (417).
- Wiesheu, A., Anger, P., Baumann, T., Niessner, R. and Ivleva, N. (2016). Raman microspectroscopic analysis of fibres in beverages. *Analytical Methods*, 8(28), pp.5722-5725.
- Yuan, W., Liu, X., Wang, W., Di, M. and Wang, J. (2019). Microplastic abundance, distribution and composition in water, sediments, and wild fish from Poyang Lake, China. *Ecotoxicology and Environmental Safety*, 170, pp.180-187.
- Zhao, S., Danley, M., Ward, J., Li, D. and Mincer, T. (2017). An approach for extraction, characterization and quantitation of microplastic in natural marine snow using Raman microscopy. *Analytical Methods*, 9(9), pp.1470-1478.

3.8. Appendix

Table A3.1. The closest residential (distance away in parenthesis) and urban (pop. >10,000; distance away in parenthesis) areas, with their respective populations, to each of the three headwater lake catchments.

Lake Catchment	Nearest residential area (km)	Population	Nearest urban centre (km)	Population
Glendalough	Laragh (2)	<500	Wicklow (20.5)	10,584
Lough Maumwee	Maum (4.7)	<500	Galway (39.3)	79,934
Lough Veagh	Termon (8.6)	<500	Letterkenny (17.5)	19,274





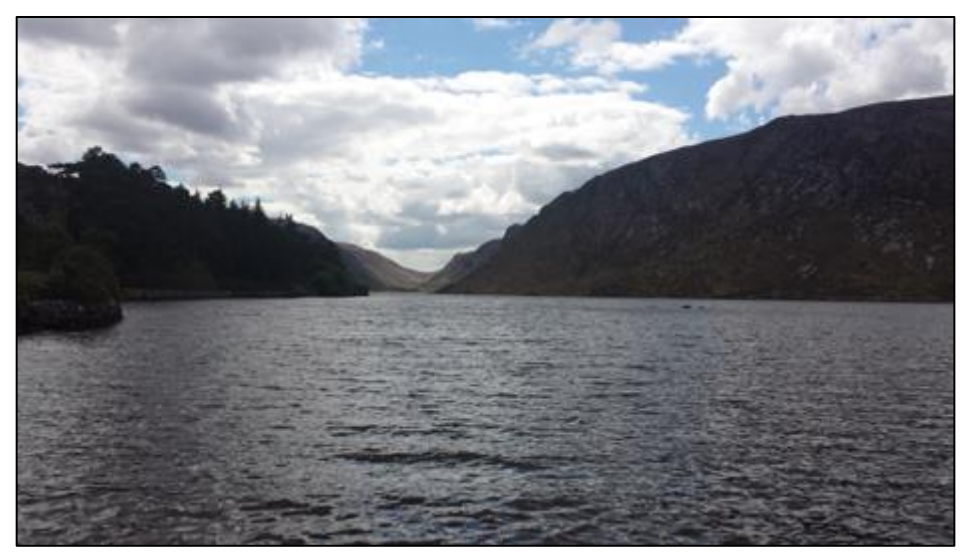


Figure A3.1. Photographs (from top to bottom) of Glendalough, Lough Maumwee and Lough Veagh.

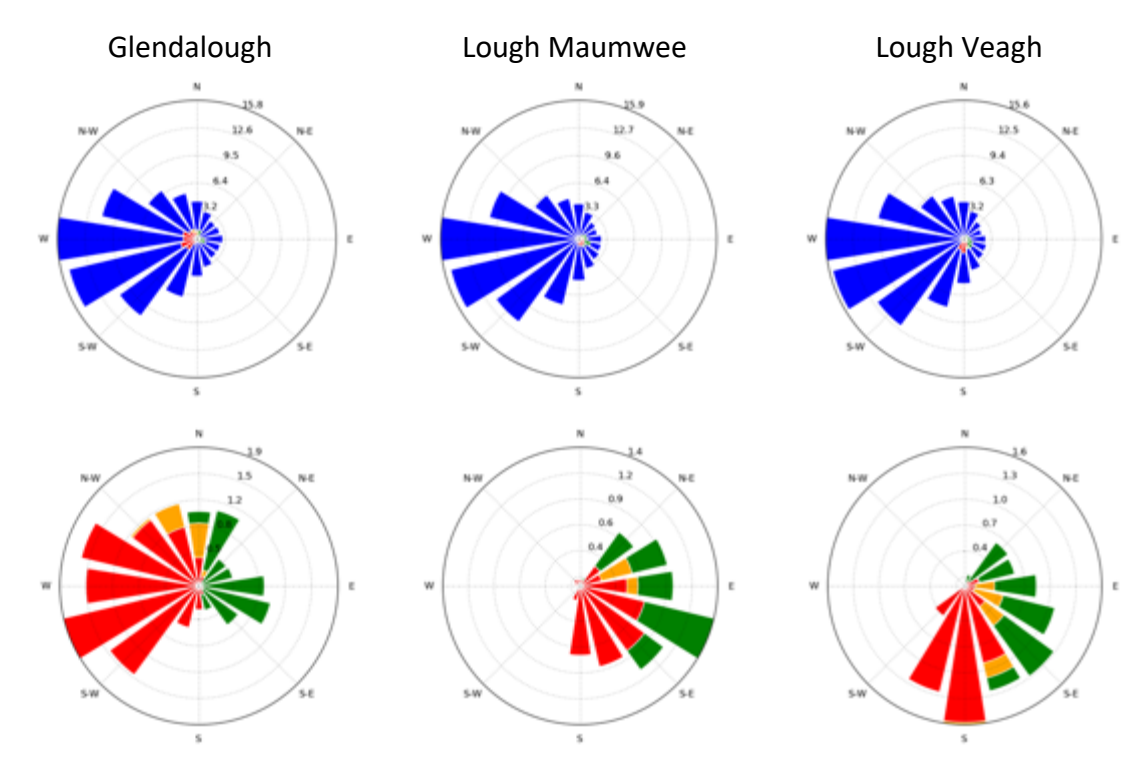


Figure A3.2. Upper: Trajectory source-receptor rose plots showing the proportion (%) of air by direction and source (Republic of Ireland (red), Northern Ireland (orange), Great Britain (green) and marine and other regions (blue)) arriving at the study sites. Lower: Close-up of proportion (%) of air from Ireland, Northern Ireland and Great Britian source regions only. Source-receptor trajectory rose plots were based on two-day back trajectories (arrival height of 850 hPa) estimated every six hours during the period 1989–2009.

Table A3.2. List of criteria used to visually identify plastic microfibres following: (A) four criteria taken from Norén (2007) as cited by Hidalgo-Ruz (2010) and Löder and Gerdts (2015), and (B) eight criteria taken from Windsor et al. (2018), with a recommendation that a positive response for at least two of the eight criteria is required for identification of microplastic particles.

	Source: Löder and Gerdts (2015) and Hidalgo-Ruz (2010) following Norén (2007)
1	No (cellular) structures of organic origin should be visible in the plastic particle or
	fibre.
2	Fibres should be equally thick throughout their entire length and have a three-
	dimensional bending to exclude a biological origin.
3	Particles should be clear and homogeneously coloured.
4	Transparent or whitish particles must be examined under high magnification and
	with the help of fluorescence microscopy to exclude a biological origin.
В	Source: Windsor et al. (2018) following Löder and Gerdts (2015)
1	Unnaturally coloured compared to the majority of other particles/detritus in the
	sample, e.g., red, bright blue and yellow.
2	Appears homogenous in material or texture, e.g., no cell structure.
3	Unnatural shape or structure, e.g. perfectly spherical, smooth or sharp edges.
4	Fibres that remain intact with a firm tug or poke with fine tweezers.
5	Shiny or glassy in appearance.
6	Flexible and can be compressed without being brittle.
7	Share similar surface characteristics to reference plastic material.

Table A3.3. The number of microfibres observed in triplicate moss, lake and lakeshore sediment samples from the three headwater lake catchments.

Triplicate sample	Glendalough	Lough Maumwee	Lough Veagh
Moss S1	13	9	8
Moss S2	27	6	9
Moss S3	36	19	33
Lake Sed. S1	30	14	10
Lake Sed. S2	9	11	10
Lake Sed. S3	5	18	16
Lakeshore Sed. S1	5	7	20
Lakeshore Sed. S2	17	5	30
lakeshore Sed. S3	6	3	11

Table A3.4. The total count of microfibres found in each media collected at the three headwater lake catchments.

Lake Catchment	Moss	Surface trawl	Subsurface	Lake sediment	Lakeshore sediment	Total
GL	162	24	42	44	28	300
LM	56	34	45	43	15	193
LV	82	38	39	36	61	256
Total	300	96	126	123	104	749
Average	100	32	42	35	41	250

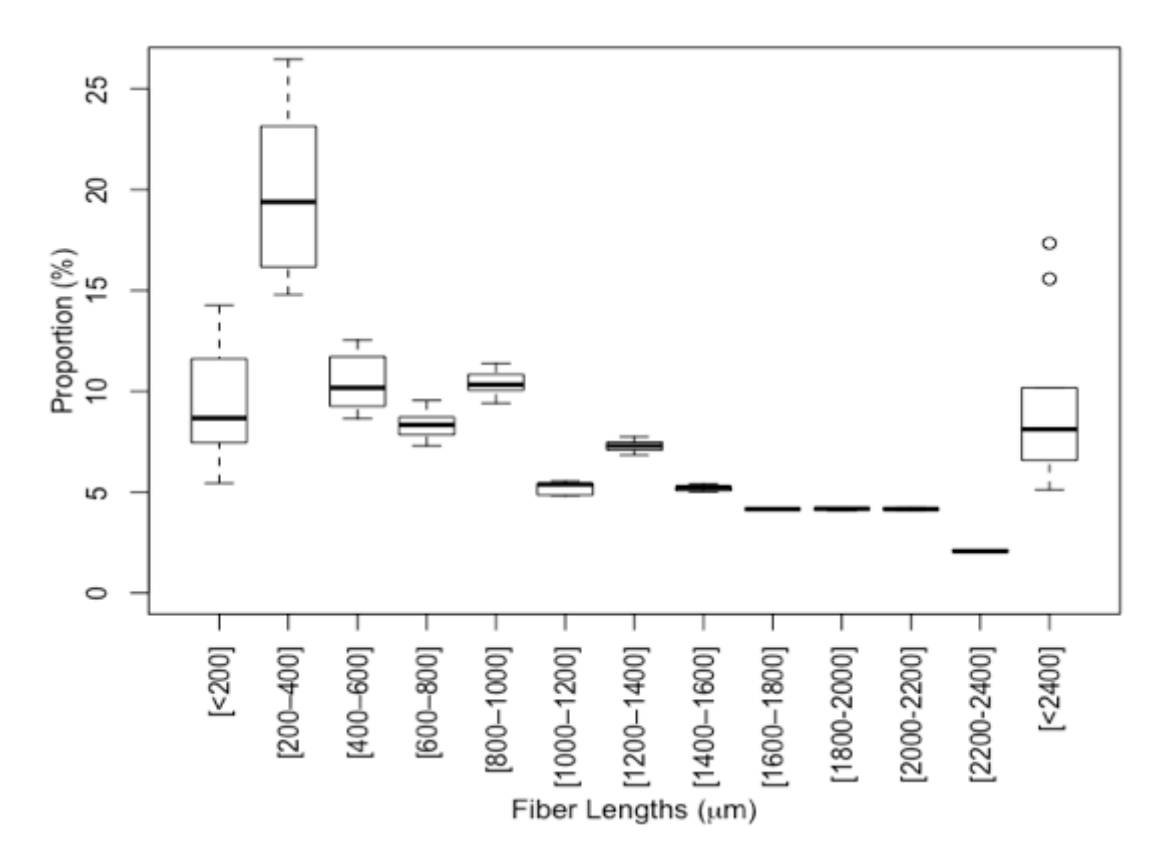


Figure A3.3A. Length distribution (μm) of microfibres in surface trawl samples from the three headwater lake catchments (Glendalough, Lough Maumwee and Lough Veagh). Black line represents the median, boxplots represent the first quartile and third quartile, whiskers represent the smallest and largest observations that fall within a distance of 1.5 times the box size and the dots represent values that are outside the 1.5 times distance.

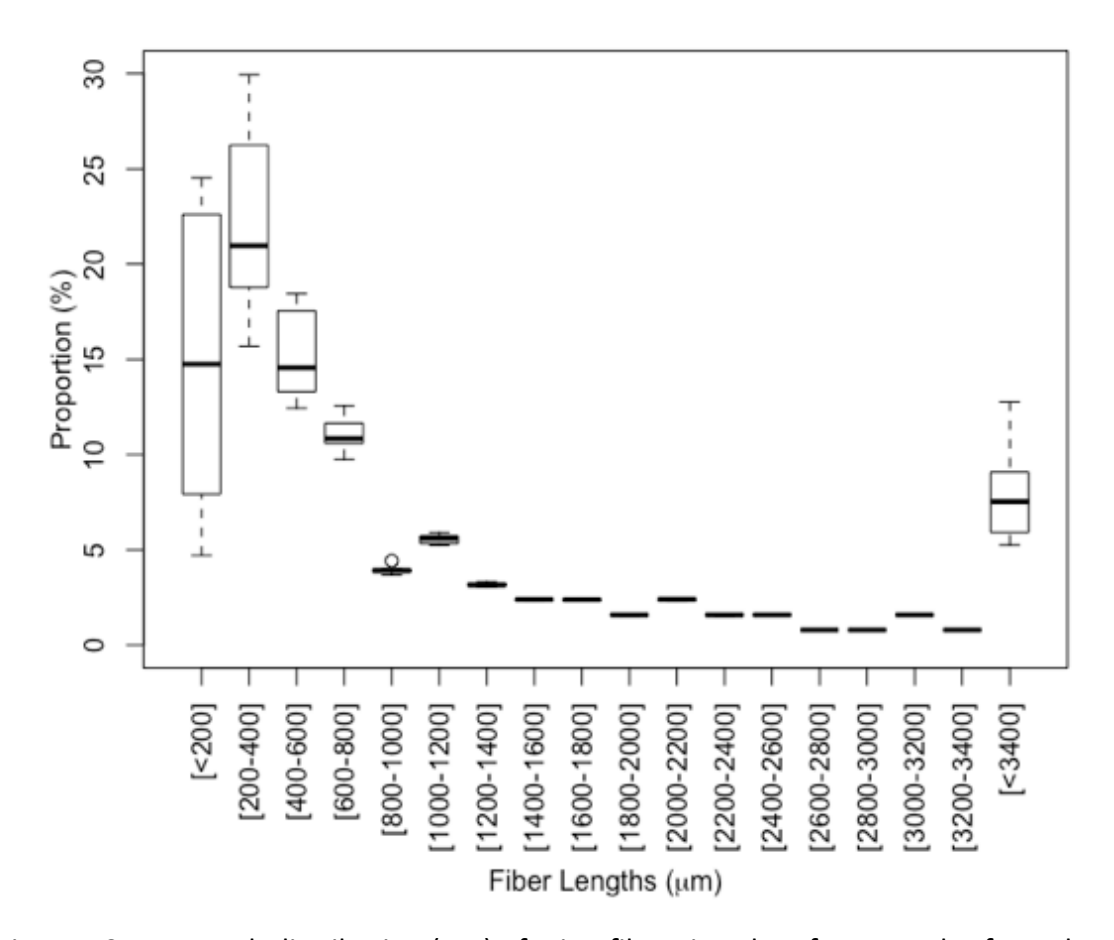


Figure A3.4B. Length distribution (μ m) of microfibres in subsurface samples from the three headwater lake catchments (Glendalough, Lough Maumwee and Lough Veagh). Black line represents the median, boxplots represent the first quartile and third quartile, whiskers represent the smallest and largest observations that fall within a distance of 1.5 times the box size and the dots represent values that are outside the 1.5 times distance.

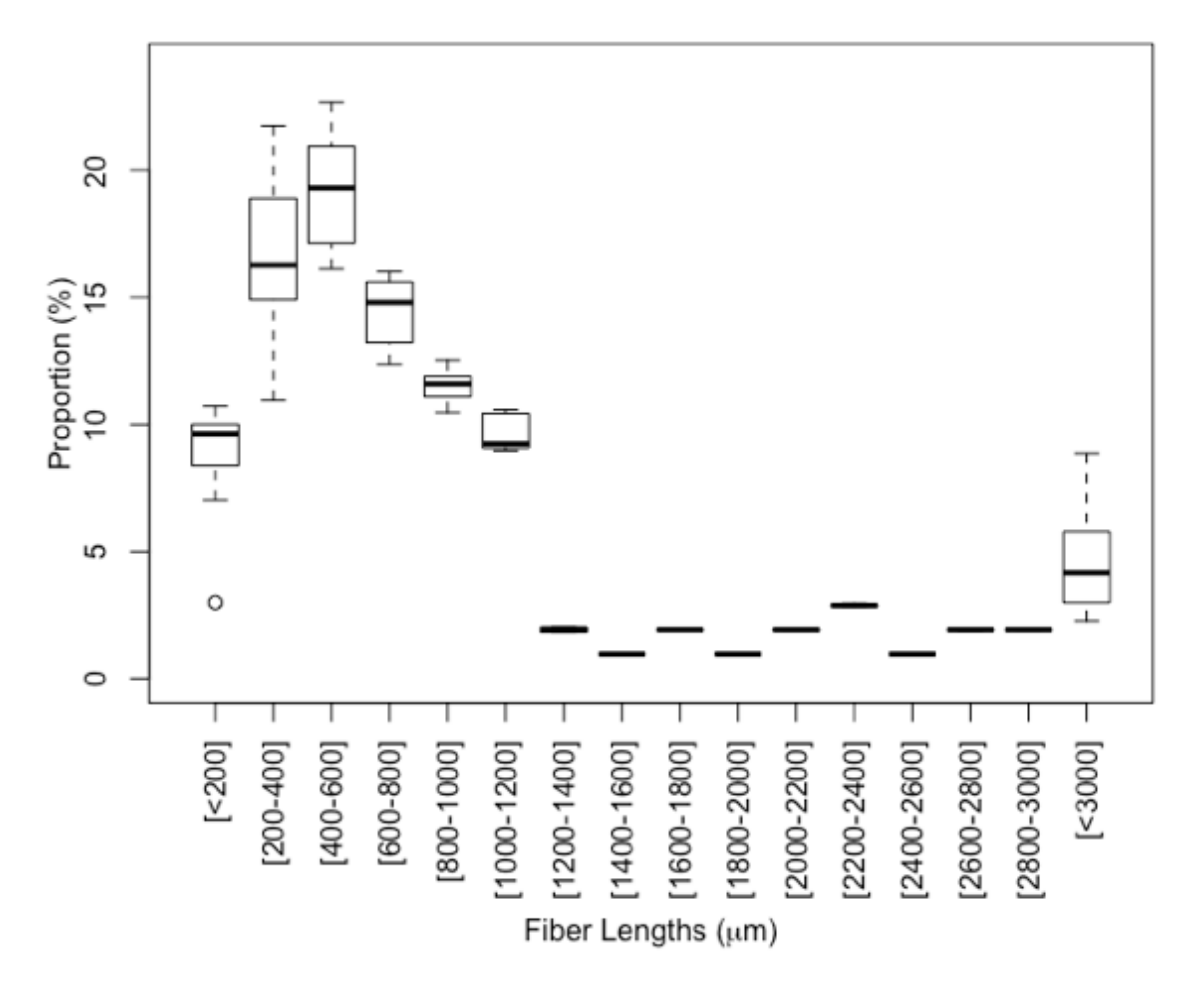


Figure A3.5C. Length distribution (μm) of microfibres in lake sediment samples from the three lake catchments (Glendalough, Lough Maumwee and Lough Veagh). Black line represents the median, boxplots represent the first quartile and third quartile, whiskers represent the smallest and largest observations that fall within a distance of 1.5 times the box size and the dots represent values that are outside the 1.5 times distance.

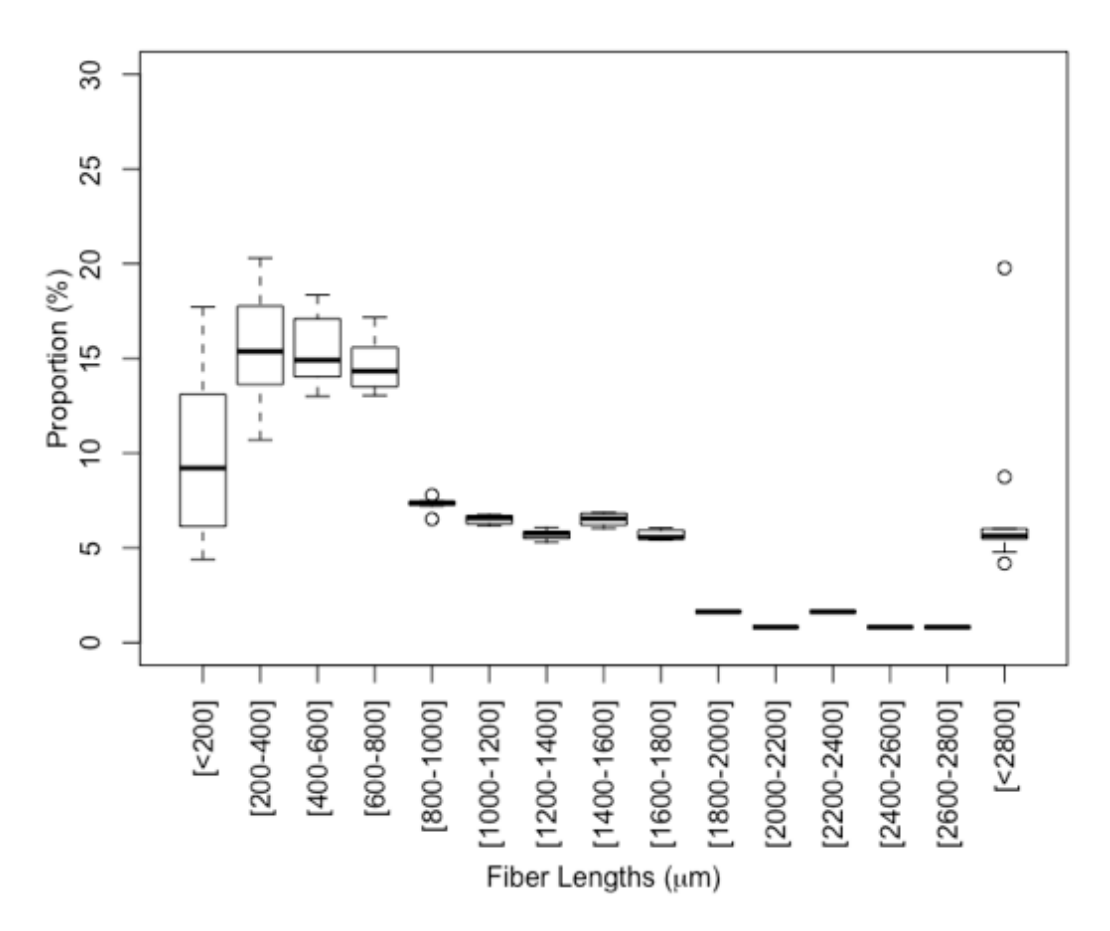


Figure A3.6D. Length distribution (μ m) of microfibres in lakeshore sediment samples from the three lake catchments (Glendalough, Lough Maumwee and Lough Veagh). Black line represents the median, boxplots represent the first quartile and third quartile, whiskers represent the smallest and largest observations that fall within a distance of 1.5 times the box size and the dots represent values that are outside the 1.5 times distance.

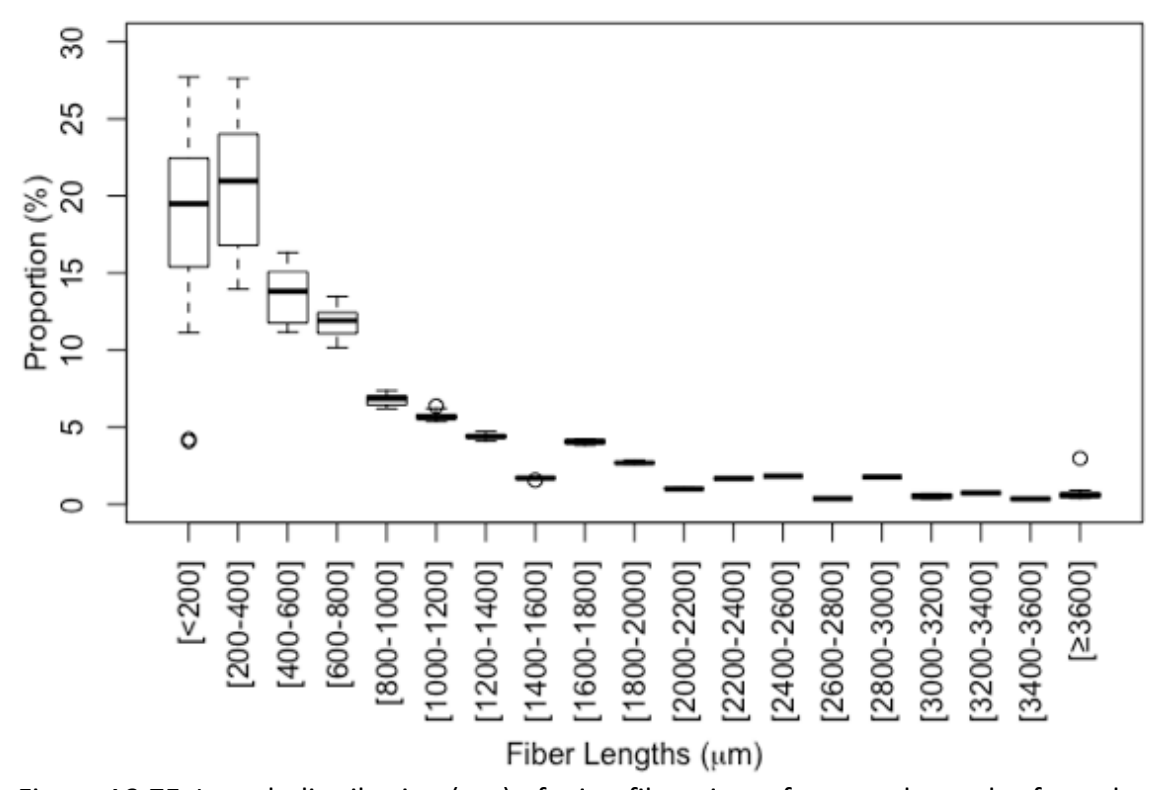


Figure A3.7E. Length distribution (μm) of microfibres in surface trawl samples from the three lake catchments (Glendalough, Lough Maumwee and Lough Veagh). Black line represents the median, boxplots represent the first quartile and third quartile, whiskers represent the smallest and largest observations that fall within a distance of 1.5 times the box size and the dots represent values that are outside the 1.5 times distance.

Appendix 3.4. Raman spectral analysis reports from Bio Rad-KnowltAll online library for media collected from headwater lake catchments.

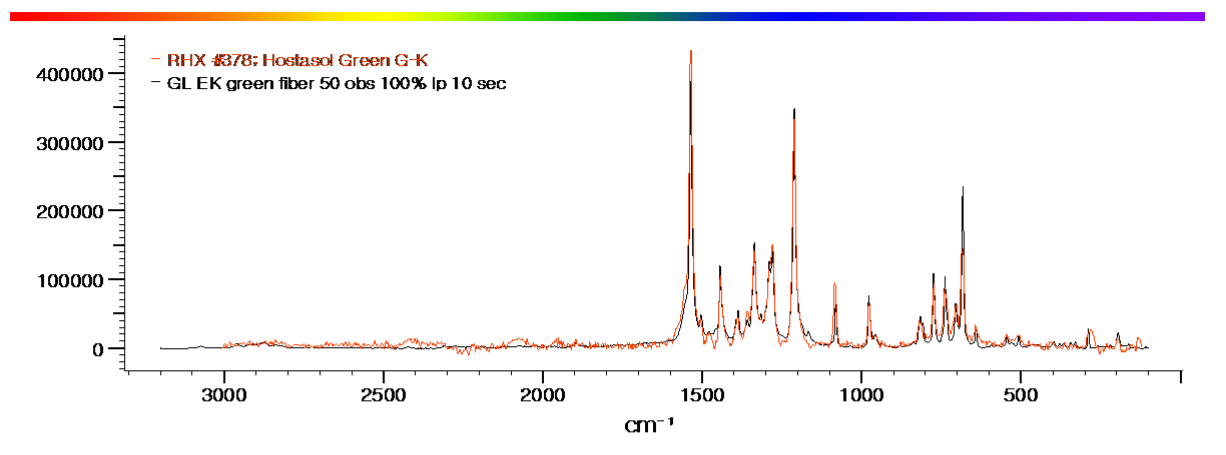
Figure A3.4A. Hostasol Green G-K pigment

Figure A3.4B. Indigo pigment

Figure A3.4C. Hostopen violet pigment

Figure A3.4D. Copper phthalocyanine pigment

Figure A3.4E. Eriochrome blue pigment



Manual Corrections: None

Ranges: Full

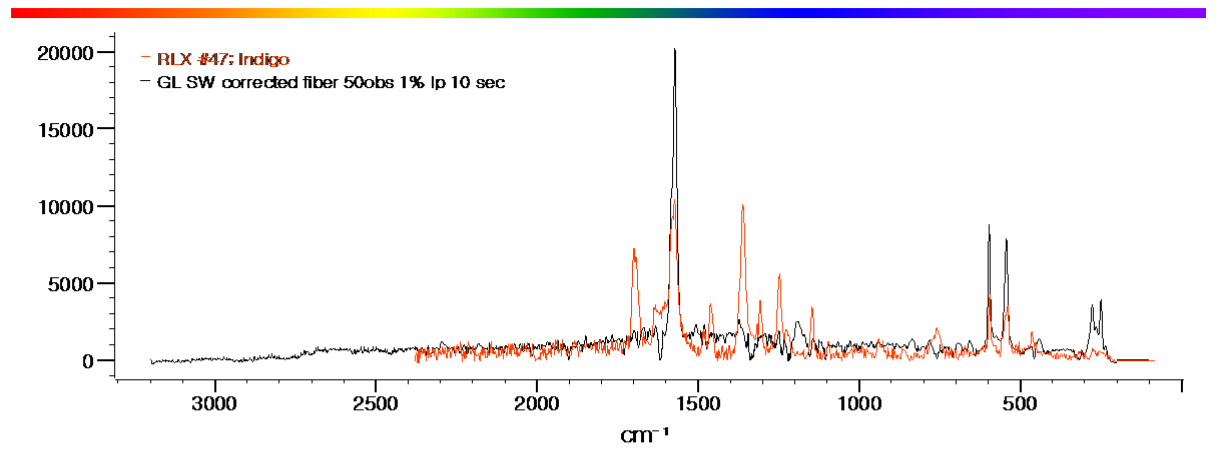
Search Algorithm: Correlation

Query Path: \text{\text{Wariftwood\text{\text{W}}}\text{tudents\text{\text{W}}\text{trettroblin\text{W}}\text{y} Documents\text{\text{W}}\text{aman Spectra\text{\text{V}}\text{L} EK green fiber 50 obs 100\text{\text{l} Ip 10 sec.txt}

Name	Value
Resulting HQI	95.44
Database Abbreviation	RHX
Database Title	Raman -Forensic -HORIBA
Record ID	378
Name	Hostasol Green G-K
Classification	dyestuff
Comments	Hoechst
Instrument Name	HORIBA LabRAM Infinity-
Laser Power	632.8
Source of Sample	LKA Berlin
Source of Spectrum	HORIBA Scientific

Score: 95.44%

Figure A3.8A. Raman spectral analysis report from Bio Rad-KnowItAll online library for Hostasol Green G-K identified from a Glendalough lake sediment microfibre.



Manual Corrections: Noise

Ranges: Full

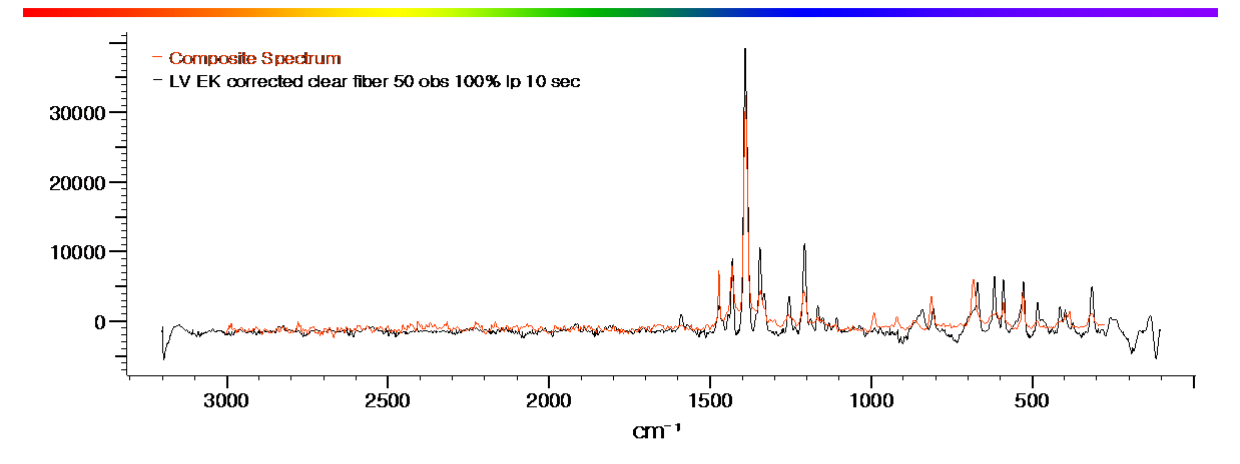
Search Algorithm: Correlation

Query Path: \text{Warriftwood\text{Mariftwood\

Name	Value
Resulting HQI	60.83
Database Abbreviation	RLX
Database Title	Raman -Biomaterials -HORIBA
Record ID	47
Name	Indigo
Comments	synthetic
Formula	C16H10N2O2
InChl	InChl=1S/C16H10N2O2/c19-15-9-
InChlKey	COHYTHOBJLSHDF-
Instrument Name	HORIBA
Laser Power	514.5
Mol.Weight	262.268 g/mol
Осситепсе	urinary pigment whose presence in stone is controversal
Source of Sample	Jobin Yvon
Source of Spectrum	HORIBA Scientific
Synonyms	Indigotin; Indigo blue

Score: 60.83 %

Figure A3.9B. Raman spectral analysis report from Bio Rad-KnowItAll online library for indigo identified from a Glendalough surface trawl microfibre.



Manual Corrections: Noise

Ranges: Full

Search Algorithm: Correlation

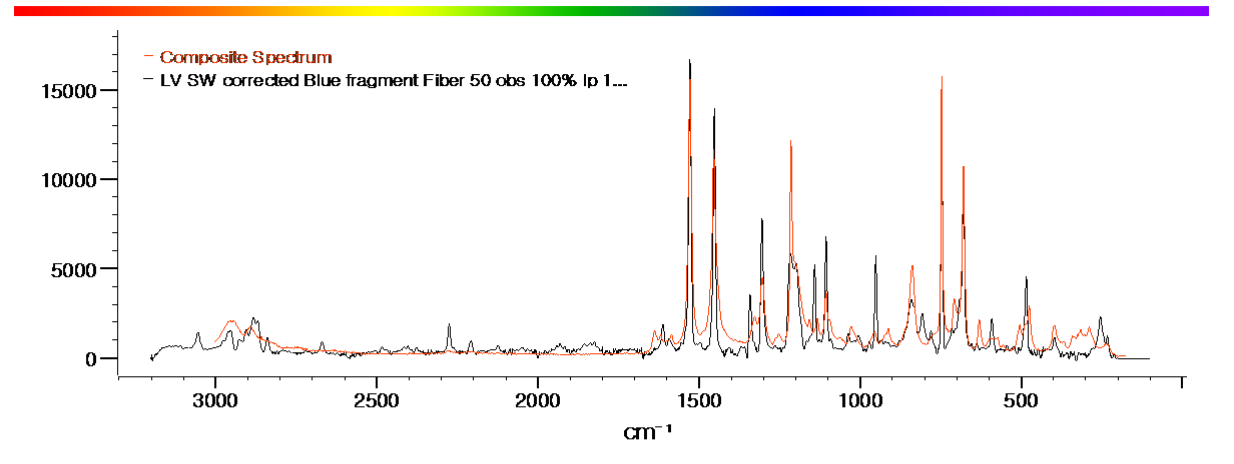
Query Path: \text{\text{WM}}riftwood\text{\text{\text{WM}}}riftwood\text{\text{\text{WM}}}riftwood\text{\text{\text{WM}}}riftwood\text{\text{\text{WM}}}riftwood\text{\text{\text{WM}}}riftwood\text{\text{\text{WM}}}riftwood\text{\text{\text{WM}}}riftwood\text{\text{\text{WM}}}riftwood\text{\text{\text{WM}}}riftwood\text{\text{\text{WM}}}riftwood\text{\text{\text{WM}}}riftwood\text{\text{\text{WM}}}riftwood\text{\text{\text{WM}}}riftwood\text{\text{WM}}riftwoo

Score	Info	Weight	Name	Chemical Structure	Spectrum
91.48		N.A.	Composite Spectrum	**************************************	Manual Ma

Score: 86.8% Hostopen violet

Composite Spectra score: 91.48% with Hostopen violet, Melamine, and Magnesium Oxalate (inorganic compound)

Figure A3.10C. Raman spectral analysis report from Bio Rad-KnowItAll online library for Hostopen violet identified from a Lough Veagh lake sediment microfibre.



Manual Corrections: Noise

Ranges: Full

Search Algorithm: Correlation

Query Path: \text{\text{Warriftwood\text{Warriftwood\text{Warriftwood\text{Warriftwood\text{Warriftwood\text{\text{Warriftwood\text{\text{Warriftwood\text{Warriftwood\text{Warriftwood\text{\text{Warriftwood\text{\text{Warriftwood\text{Warriftwoo

100% lp 10sec.txt

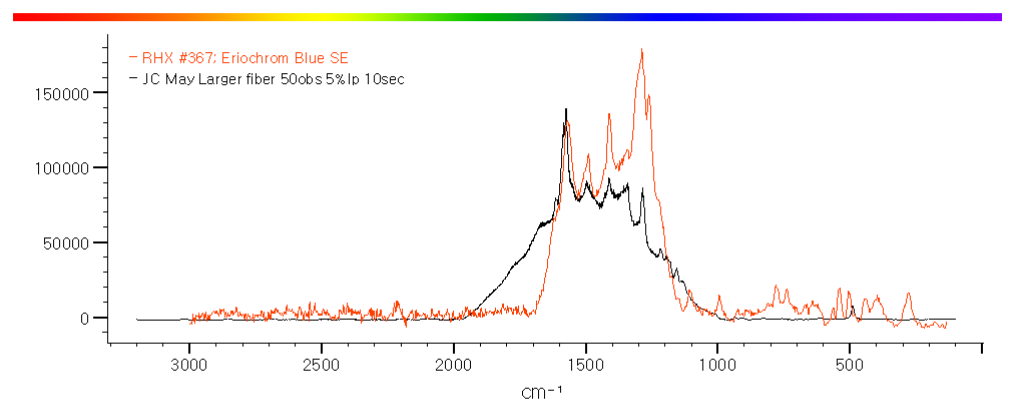
Score	Info	Weight	Name	Chemical Structure	Spectrum
82.71		N.A.	Composite Spectrum	α{}po~è-¢	- Muhamhama

Score: 73.4% Copper phthalocyanine

Composite Spectra score: 82.71% with Cobalt phthalocyanine, Ammonium hexafluorophosphate and imidazole

Figure A3.11D. Raman spectral analysis report from Bio Rad-KnowltAll online library for Copper phthalocyanine identified from a Lough Veagh surface trawl microfibre.





Manual Corrections: Baseline

Ranges: Full

Search Algorithm: Correlation

Query Path: ₩ariftwood ₩hudents\rettroblin ₩y Documents\rettraman Spectra ₩C May Larger fiber 50obs 5%lp 10sec.txt

Name	Value
Resulting HQI	84.36
Database Abbreviation	RHX
Database Title	Raman -Forensic -HORIBA
Record ID	367
Name	Eriochrom Blue SE
CAS Registry Number	1058-92-0
Classification	dyestuff, stain
Comments	Merck 285
Formula	C16H9CIN2O9S2Na8
InChl	InChl=1S/C16H11CIN2O9S2.2Na/c
InChlKey	LNXMAD NIU WFTPP-
Instrument Name	HORIBA LabRAM Infinity-
Laser Power	632.8
Source of Sample	LKA Berlin
Source of Spectrum	HORIBA Scientific
Synonyms	C.I. Generic name: Mordant Blue 13; MB13; C.I. Constitution No:

Score: 84.36%

Figure A3.12E. Raman spectral analysis reports from Bio Rad-KnowItAll online library for Eriochrome blue.

Table A3.5. Previous studies on microplastics, with the location, sample type, abundance (range in parentheses), and dominant type of microplastic.

Location	Sample Type	Particle Abundance	Dominant Type	Reference
Chiusi Lake	Surface trawl	3.02 m ⁻³	Fibre	Fischer et
	(300 μm) and sediments	168 kg ⁻¹ dw		al., 2016
Taihu Lake	Surface trawl	(10,000-6.5x10 ⁶ km ⁻²)	Fibre (48-84%)	Su et al.,
	(333 μm), bulk	(3.4-25.8 L ⁻¹)		2016
	water (30 cm) and sediments	(11-235 kg ⁻¹ dw)		
Lake	Surface trawl	193,420 km ⁻²	Fibre (90%)	Anderson et
Winnipeg	(333 μm)			al., 2017
Wuhan lakes	Bulk water (0-20 cm)	(1660-8925 m ⁻³)	Fibre	Wang et al., 2017
Dongting	Bulk water (0-20	1191/2282 m ⁻³	Fibre (41-91%)	Wang et al.,
and Hong Lake	cm)		Fibre (44-84%)	2018
Poyang	Bulk water (0-1	(5-34 L ⁻¹)	Fibre (41% and	Yuan et al.,
Lake	m) and sediments	(54-506 kg ⁻¹ dw)	44%)	2019

Chapter 4: Conclusion

4.1 General conclusions

Most of the scientific literature regarding microfibres has focused on marine systems, with limited research in other environments (Horton et al., 2017; Li et al., 2018). Yet, annual atmospheric deposition of microfibres has been estimated to range from 14,000 mf m $^{-2}$ to > 74,000 mf m $^{-2}$, depending on the geographic location (Cai et al., 2017; Allen et al., 2019). As such, atmospheric deposition may be an important source / vector for microfibre pollution transport into remote, environments. The objective of this thesis was to evaluate the level of anthropogenic microfibre contamination in background natural environments.

Chapter 2 focused on estimating and characterizing the atmospheric deposition of microfibres in precipitation. Precipitation was collected from four long term precipitation chemistry monitoring stations in Ireland from June 2017 to May 2018. Anthropogenic microfibres were present in all precipitation samples collected from the four monitoring stations. Microfibres were visual identified using modified methods supported by Raman spectroscopic analysis. Raman analysis verified the visual method by identifying polyester film and synthetic pigments, Indigo, Eriochrome blue, Levafix blue, Drimarene turquoise X-2G and Mortoperm. This is the first study to estimate wet deposition of microfibres across three stations with wet-only precipitation collectors, which had an average annual wet deposition of ~26,300 mf m⁻². Meteorological

variables such as rain, wind direction, wind speed, relative humidity, vapor pressure, and mean sea level pressure were correlated with the amount of microfibres in deposition. There was no difference in the magnitude and size of microfibres between the four meteorological stations. There was a difference in the deposition of microfibres between wet-only and bulk collectors, as bulk deposition is a mix of wet and a fraction of dry deposition.

In Chapter 3, the abundance, size and colour of microfibres were evaluated in moss, water and sediment collected at three background headwater lake catchments in Ireland. Anthropogenic microfibres were present in all media samples from the three lake catchments. Microfibres were visual identified using modified methods supported by Raman spectroscopic analysis. Raman analysis verified the visual method by identifying synthetic pigments, Indigo, Eriochrome blue, Cobalt phthalocyanine,

Hostasol green G-K and Hostopen Violet. The average number of microfibres per lake catchment was 47,700 mf m⁻² in moss, 0.70 mf m⁻³ in surface trawl, 9, 690 mf m⁻³ in subsurface, 915 mf kg⁻¹ in lake sediment and 576 mf kg⁻¹ in lakeshore sediment. This was the first study to estimate atmospheric deposition from moss, which suggests it may be suitable as a biomonitor for the atmospheric deposition of microfibres. There was no difference in the microfibre abundance and length in the moss, lake water and lake sediment samples collected at the three headwater lake catchments

4.2 Contributions to research

There have been few studies focusing on the atmospheric deposition of microfibres (Dris et al., 2016; Cai et al., 2017; Stanton et al., 2019; Allen et al., 2019) with the majority of them being conducted in urban centres (e.g., Dris et al., 2016; Cai et al., 2017; Stanton et al., 2019). Additionally, these studies have only collected bulk deposition (wet and a fraction of dry deposition) (Allen et al., 2019). The research in this thesis contributes to the literature surrounding the presence of anthropogenic microfibres in background headwater lake catchments and atmospheric deposition.

Specifically, Chapter 2 is the first study to characterize the abundance of microfibres in wet-only deposition. This study also determined meteorological variables, such as rain, relative humidity, mean sea level pressure, vapor pressure, wind direction, and wind speed, were correlated with the abundance of microfibres. Chapter 3 characterized microfibres from a catchment approach, which indicated that microfibres input from atmospheric deposition are likely to sink and concentrate in lake sediment. This was the first study to estimate deposition of microfibres from moss samples, which suggests that moss may be a suitable biomonitor for atmospheric deposition of microfibres.

4.3 Recommendations

The results determined from Chapter 2 of this study are the first to analyse wet and bulk deposition of microfibres. Only a fraction of microfibre dry deposition was collected in the current study, therefore it is recommended that further research is conducted to

determine total microfibre dry deposition. Due to the majority of published papers having different methods, it is recommended that methods become standardized in order to properly compare studies.

There is a need to assess the impacts that microfibres have on human health. Studies have indicated that depending on the demographic, people could ingest 26–146 microplastics per day, with an additional 97–170 daily from inhalation, and the majority of these microplastics are microfibres (Prata, 2018; Cox et al., 2019). This indicates that people are estimated to ingest 81,000–123,000 microplastics per year (Cox et al., 2019). The biggest risks to people have been identified as inhalation and drinking water (Cox et al., 2019). There is currently no known risk associated with the ingestion of microfibres into the digestive tract or lungs (Wright and Kelly, 2017; Cox et al., 2019). Due to the lack of knowledge surrounding health impacts, it is recommended that the potential health impacts from microfibres should be further assessed.

4.4. References

- Allen, S., Allen, D., Phoenix, V., Le Roux, G., Durántez Jiménez, P., Simonneau, A., Binet, S. and Galop, D. (2019). Atmospheric transport and deposition of microplastics in a remote mountain catchment. *Nature Geoscience*, 12(5), pp.339-344.
- Cai, L., Wang, J., Peng, J., Tan, Z., Zhan, Z., Tan, X. and Chen, Q. (2017). Characteristic of microplastics in the atmospheric fallout from Dongguan city, China: preliminary research and first evidence. *Environmental Scence andi Pollution Research*, 24(32), pp. 24928–24935.
- Cox, K., Covernton, G., Davies, H., Dower, J., Juanes, F., and Sarah E. Dudas. (2019). Environmental Science & Technology, pp. A-G. doi: 10.1021/acs.est.9b01517
- Horton, A. A., Walton, A., Spurgeon, D. J., Lahive, E. and Svendsen, C. (2017).

 Microplastics in freshwater and terrestrial environments: Evaluating the current understanding to identify the knowledge gaps and future research priorities.

 Science of the Total Environment, 586, pp. 127–141.
- Li, J., Liu, H. and Paul Chen, J. (2018). Microplastics in freshwater systems: A review on occurrence, environmental effects, and methods for microplastics detection. *Water Research*, 137, pp.362-374.
- Prata, J. (2018). Airborne microplastics: Consequences to human health. *Environmental Pollution*, 234, pp.115-126.
- Stanton, T., Johnson, M., Nathanail, P., MacNaughtan, W. and Gomes, R. (2019). Freshwater and airborne textile fibre populations are dominated by 'natural', not microplastic, fibres. *Science of The Total Environment*, 666, pp.377-389.
- Wright, S. and Kelly, F. (2017). Plastic and Human Health: A Micro Issue. *Environmental Science & Technology*, 51(12), pp.6634-6647.